# Single chain conformations

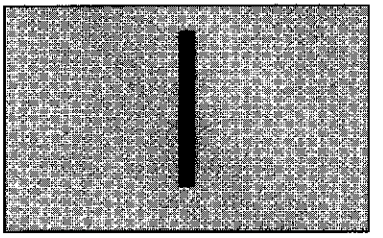

This page is intentionally left blank

# Ideal chains

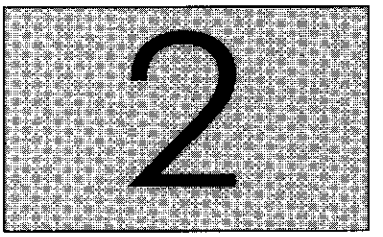


In this chapter, we consider the conformations of chains with no interactions between monomers that are far apart along the chain, even if they approach each other in space. Such chains are called **ideal chains**. This situation is never completely realized for real chains, but there are several types of polymeric systems with nearly ideal chains. Real chains interact with both their solvent and themselves. The relative strength of these interactions determines whether the monomers effectively attract or repel one another. In Chapter 3, we will learn that real chains in a solvent at low temperatures can be found in a collapsed conformation due to a dominance of attractive over repulsive interactions between monomers. At high temperatures, chains swell due to dominance of repulsive interactions. At a special intermediate temperature, called the **$\theta$-temperature**, chains are in nearly ideal conformations because the attractive and repulsive parts of monomer–monomer interactions cancel each other. This $\theta$-temperature is analogous to the Boyle temperature of a gas, where the ideal gas law happens to work at low pressures. Even more importantly, linear polymer melts and concentrated solutions have practically ideal chain conformations because the interactions between monomers are almost completely screened by surrounding chains.

The conformation of an ideal chain, with no interactions between monomers, is the essential starting point of most models in polymer physics. In this sense, the role of the ideal chain is similar to the role of the harmonic oscillator or the hydrogen atom in other branches of physics.

## 2.1 Flexibility mechanisms

In order to understand the multitude of conformations available for a polymer chain, consider an example of a polyethylene molecule. The distance between carbon atoms in the molecule is almost constant $l = 1.54$ Å. The fluctuations in the bond length (typically $\pm 0.05$ Å) do not affect chain conformations. The angle between neighbouring bonds, called the **tetrahedral angle** $\theta = 68°$ is also almost constant.

The main source of polymer flexibility is the variation of **torsion angles** [see Fig. 2.1(a)]. In order to describe these variations, consider a plane defined by three neighbouring carbon atoms $C_{i-2}$, $C_{i-1}$, and $C_i$. The bond

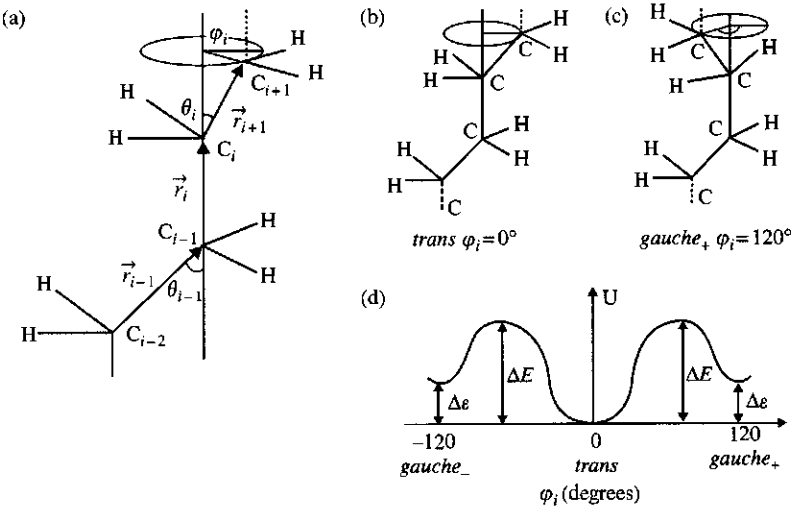


**Fig. 2.1**
(a) Torsion angle $\varphi_i$ for a sequence of three main-chain bonds. (b) *Trans* state. (c) *Gauche*-plus state. (d) Torsion angle dependence of energy.

vector $\vec{r}_i$ between atoms $C_{i-1}$ and $C_i$ defines the axis of rotation for the bond vector $\vec{r}_{i+1}$ between atoms $C_i$ and $C_{i+1}$ at constant bond angle $\theta_i$. The zero value of the torsion angle $\varphi_i$ corresponds to the bond vector $\vec{r}_{i+1}$ being colinear to the bond vector $\vec{r}_{i-1}$ and is called the **trans** state ($t$) of the torsion angle $\varphi_i$ [Fig. 2.1(b)].

The *trans* state of the torsion angle $\varphi_i$ is the lowest energy conformation of the four consecutive $CH_2$ groups. The changes of the torsion angle $\varphi_i$ lead to the energy variations shown in Fig. 2.1(d). These energy variations are due to changes in distances and therefore interactions between carbon atoms and hydrogen atoms of this sequence of four $CH_2$ groups. The two secondary minima corresponding to torsion angles $\varphi_i = \pm 120°$ are called **gauche-plus** ($g+$) [Fig. 2.1(c)] and **gauche-minus** ($g-$). The energy difference between *gauche* and *trans* minima $\Delta\varepsilon$ determines the relative probability of a torsion angle being in a *gauche* state in thermal equilibrium. In general, this probability is also influenced by the values of torsion angles of neighbouring monomers. These correlations are included in the rotational isomeric state model (Section 2.3.4). The value of $\Delta\varepsilon$ for polyethylene at room temperature is $\Delta\varepsilon \cong 0.8kT$. The energy barrier $\Delta E$ between *trans* and *gauche* states determines the dynamics of conformational rearrangements.

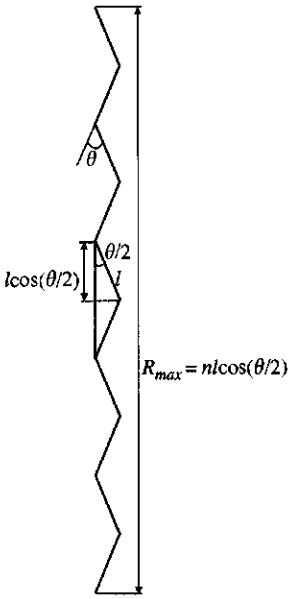


**Fig. 2.2**
All-*trans* (zig-zag) conformation of a short polymer with $n = 10$ main-chain bonds.

Any section of the chain with consecutive *trans* states of torsion angles is in a rod-like zig-zag conformation (see Fig. 2.2). If all torsion angles of the whole chain are in the *trans* state (Fig. 2.2), the chain has the largest possible value of its end-to-end distance $R_{max}$. This largest end-to-end distance is determined by the product of the number of skeleton bonds $n$ and their projected length $l\cos(\theta/2)$ along the contour, and is referred to as the **contour length** of the chain:

$$R_{max} = nl\cos\frac{\theta}{2}. \tag{2.1}$$

*Gauche* states of torsion angles lead to flexibility in the chain conformation since each *gauche* state alters the conformation from the all-*trans* zig-zag of

Fig. 2.2. In general, there will be a variable number of consecutive torsion angles in the *trans* state. Each of these all-*trans* rod-like sections will be broken up by a *gauche*. The chain is rod-like on scales smaller than these all-*trans* sections, but is flexible on larger length scales. Typically, all-*trans* sections comprise fewer than ten main-chain bonds and most synthetic polymers are quite flexible.

A qualitatively different mechanism of flexibility of many polymers, such as double-helix DNA is uniform flexibility over the whole polymer length. These chains are well described by the worm-like chain model (see Section 2.3.2).

## 2.2 Conformations of an ideal chain

Consider a flexible polymer of $n+1$ backbone atoms $A_i$ (with $0 \leq i \leq n$) as sketched in Fig. 2.3. The bond vector $\vec{r}_i$ goes from atom $A_{i-1}$ to atom $A_i$. The backbone atoms $A_i$ may all be identical (such as polyethylene) or may be of two or more atoms [Si and O for poly(dimethyl siloxane)]. The polymer is in its ideal state if there are no net interactions between atoms $A_i$ and $A_j$ that are separated by a sufficient number of bonds along the chain so that $|i-j| \gg 1$.

The **end-to-end vector** is the sum of all $n$ bond vectors in the chain:

$$\vec{R}_n = \sum_{i=1}^{n} \vec{r}_i. \tag{2.2}$$

Different individual chains will have different bond vectors and hence different end-to-end vectors. The distribution of end-to-end vectors shall be discussed in Section 2.5. It is useful to talk about average properties of this distribution. The average end-to-end vector of an isotropic collection of chains of $n$ backbone atoms is zero:

$$\langle \vec{R}_n \rangle = 0. \tag{2.3}$$

The **ensemble average** $\langle\,\rangle$ denotes an average over all possible states of the system (accessed either by considering many chains or many

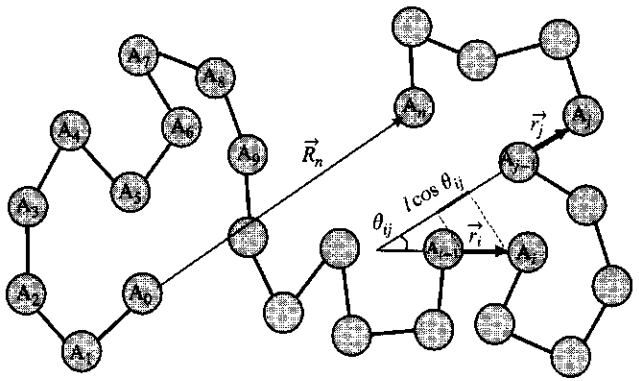


**Fig. 2.3**
One conformation of a flexible polymer.

different conformations of the same chain). In this particular case the ensemble average corresponds to averaging over an ensemble of chains of $n$ bonds with all possible bond orientations. Since there is no preferred direction in this ensemble, the average end-to-end vector is zero [Eq. (2.3)]. The simplest non-zero average is the mean-square end-to-end distance:

$$\langle R^2 \rangle \equiv \langle \vec{R}_n^2 \rangle = \langle \vec{R}_n \cdot \vec{R}_n \rangle = \left\langle \left( \sum_{i=1}^{n} \vec{r}_i \right) \cdot \left( \sum_{j=1}^{n} \vec{r}_j \right) \right\rangle$$
$$= \sum_{i=1}^{n} \sum_{j=1}^{n} \langle \vec{r}_i \cdot \vec{r}_j \rangle. \tag{2.4}$$

If all bond vectors have the same length $l = |\vec{r}_i|$, the scalar product can be represented in terms of the angle $\theta_{ij}$ between bond vectors $\vec{r}_i$ and $\vec{r}_j$ as shown in Fig. 2.3:

$$\vec{r}_i \cdot \vec{r}_j = l^2 \cos \theta_{ij}. \tag{2.5}$$

The mean-square end-to-end distance becomes a double sum of average cosines:

$$\langle R^2 \rangle = \sum_{i=1}^{n} \sum_{j=1}^{n} \langle \vec{r}_i \cdot \vec{r}_j \rangle = l^2 \sum_{i=1}^{n} \sum_{j=1}^{n} \langle \cos \theta_{ij} \rangle. \tag{2.6}$$

One of the simplest models of an ideal polymer is the **freely jointed chain model** with a constant bond length $l = |\vec{r}_i|$ and no correlations between the directions of different bond vectors, $\langle \cos \theta_{ij} \rangle = 0$ for $i \neq j$. There are only $n$ non-zero terms in the double sum ($\cos \theta_{ij} = 1$ for $i = j$). The mean-square end-to-end distance of a freely jointed chain is then quite simple:

$$\langle R^2 \rangle = nl^2. \tag{2.7}$$

In a typical polymer chain, there are correlations between bond vectors (especially between neighbouring ones) and $\langle \cos \theta_{ij} \rangle \neq 0$. But in an ideal chain there is no interaction between monomers separated by a great distance along the chain contour. This implies that there are no correlations between the directions of distant bond vectors.

$$\lim_{|i-j| \to \infty} \langle \cos \theta_{ij} \rangle = 0. \tag{2.8}$$

It can be shown (see Section 2.3.1) that for any bond vector $i$, the sum over all other bond vectors $j$ converges to a finite number, denoted by $C_i'$:

$$C_i' \equiv \sum_{j=1}^{n} \langle \cos \theta_{ij} \rangle. \tag{2.9}$$

Therefore, Eq. (2.6) reduces to

$$\langle R^2 \rangle = l^2 \sum_{i=1}^{n} \sum_{j=1}^{n} \langle \cos \theta_{ij} \rangle = l^2 \sum_{i=1}^{n} C_i' = C_n n l^2, \tag{2.10}$$

where the coefficient $C_n$, called Flory's **characteristic ratio**, is the average value of the constant $C_i'$ over all main-chain bonds of the polymer:

$$C_n = \frac{1}{n} \sum_{i=1}^{n} C_i'. \tag{2.11}$$

The main property of ideal chains is that $\langle R^2 \rangle$ is proportional to the product of the number of bonds $n$ and the square of the bond length $l^2$ [Eq. (2.10)].

An infinite chain has a $C_i'$ value for all $i$ given by $C_\infty$. A real chain has a cutoff in the sum [Eq. (2.9)] at finite $j$ that results in a smaller $C_i'$. This effect is more pronounced near chain ends.

The characteristic ratio is larger than unity ($C_n > 1$) for all polymers. The physical origins of these local correlations between bond vectors are restricted bond angles and steric hindrance. All models of ideal polymers ignore steric hindrance between monomers separated by many bonds and result in characteristic ratios saturating at a finite value $C_\infty$ for large numbers of main-chain bonds ($n \to \infty$) (see Fig. 2.4). Thus, the mean-square end-to-end distance [Eq. (2.10)] can be approximated for long chains:

$$\langle R^2 \rangle \cong C_\infty n l^2. \tag{2.12}$$

The numerical value of Flory's characteristic ratio depends on the local stiffness of the polymer chain with typical numbers of 7–9 for many flexible polymers. The values of the characteristic ratios of some common polymers are listed in Table 2.1. There is a tendency for polymers with bulkier side groups to have higher $C_\infty$, owing to the side groups sterically hindering bond rotation (as in polystyrene), but there are many exceptions to this general tendency (such as polyethylene).

Flexible polymers have many universal properties that are independent of local chemical structure. A simple unified description of all ideal

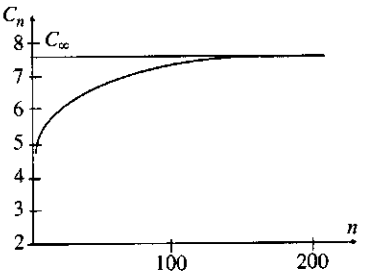


**Fig. 2.4**
Flory's characteristic ratio $C_n$ saturates at $C_\infty$ for long chains.

**Table 2.1** Characteristic ratios, Kuhn lengths, and molar masses of Kuhn monomers for common polymers

| Polymer | Structure | $C_\infty$ | $b$ (Å) | $\rho$ (g cm$^{-3}$) | $M_0$ (g mol$^{-1}$) |
|---|---|---|---|---|---|
| 1,4-Polyisoprene (PI) | –($CH_2CH$=$CHCH(CH_3)$)– | 4.6 | 8.2 | 0.830 | 113 |
| 1,4-Polybutadiene (PB) | –($CH_2CH$=$CHCH_2$)– | 5.3 | 9.6 | 0.826 | 105 |
| Polypropylene (PP) | –($CH_2CH_2(CH_3)$)– | 5.9 | 11 | 0.791 | 180 |
| Poly(ethylene oxide) (PEO) | –($CH_2CH_2O$)– | 6.7 | 11 | 1.064 | 137 |
| Poly(dimethyl siloxane) (PDMS) | –($OSi(CH_3)_2$)– | 6.8 | 13 | 0.895 | 381 |
| Polyethylene (PE) | –($CH_2CH_2$)– | 7.4 | 14 | 0.784 | 150 |
| Poly(methyl methacrylate) (PMMA) | –($CH_2C(CH_3)(COOCH_3)$)– | 9.0 | 17 | 1.13 | 655 |
| Atactic polystyrene (PS) | –($CH_2CHC_6H_5$)– | 9.5 | 18 | 0.969 | 720 |

polymers is provided by an **equivalent freely jointed chain**. The equivalent chain has the same mean-square end-to-end distance $\langle R^2 \rangle$ and the same maximum end-to-end distance $R_{max}$ as the actual polymer, but has $N$ freely-jointed effective bonds of length $b$. This effective bond length $b$ is called the **Kuhn length**. The contour length of this equivalent freely jointed chain is

$$Nb = R_{max}, \tag{2.13}$$

and its mean-square end-to-end distance is

$$\langle R^2 \rangle = Nb^2 = bR_{max} = C_\infty nl^2. \tag{2.14}$$

Therefore, the equivalent freely jointed chain has

$$N = \frac{R_{max}^2}{C_\infty nl^2} \tag{2.15}$$

equivalent bonds (**Kuhn monomers**) of length

$$b = \frac{\langle R^2 \rangle}{R_{max}} = \frac{C_\infty nl^2}{R_{max}}. \tag{2.16}$$

**Example**: Calculate the Kuhn length $b$ of a polyethylene chain with $C_\infty = 7.4$, main-chain bond length $l = 1.54$ Å, and bond angle $\theta = 68°$.

Substituting the maximum end-to-end distance from Eq. (2.1) into Eq. (2.16) determines the Kuhn length:

$$b = \frac{C_\infty l^2 n}{nl\cos(\theta/2)} = \frac{C_\infty l}{\cos(\theta/2)}. \tag{2.17}$$

For polyethylene $b \cong 1.54\,\text{Å} \times 7.4/0.83 \cong 14\,\text{Å}$.

The values of the Kuhn length $b$ and corresponding molar mass of a Kuhn monomer $M_0$ for various polymers are listed in Table 2.1. Throughout this book, we will use the equivalent freely jointed chain to describe all flexible polymers and will call $N$ the 'degree of polymerization' or number of 'monomers' (short for Kuhn monomers) and call $b$ the monomer length (instead of the Kuhn monomer length) and

$$R_0 = \sqrt{\langle R^2 \rangle} = bN^{1/2}, \tag{2.18}$$

the root-mean-square end-to-end distance (the subscript 0 refers to the ideal state). This is not to be confused with the chemical definitions of the degree of polymerization and of monomer size. By renormalizing the monomer, Eq. (2.18) holds for *all* flexible linear polymers in the ideal state with $N \gg 1$, with all chemical-specific characteristics contained within that monomer size (Kuhn length).

## 2.3 Ideal chain models

Below we describe several models of ideal chains. Each model makes different assumptions about the allowed values of torsion and bond angles. However, every model ignores interactions between monomers separated

by large distance along the chain and is therefore a model of an ideal polymer. The chemical structure of polymers determines the populations of torsion and bond angles. Some polymers (like 1,4-polyisoprene) are very flexible chains while others (like double-stranded DNA) are locally very rigid, becoming random walks only on quite large length scales.

### 2.3.1 Freely rotating chain model

As the name suggests, this model ignores differences between the probabilities of different torsion angles and assumes all torsion angles $-\pi < \varphi_i \leq \pi$ to be equally probable. Thus, the **freely rotating chain model** ignores the variations of the potential $U(\varphi_i)$. This model assumes all bond lengths and bond angles are fixed (constant) and all torsion angles are equally likely and independent of each other.

To calculate the mean-square end-to-end distance [Eq. (2.4)]

$$\langle R^2 \rangle = \langle \vec{R}_n \cdot \vec{R}_n \rangle = \sum_{i=1}^{n} \sum_{j=1}^{n} \langle \vec{r}_i \cdot \vec{r}_j \rangle, \tag{2.19}$$

the correlation between bond vectors $\vec{r}_i$ and $\vec{r}_j$ must be determined. This correlation is passed along through the chain of bonds connecting bonds $\vec{r}_i$ and $\vec{r}_j$. For the freely rotating chain, the component of $\vec{r}_j$ normal to vector $\vec{r}_{j-1}$ averages out to zero due to free rotations of the torsion angle $\varphi_j$ (see Fig. 2.5). The only correlation between the bond vectors that is transmitted down the chain is the component of vector $\vec{r}_j$ along the bond vector $\vec{r}_{j-1}$. The value of this component is $l \cos\theta$. Bond vector $\vec{r}_{j-1}$ passes this correlation down to vector $\vec{r}_{j-2}$, but again only the component along $\vec{r}_{j-2}$ survives due to free rotations of torsion angle $\varphi_{j-1}$. The leftover memory of the vector $\vec{r}_j$ at this stage is $l(\cos\theta)^2$. The correlations from bond vector $\vec{r}_j$ at bond vector $\vec{r}_i$ are reduced by the factor $(\cos\theta)^{|j-i|}$ due to independent free rotations of $|j-i|$ torsion angles between these two vectors. Therefore, the correlation between bond vectors $\vec{r}_i$ and $\vec{r}_j$ is

$$\langle \vec{r}_i \cdot \vec{r}_j \rangle = l^2 (\cos\theta)^{|j-i|}. \tag{2.20}$$

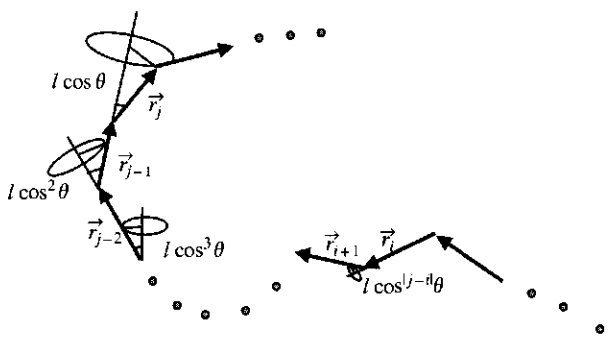


**Fig. 2.5**
All torison angles are equally likely in a freely rotating chain.

The mean-square end-to-end distance of the freely rotating chain can now be written in terms of cosines:

$$\begin{aligned}\langle R^2\rangle &= \sum_{i=1}^{n}\sum_{j=1}^{n}\langle \vec{r}_i\cdot\vec{r}_j\rangle = \sum_{i=1}^{n}\left(\sum_{j=1}^{i-1}\langle \vec{r}_i\cdot\vec{r}_j\rangle + \langle \vec{r}_i^{\,2}\rangle + \sum_{j=i+1}^{n}\langle \vec{r}_i\cdot\vec{r}_j\rangle\right)\\ &= \sum_{i=1}^{n}\langle \vec{r}_i^{\,2}\rangle + l^2\sum_{i=1}^{n}\left(\sum_{j=1}^{i-1}(\cos\theta)^{i-j} + \sum_{j=i+1}^{n}(\cos\theta)^{j-i}\right)\\ &= nl^2 + l^2\sum_{i=1}^{n}\left(\sum_{k=1}^{i-1}\cos^k\theta + \sum_{k=1}^{n-i}\cos^k\theta\right).\end{aligned} \tag{2.21}$$

Note that $(\cos\theta)^{|j-i|}$ decays rapidly as the number of bonds between bond vectors $\vec{r}_i$ and $\vec{r}_j$ is increased.

$$(\cos\theta)^{|j-i|} = \exp[|j-i|\ln(\cos\theta)] = \exp\left[-\frac{|j-i|}{s_p}\right]. \tag{2.22}$$

The final relation defines $s_p$ as the number of main-chain bonds in a persistence segment, which is the scale at which local correlations between bond vectors decay:

$$s_p = -\frac{1}{\ln(\cos\theta)}. \tag{2.23}$$

Since the decay is so rapid, the summation in Eq. (2.21) can be replaced by an infinite series over $k$:

$$\begin{aligned}\sum_{i=1}^{n}\left(\sum_{k=1}^{i-1}\cos^k\theta + \sum_{k=1}^{n-i}\cos^k\theta\right) &\cong 2\sum_{i=1}^{n}\sum_{k=1}^{\infty}\cos^k\theta = 2n\sum_{k=1}^{\infty}\cos^k\theta\\ &= 2n\frac{\cos\theta}{1-\cos\theta}.\end{aligned} \tag{2.24}$$

The mean-square end-to-end distance of the freely rotating chain is a simple function of the number of bonds in the chain backbone $n$, the length of each backbone bond $l$ and the bond angle $\theta$:

$$\langle R^2\rangle = nl^2 + 2nl^2\frac{\cos\theta}{1-\cos\theta} = nl^2\frac{1+\cos\theta}{1-\cos\theta}. \tag{2.25}$$

Polymers with carbon single bonds making up their backbone have a bond angle of $\theta = 68°$.

$$C_\infty = \frac{1+\cos\theta}{1-\cos\theta} \cong 2 \quad \text{and} \quad s_p \cong 1. \tag{2.26}$$

Polymer chains are never as flexible as the freely rotating chain model predicts, since the most flexible polymers with $\theta = 68°$ have $C_\infty > 4$

(see Table 2.1). This is because there is steric hindrance to bond rotation in all polymers.

### 2.3.2 Worm-like chain model

The **worm-like chain model** (sometimes called the Kratky–Porod model) is a special case of the freely rotating chain model for very small values of the bond angle. This is a good model for very stiff polymers, such as double-stranded DNA for which the flexibility is due to fluctuations of the contour of the chain from a straight line rather than to *trans–gauche* bond rotations. For small values of the bond angle ($\theta \ll 1$), the $\cos\theta$ in Eq. (2.23) can be expanded about its value of unity at $\theta = 0$:

$$\cos\theta \cong 1 - \frac{\theta^2}{2}. \tag{2.27}$$

For small $x$, $\ln(1-x) \cong -x$.

$$\ln(\cos\theta) \cong -\frac{\theta^2}{2}. \tag{2.28}$$

Since $\theta$ is small, the persistence segment of the chain [Eq. (2.23)] contains a large number of main-chain bonds.

$$s_p = -\frac{1}{\ln(\cos\theta)} \cong \frac{2}{\theta^2}. \tag{2.29}$$

The **persistence length** is the length of this persistence segment:

$$l_p \equiv s_p l = l\frac{2}{\theta^2}. \tag{2.30}$$

The Flory characteristic ratio of the worm-like chain is very large:

$$C_\infty = \frac{1+\cos\theta}{1-\cos\theta} \cong \frac{2-(\theta^2/2)}{(\theta^2/2)} \cong \frac{4}{\theta^2}. \tag{2.31}$$

The corresponding Kuhn length [see Eq. (2.16)] is twice the persistence length:

$$b = l\frac{C_\infty}{\cos(\theta/2)} \cong l\frac{4}{\theta^2} = 2l_p. \tag{2.32}$$

For example, the persistence length of a double-helical DNA $l_p \approx 50\,\text{nm}$ and the Kuhn length is $b \approx 100\,\text{nm}$.

The combination of parameters $l/\theta^2$ enters in the expressions of the persistence length $l_p$ and the Kuhn length $b$. The worm-like chain is defined as the limit $l \to 0$ and $\theta \to 0$ at constant persistence length $l_p$ (constant $l/\theta^2$) and constant chain contour length $R_{max} = nl\cos(\theta/2) \cong nl$.

The mean-square end-to-end distance of the worm-like chain can be evaluated using the exponential decay of correlations between tangent vectors along the chain [Eq. (2.22)]:

$$\langle R^2\rangle = l^2\sum_{i=1}^{n}\sum_{j=1}^{n}\langle\cos\theta_{ij}\rangle = l^2\sum_{i=1}^{n}\sum_{j=1}^{n}(\cos\theta)^{|j-i|}$$
$$= l^2\sum_{i=1}^{n}\sum_{j=1}^{n}\exp\left(-\frac{|j-i|}{l_p}l\right). \tag{2.33}$$

The summation over bonds can be changed into integration over the contour of the worm-like chain:

$$l\sum_{i=1}^{n}\to\int_0^{R_{max}}\mathrm{d}u \quad\text{and}\quad l\sum_{j=1}^{n}\to\int_0^{R_{max}}\mathrm{dv}. \tag{2.34}$$

$$\begin{aligned}\langle R^2\rangle &= \int_0^{R_{max}}\left[\int_0^{R_{max}}\exp\left(-\frac{|u-v|}{l_p}\right)\mathrm{dv}\right]\mathrm{d}u\\ &= \int_0^{R_{max}}\left[\left(\exp\left(-\frac{u}{l_p}\right)\int_0^{u}\exp\left(\frac{v}{l_p}\right)\mathrm{dv}\right.\right.\\ &\qquad\left.\left.+\exp\left(\frac{u}{l_p}\right)\int_u^{R_{max}}\exp\left(-\frac{v}{l_p}\right)\mathrm{dv}\right)\right]\mathrm{d}u\\ &= l_p\int_0^{R_{max}}\left[\exp\left(-\frac{u}{l_p}\right)\left(\exp\left(\frac{u}{l_p}\right)-1\right)\right.\\ &\qquad\left.+\exp\left(\frac{u}{l_p}\right)\left(-\exp\left(-\frac{R_{max}}{l_p}\right)+\exp\left(-\frac{u}{l_p}\right)\right)\right]\mathrm{d}u\\ &= l_p\int_0^{R_{max}}\left[2-\exp\left(-\frac{u}{l_p}\right)-\exp\left(-\frac{R_{max}}{l_p}\right)\exp\left(\frac{u}{l_p}\right)\right]\mathrm{d}u\\ &= l_p\left[2R_{max}+l_p\left(\exp\left(-\frac{R_{max}}{l_p}\right)-1\right)\right.\\ &\qquad\left.-l_p\exp\left(-\frac{R_{max}}{l_p}\right)\left(\exp\left(\frac{R_{max}}{l_p}\right)-1\right)\right]\\ &= 2l_pR_{max}-2l_p^2\left(1-\exp\left(-\frac{R_{max}}{l_p}\right)\right).\end{aligned} \tag{2.35}$$

There are two simple limits of this expression. The ideal chain limit is for worm-like chains much longer than their persistence length.

$$\langle R^2\rangle \cong 2l_pR_{max} = bR_{max} \quad \text{for } R_{max}\gg l_p. \tag{2.36}$$

The rod-like limit is for worm-like chains much shorter than their persistence length. The exponential in Eq. (2.35) can be expanded in this limit:

$$\exp\left(-\frac{R_{max}}{l_p}\right)\cong 1-\frac{R_{max}}{l_p}+\frac{1}{2}\left(\frac{R_{max}}{l_p}\right)^2+\cdots \quad \text{for } R_{max}\ll l_p, \tag{2.37}$$

$$\langle R^2 \rangle \cong R_{\max}^2 \quad \text{for } R_{\max} \ll l_p. \tag{2.38}$$

The mean-square end-to-end distance of the worm-like chain [Eq. (2.35)] is a smooth crossover between these two simple limits.

The important difference between freely jointed chains and worm-like chains is that each bond of Kuhn length $b$ of the freely jointed chain is assumed to be completely rigid. Worm-like chains are also stiff on length scales shorter than the Kuhn length, but are not completely rigid and can fluctuate and bend. These bending modes lead to a qualitatively different dependence of extensional force on elongation near maximum extension, as will be discussed in Section 2.6.2.

### 2.3.3 Hindered rotation model

The **hindered rotation model** also assumes bond lengths and bond angles are constant and torsion angles are independent of each other. As its name suggests, the torsion angle rotation is taken to be hindered by a potential $U(\varphi_i)$ [see Fig. 2.1(d)]. The probability of any value of the torsion angle $\varphi_i$ is taken to be proportional to the **Boltzmann factor** $\exp[-U(\varphi_i)/kT]$. Most of the torsion angles are in low energy states [near the minima in Fig. 2.1(d)] but for ordinary temperatures there are some torsion angles corresponding to high energy states as well. The Boltzmann factor ensures that states with higher energy are progressively less likely to be populated.

The hindered rotation model assumes independent but hindered rotations of torsion angles at constant bond lengths and bond angles with different potential profiles $U(\varphi_i)$ corresponding to different polymers. The hindered rotation model predicts the mean-square end-to-end distance

$$\langle R^2 \rangle = C_\infty l^2 n, \tag{2.39}$$

with the characteristic ratio (see problem 2.9)

$$C_\infty = \left(\frac{1+\cos\theta}{1-\cos\theta}\right)\left(\frac{1+\langle\cos\varphi\rangle}{1-\langle\cos\varphi\rangle}\right), \tag{2.40}$$

where $\langle\cos\varphi\rangle$ is the average value of the cosine of the torsion angle with probabilities determined by Boltzmann factors, $\exp[-U(\varphi_i)/kT]$:

$$\langle\cos\varphi\rangle = \frac{\int_0^{2\pi} \cos\varphi \exp(-U(\varphi)/kT)\,d\varphi}{\int_0^{2\pi} \exp(-U(\varphi)/kT)\,d\varphi}. \tag{2.41}$$

### 2.3.4 Rotational isomeric state model

This is the most successful ideal chain model used to calculate the details of conformations of different polymers. In this model, bond lengths $l$ and bond angles $\theta$ are fixed (constant).

For a relatively high barrier between *trans* and *gauche* states $\Delta E \gg kT$ the values of the torsion angles $\varphi_i$ are close to the minima $(t, g_+, g_-)$ [see Fig. 2.1(d)]. In the **rotational isomeric state model** each molecule is assumed to exist only in discrete torsional states corresponding to the potential

energy minima. The fluctuations about these minima are ignored. A conformation of a chain with $n$ main-chain bonds is thus represented by a sequence of $n-2$ torsion angles:

$$\cdots t g_- t t g_+ t g_+ t t g_- t \cdots. \tag{2.42}$$

Each of these $n-2$ torsion angles can be in one of three states $(t, g_+, g_-)$ and therefore the whole chain has $3^{n-2}$ rotational isomeric states. For example, $n$-pentane, with $n=4$ main-chain bonds and $n-2=2$ torsion angles, has $3^2=9$ rotational isomeric states:[1]

$$tt,\ tg_+,\ tg_-,\ g_+t,\ g_-t,\ g_+g_+,\ g_+g_-,\ g_-g_+,\ g_-g_-. \tag{2.43}$$

In the rotational isomeric state model, these states are *not* equally probable. Correlations between neighbouring torsional states are included in the model. For example, a consecutive sequence of $g_+$ and $g_-$ has high energy due to overlap between atoms and therefore is taken to have very low probability in the rotational isomeric state model. The relative probabilities of the states of neighboring torsional angles are used to calculate the mean-square end-to-end distance and $C_\infty$ [Eq. (2.12)].

Table 2.2 summarizes the assumptions of the ideal chain models. The worm-like chain model is a special case of the freely rotating chain with a small value of the bond angle $\theta$. Moving from left to right in Table 2.2, the models become progressively more specific (and more realistic). As more constraints are adopted, the chain becomes stiffer, reflected in larger $C_\infty$.

**Table 2.2** Assumptions and predictions of ideal chain models: FJC, freely jointed chain; FRC, freely rotating chain; HR, hindered rotation; RIS, rotational isomeric state

| Models | FJC | FRC | HR | RIS |
|---|---|---|---|---|
| Bond length $l$ | Fixed | Fixed | Fixed | Fixed |
| Bond angle $\theta$ | Free | Fixed | Fixed | Fixed |
| Torsion angle $\varphi$ | Free | Free | Controlled by $U(\varphi)$ | $t, g+, g-$ |
| Next $\varphi$ independent? | Yes | Yes | Yes | No |
| $C_\infty$ | 1 | $\frac{1+\cos\theta}{1-\cos\theta}$ | $\left(\frac{1+\cos\theta}{1-\cos\theta}\right)\left(\frac{1+\langle\cos\theta\rangle}{1-\langle\cos\varphi\rangle}\right)$ | Specific |

## 2.4 Radius of gyration

The size of linear chains can be characterized by their mean-square end-to-end distance. However, for branched or ring polymers this quantity is not well defined, because they either have too many ends or no ends at all. Since all objects possess a radius of gyration, it can characterize the size of polymers of any architecture. Consider, for example, the branched polymer sketched in Fig. 2.6. The square **radius of gyration** is defined as the average square distance between monomers in a given conformation (position vector $\vec{R}_i$) and the polymer's centre of mass (position vector $\vec{R}_{cm}$):

$$R_g^2 \equiv \frac{1}{N}\sum_{i=1}^{N}(\vec{R}_i - \vec{R}_{cm})^2. \tag{2.44}$$

[1] Six of the nine rotational isomers are distinguishable.

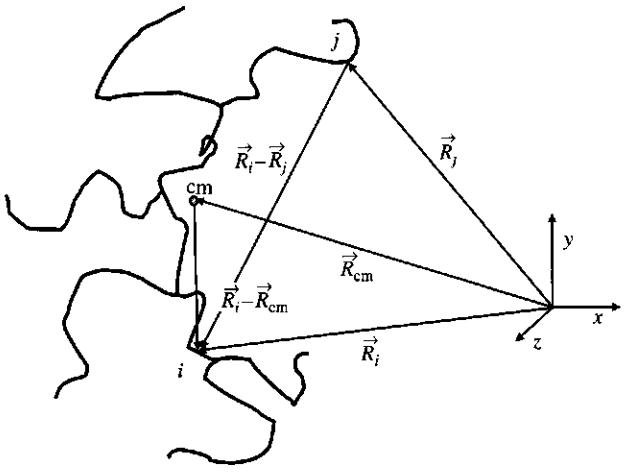


**Fig. 2.6**
One conformation of a randomly branched polymer and its centre of mass, denoted by cm.

The position vector of the centre of mass of the polymer is the number-average of all monomer position vectors:[2]

$$\vec{R}_{cm} \equiv \frac{1}{N}\sum_{j=1}^{N} \vec{R}_j. \tag{2.45}$$

Substituting the definition of the position vector of the centre of mass [Eq. (2.45)] into Eq. (2.44) gives an expression for the square radius of gyration as a double sum of squares over all inter-monomer distances:

$$\begin{aligned} R_g^2 &= \frac{1}{N}\sum_{i=1}^{N}(\vec{R}_i^2 - 2\vec{R}_i\vec{R}_{cm} + \vec{R}_{cm}^2) \\ &= \frac{1}{N}\sum_{i=1}^{N}\left[\vec{R}_i^2\frac{1}{N}\sum_{j=1}^{N}1 - 2\vec{R}_i\frac{1}{N}\sum_{j=1}^{N}\vec{R}_j + \left(\frac{1}{N}\sum_{j=1}^{N}\vec{R}_j\right)^2\right]. \end{aligned} \tag{2.46}$$

The last term in the sum can be rewritten as

$$\begin{aligned} \frac{1}{N}\sum_{i=1}^{N}\left(\frac{1}{N}\sum_{j=1}^{N}\vec{R}_j\right)^2 &= \left(\frac{1}{N}\sum_{j=1}^{N}\vec{R}_j\right)^2 = \left(\frac{1}{N}\sum_{i=1}^{N}\vec{R}_i\right)\left(\frac{1}{N}\sum_{j=1}^{N}\vec{R}_j\right) \\ &= \frac{1}{N^2}\sum_{i=1}^{N}\sum_{j=1}^{N}\vec{R}_i\vec{R}_j. \end{aligned}$$

Therefore, the expression for the square radius of gyration takes the form

$$R_g^2 = \frac{1}{N^2}\sum_{i=1}^{N}\sum_{j=1}^{N}(\vec{R}_i^2 - 2\vec{R}_i\vec{R}_j + \vec{R}_i\vec{R}_j) = \frac{1}{N^2}\sum_{i=1}^{N}\sum_{j=1}^{N}(\vec{R}_i^2 - \vec{R}_i\vec{R}_j).$$

[2] In general, the mass of the monomers $M_j$ should be included in the definitions of the radius of gyration and of the centre of mass. For example, the proper centre of mass definition is

$$\vec{R}_{cm} \equiv \frac{\sum_{j=1}^{N} M_j\vec{R}_j}{\sum_{j=1}^{N} M_j}.$$

We assume that all the monomers have the same mass $M_j = M_0$ for all $j$.

This expression does not depend on the choice of summation indices and can be rewritten in a symmetric form:

$$\begin{aligned} R_g^2 &= \frac{1}{N^2}\sum_{i=1}^{N}\sum_{j=1}^{N}(\vec{R}_i^2 - \vec{R}_i\vec{R}_j) \\ &= \frac{1}{2}\left[\frac{1}{N^2}\sum_{i=1}^{N}\sum_{j=1}^{N}(\vec{R}_i^2 - \vec{R}_i\vec{R}_j) + \frac{1}{N^2}\sum_{j=1}^{N}\sum_{i=1}^{N}(\vec{R}_j^2 - \vec{R}_j\vec{R}_i)\right] \\ &= \frac{1}{2N^2}\sum_{i=1}^{N}\sum_{j=1}^{N}(\vec{R}_i^2 - 2\vec{R}_i\vec{R}_j + \vec{R}_j^2) \\ &= \frac{1}{2N^2}\sum_{i=1}^{N}\sum_{j=1}^{N}(\vec{R}_i - \vec{R}_j)^2. \end{aligned} \tag{2.47}$$

Each pair of monomers enters twice in the double sum of Eq. (2.47). Alternatively, this expression for the square radius of gyration can be written with each pair of monomers entering only once in the double sum:

$$R_g^2 = \frac{1}{N^2}\sum_{i=1}^{N}\sum_{j=i}^{N}(\vec{R}_i - \vec{R}_j)^2. \tag{2.48}$$

For polymers and other fluctuating objects, the square radius of gyration is usually averaged over the ensemble of allowed conformations giving the mean-square radius of gyration:

$$\langle R_g^2\rangle = \frac{1}{N}\sum_{i=1}^{N}\langle(\vec{R}_i - \vec{R}_{cm})^2\rangle = \frac{1}{N^2}\sum_{i=1}^{N}\sum_{j=i}^{N}\langle(\vec{R}_i - \vec{R}_j)^2\rangle. \tag{2.49}$$

For non-fluctuating (solid) objects such averaging is unnecessary. The expression with the centre of mass is useful only if the position of the centre of mass $\vec{R}_{cm}$ of the object is known or is easy to evaluate. Otherwise the expression for the radius of gyration in terms of the average square distances between all pairs of monomers is used.

### 2.4.1 Radius of gyration of an ideal linear chain

To illustrate the use of Eq. (2.48), we now calculate the mean-square radius of gyration for an ideal linear chain. For the linear chain, the summations over the monomers can be changed into integrations over the contour of the chain, by replacing monomer indices $i$ and $j$ with continuous coordinates $u$ and v along the contour of the chain:

$$\sum_{i=1}^{N} \to \int_0^N \mathrm{d}u \quad \text{and} \quad \sum_{j=i}^{N} \to \int_u^N \mathrm{dv}. \tag{2.50}$$

This transformation results in the integral form for the mean-square radius of gyration

$$\langle R_g^2 \rangle = \frac{1}{N^2} \int_0^N \int_u^N \langle (\vec{R}(u) - \vec{R}(v))^2 \rangle \, dv \, du, \tag{2.51}$$

where $\vec{R}(u)$ is the position vector corresponding to the contour coordinate $u$. The mean-square distance between points $u$ and v along the contour of the chain can be obtained by treating each section of $v - u$ monomers as a shorter ideal chain. The outer sections of $u$ and of $N - v$ monomers do not affect the conformations of this inner section. The mean-square end-to-end distance for an ideal chain of $v - u$ monomers is given by Eq. (2.18):

$$\langle (\vec{R}(u) - \vec{R}(v))^2 \rangle = (v - u) b^2. \tag{2.52}$$

The mean-square radius of gyration is then calculated by a simple integration using the change of variables $v' \equiv v - u$ and $u' \equiv N - u$:

$$\begin{aligned} \langle R_g^2 \rangle &= \frac{b^2}{N^2} \int_0^N \int_u^N (v - u) \, dv \, du = \frac{b^2}{N^2} \int_0^N \int_0^{N-u} v' \, dv' \, du \\ &= \frac{b^2}{N^2} \int_0^N \frac{(N-u)^2}{2} du = \frac{b^2}{2N^2} \int_0^N (u')^2 \, du' = \frac{b^2}{2N^2} \frac{N^3}{3} = \frac{Nb^2}{6} \end{aligned} \tag{2.53}$$

Comparing this result with Eq. (2.18), we obtain the classic Debye result relating the mean-square radius of gyration and the mean-square end-to-end distance of an ideal linear chain:

$$\langle R_g^2 \rangle = \frac{b^2 N}{6} = \frac{\langle R^2 \rangle}{6}. \tag{2.54}$$

The radius of gyration of other shapes of flexible ideal chains can be calculated in a similar way and examples of the results are given in Table 2.3.

**Table 2.3** Mean-square radii of gyration of ideal polymers with $N$ Kuhn monomers of length $b$: linear chain, ring, $f$-arm star with each arm containing $N/f$ Kuhn monomers, and H-polymer with all linear sections containing $N/5$ Kuhn monomers

| Ideal chains | Linear | Ring | $f$-arm star | H-polymer |
|---|---|---|---|---|
| $\langle R_g^2 \rangle$ | $Nb^2/6$ | $Nb^2/12$ | $[(N/f)b^2/6]\,(3 - 2/f)$ | $(Nb^2/6)\ 89/625$ |

## 2.4.2 Radius of gyration of a rod polymer

Consider a rod polymer of $N$ monomers of length $b$, with end-to-end distance $L = Nb$. It is convenient to calculate the radius of gyration of a rod polymer using the original definition, Eq. (2.44), written in integral form:

$$R_g^2 \equiv \frac{1}{N} \int_0^N \left[ (\vec{R}(u) - \vec{R}_{cm})^2 \right] du. \tag{2.55}$$

A rigid rod polymer has only one conformation with the distance between coordinate $u$ along the chain and its centre of mass (coordinate $N/2$):

$$|\vec{R}(u) - \vec{R}_{cm}| = \left|u - \frac{N}{2}\right| b. \tag{2.56}$$

Therefore, no averaging is needed for calculation of the radius of gyration of a rod. The square radius of gyration of the rod polymer is calculated by a simple integration

$$R_g^2 \equiv \frac{b^2}{N}\int_0^N \left(u - \frac{N}{2}\right)^2 du = \frac{b^2}{N}\int_{-N/2}^{N/2} x^2\, dx = \frac{N^2 b^2}{12}, \tag{2.57}$$

where the change of variables $x = u - N/2$ has been used. Note that the relation between the end-to-end distance and the radius of gyration for a rod polymer is different from that for an ideal linear chain [Eq. (2.54)]:

$$R_g^2 = \frac{N^2 b^2}{12} = \frac{L^2}{12}. \tag{2.58}$$

Examples of the radii of gyration of other rigid objects are listed in Table 2.4.

**Table 2.4** Square radii of gyration of rigid objects: uniform thin disc of radius $R$, uniform sphere of radius $R$, thin rod of length $L$, and uniform right cylinder of radius $R$ and length $L$

| Rigid objects | Disk | Sphere | Rod | Cylinder |
|---|---|---|---|---|
| $R_g^2$ | $R^2/2$ | $3R^2/5$ | $L^2/12$ | $(R^2/2)+(L^2/12)$ |

### 2.4.3 Radius of gyration of an ideal branched polymer (Kramers theorem)

Consider an ideal molecule that contains an arbitrary number of branches, but no loops. This molecule consists of $N$ freely jointed segments (Kuhn monomers) of length $b$. The mean-square radius of gyration of this molecule is calculated using Eq. (2.48):

$$\langle R_g^2 \rangle = \frac{1}{N^2}\sum_{i=1}^{N}\sum_{j=i}^{N}\langle(\vec{R}_j - \vec{R}_i)^2\rangle. \tag{2.59}$$

The vector $\vec{R}_j - \vec{R}_i$ between monomers $i$ and $j$ can be represented by the sum over the bond vectors $\vec{r}_k$ of a linear strand connecting these two monomers:

$$\vec{R}_j - \vec{R}_i = \sum_{k=i+1}^{j} \vec{r}_k. \tag{2.60}$$

Since we have assumed freely jointed chain statistics with no correlations between different segments,

$$\langle \vec{r}_k \vec{r}_{k'} \rangle = 0 \quad \text{if } k \neq k', \tag{2.61}$$

the mean-square distance between monomers $i$ and $j$ can be rewritten:

$$\langle(\vec{R}_j - \vec{R}_i)^2\rangle = \sum_{k=i+1}^{j}\sum_{k'=i+1}^{j}\langle\vec{r}_k\vec{r}_{k'}\rangle = \sum_{k=i+1}^{j}(\vec{r}_k)^2. \tag{2.62}$$

Each segment of a linear strand connecting monomers $i$ and $j$ contributes $(\vec{r}_k)^2 = b^2$ to the double sum in Eq. (2.59). There is only one such strand connecting each pair of monomers because the molecule is assumed to have no loops. Therefore, the contribution of each segment of the molecule to the double sum in Eq. (2.59) is equal to $b^2$ times the number of strands between different monomers $i$ and $j$ that pass through this segment. Consider, for example, segment $k$ in Fig. 2.7. It divides the molecule into two tree-like parts. The lower part contains $N_1$ monomers and the upper part contains $N - N_1$ monomers. Monomer $i$ could be any one of $N - N_1$ monomers of the upper part, while monomer $j$ could be any one of $N_1$ monomers of the lower part of the molecule. Therefore, there are $N_1(N - N_1)$ different strands between all pairs of monomers $i$ and $j$ passing through segment $k$. Thus, the segment $k$ contributes $N_1(k)[N - N_1(k)]b^2$ to the double sum in Eq. (2.59).

The radius of gyration can be expressed as the sum over all $N$ molecular bonds, of the product of the number of monomers of the two branches $N_1(k)$ and $N - N_1(k)$ that each bond $k$ divides the molecule into:

$$\langle R_g^2\rangle = \frac{b^2}{N^2}\sum_{k=1}^{N} N_1(k)[N - N_1(k)]. \tag{2.63}$$

The average value of this product is:

$$\langle N_1(N - N_1)\rangle = \frac{1}{N}\sum_{k=1}^{N} N_1(k)[N - N_1(k)]. \tag{2.64}$$

The **Kramers theorem** is expressed in terms of this average over all possible ways of dividing the molecule into two parts:

$$\langle R_g^2\rangle = \frac{b^2}{N}\langle N_1(N - N_1)\rangle. \tag{2.65}$$

This expression is valid for a linear polymer with the average evaluated by integration.

$$\begin{aligned}\langle N_1(N - N_1)\rangle &= \frac{1}{N}\int_0^N N_1(N - N_1)\,\mathrm{d}N_1 \\ &= \int_0^N N_1\,\mathrm{d}N_1 - \frac{1}{N}\int_0^N N_1^2\,\mathrm{d}N_1 \\ &= \frac{N^2}{2} - \frac{N^2}{3} = \frac{N^2}{6}.\end{aligned} \tag{2.66}$$

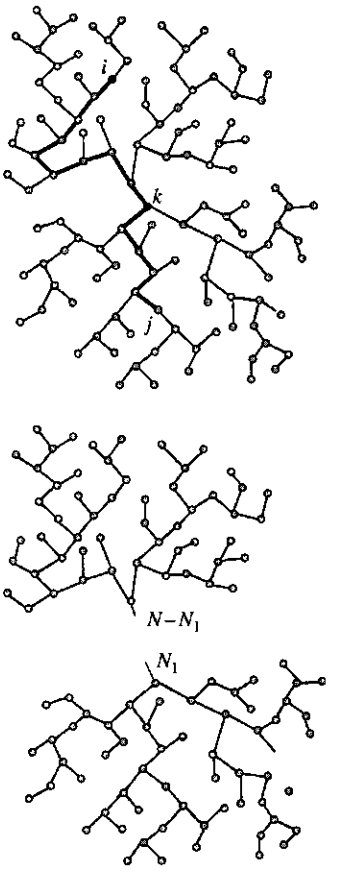


**Fig. 2.7**
The Kramers theorem effectively cuts a randomly branched polymer with $N$ monomers into two parts, with $N_1$ and $N - N_1$ monomers.

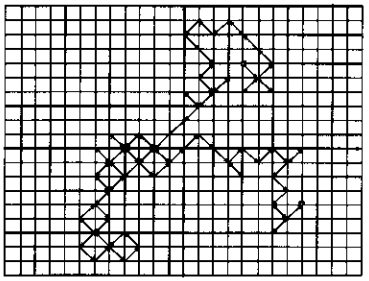

**Fig. 2.8**
A two-dimensional random walk on a square lattice. The direction of each step is randomly chosen from four possible diagonals.

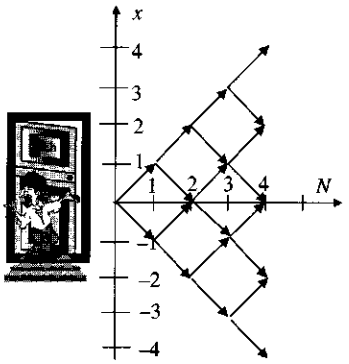


**Fig. 2.9**
A one-dimensional random walk of a drunk in an alley, showing all possible trajectories up to $N = 4$ steps.

**Table 2.5** The number of trajectories $W(N, x)$ for one-dimensional random walks of $N$ steps that start at the origin and end at position $x$

| | $N=1$ | $N=2$ | $N=3$ | $N=4$ |
|---|---|---|---|---|
| $x=-4$ | 0 | 0 | 0 | 1 |
| $x=-3$ | 0 | 0 | 1 | 0 |
| $x=-2$ | 0 | 1 | 0 | 4 |
| $x=-1$ | 1 | 0 | 3 | 0 |
| $x=0$ | 0 | 2 | 0 | 6 |
| $x=1$ | 1 | 0 | 3 | 0 |
| $x=2$ | 0 | 1 | 0 | 4 |
| $x=3$ | 0 | 0 | 1 | 0 |
| $x=4$ | 0 | 0 | 0 | 1 |

Substituting this average [Eq. (2.66)] into the Kramers theorem [Eq. (2.65)] recovers the classical result for the radius of gyration of an ideal linear chain [Eq. (2.54)]. In Section 6.4.6, we apply the Kramers theorem [Eq. (2.65)] to ideal randomly branched polymers. In this case the average is not only over different ways of dividing a molecule into two parts, but also over different branched molecules with the same degree of polymerization $N$.

## 2.5 Distribution of end-to-end vectors

A polydisperse collection of polymers can be described by an average molar mass (such as the number-average or weight-average discussed in Chapter 1). Much more information is contained in the whole molar mass distribution than in any of its moments or averages. Similarly, the average polymer conformation can be described by the mean-square end-to-end distance (or mean-square radius of gyration). Much more information is contained in the distribution of end-to-end vectors than in the mean-square end-to-end vector. In this section, we derive the distribution of end-to-end vectors for an ideal chain.

Every possible conformation of an ideal chain can be mapped onto a **random walk**. A particle making random steps defines a random walk. If the length of each step is constant and the direction of each step is independent of all previous steps, the trajectory of this random walk is one conformation of a freely jointed chain. Hence, random walk statistics and ideal chain statistics are similar.

Consider a particular random walk on a lattice with each step having independent Cartesian coordinates of either $+1$ or $-1$. The projection of this three-dimensional random walk onto each of the Cartesian coordinate axes is an independent one-dimensional random walk of unit step length (see Fig. 2.8 for an example of a two-dimensional projection). The fact that the one-dimensional components are independent of each other is an important property of any random walk (as well as any ideal polymer chain).

An example of a one-dimensional random walk is a drunk in a dark narrow alley. Let the drunk start at the doors of the pub at the origin of the one-dimensional coordinate system and make unit steps randomly up and down the alley. Figure 2.9 represents random wandering of the drunk up and down the alley as a function of the number of steps taken. Let $W(N, x)$ be the number of different possible trajectories for a drunk to get from the pub to the position $x$ in $N$ steps. For example, after the first step he could have reached either position $x = +1$ or $x = -1$, making $W(1, 1) = W(1, -1) = 1$. The numbers of different trajectories $W(N, x)$ for the first four steps of the drunk are shown in Table 2.5.

A general expression for $W(N, x)$ can be obtained in the following way. Any trajectory of our drunk consists of $N_+$ steps up the alley and $N_-$ steps down the alley. The total number of steps made by the drunk is $N = N_+ + N_-$ and his final position is $x = N_+ - N_-$. The numbers of steps up $N_+$ and down $N_-$ the alley uniquely specify both the total number of steps $N$ and the final position $x$. Therefore, the total number of trajectories $W(N, x)$ is

equal to the number of combinations of $N_+$ steps up and $N_-$ steps down, that reach $x$ in a total of $N$ steps, which is a binomial coefficient:

$$W(N,x) = \frac{(N_+ + N_-)!}{N_+!N_-!} = \frac{N!}{[(N+x)/2]![(N-x)/2]!}. \tag{2.67}$$

The factorial is defined as $N! = 1 \cdot 2 \cdot 3 \cdot 4 \cdots N$.

The total number of $N$-step walks is $2^N$ because on each step the drunk has two possibilities, which are independent from step to step. All of these $2^N$ walks are equally likely (if there is no wind or stairway in the alley) and therefore, the probability to find the drunk at position $x$ after $N$ steps is $W(N,x)$ divided by $2^N$:

$$\frac{W(N,x)}{2^N} = \frac{1}{2^N}\frac{N!}{[(N+x)/2]![(N-x)/2]!}. \tag{2.68}$$

This is an exact probability distribution for a one-dimensional random walk. However, it is not convenient to use for large $N$ because of the difficulty of calculating factorials for large $N$ (try your calculator for $N = 100$). For any $N$, the probability of finding the drunk is highest at the pub (at $x = 0$ for even $N$ and at $x = \pm 1$ for odd $N$). This probability falls off very fast for large $|x|$ and it is therefore convenient to use the Gaussian approximation of the distribution function, valid for $x \ll N$, derived next.

First, take the natural logarithm of the distribution function:

$$\ln\left(\frac{W(N,x)}{2^N}\right) = -N \ln 2 + \ln(N!) - \ln\left(\frac{N+x}{2}\right)! - \ln\left(\frac{N-x}{2}\right)!. \tag{2.69}$$

Each of the last two terms can be rewritten using the definition of the factorial function:

$$\begin{aligned}\ln\left(\frac{N+x}{2}\right)! &= \ln\left[\left(\frac{N}{2}\right)!\left(\frac{N}{2}+1\right)\left(\frac{N}{2}+2\right)\cdots\left(\frac{N}{2}+\frac{x}{2}\right)\right] \\ &= \ln\left(\frac{N}{2}\right)! + \sum_{s=1}^{x/2} \ln\left(\frac{N}{2}+s\right),\end{aligned} \tag{2.70}$$

$$\ln\left(\frac{N-x}{2}\right)! = \ln\left(\frac{N}{2}\right)! - \sum_{s=1}^{x/2} \ln\left(\frac{N}{2}+1-s\right). \tag{2.71}$$

The logarithm of the probability distribution can now be rewritten as

$$\begin{aligned}\ln\left(\frac{W(N,x)}{2^N}\right) &= -N \ln 2 + \ln(N!) - \ln\left(\frac{N}{2}\right)! - \sum_{s=1}^{x/2} \ln\left(\frac{N}{2}+s\right) \\ &\quad - \ln\left(\frac{N}{2}\right)! + \sum_{s=1}^{x/2} \ln\left(\frac{N}{2}+1-s\right) \\ &= -N \ln 2 + \ln(N!) - 2\ln\left(\frac{N}{2}\right)! - \sum_{s=1}^{x/2} \ln\left(\frac{(N/2)+s}{(N/2)+1-s}\right).\end{aligned}$$

The logarithm in the last term can be expanded for $s \ll N/2$ up to a linear term ($\ln(1+y) \cong y$ for $|y| \ll 1$). This expansion is the essence of the Gaussian approximation.

$$\ln\left(\frac{(N/2)+s}{(N/2)+1-s}\right) = \ln\left(\frac{1+(2s/N)}{1-(2s/N)+(2/N)}\right)$$
$$= \ln\left(1+\frac{2s}{N}\right) - \ln\left(1-\frac{2s}{N}+\frac{2}{N}\right)$$
$$\cong \frac{4s}{N} - \frac{2}{N}. \tag{2.72}$$

The logarithm of the probability distribution can be simplified using this approximation.

$$\ln\left(\frac{W(N,x)}{2^N}\right) \cong -N\ln 2 + \ln(N!) - 2\ln\left(\frac{N}{2}\right)! - \sum_{s=1}^{x/2}\left(\frac{4s}{N} - \frac{2}{N}\right)$$
$$\cong -N\ln 2 + \ln(N!) - 2\ln\left(\frac{N}{2}\right)! - \frac{4}{N}\sum_{s=1}^{x/2} s + \frac{2}{N}\sum_{s=1}^{x/2} 1$$
$$\cong -N\ln 2 + \ln(N!) - 2\ln\left(\frac{N}{2}\right)! - \frac{4}{N}\frac{(x/2)(x/2+1)}{2} + \frac{x}{N}$$
$$\cong -N\ln 2 + \ln(N!) - 2\ln\left(\frac{N}{2}\right)! - \frac{x^2}{2N}. \tag{2.73}$$

This gives the Gaussian approximation of the probability distribution:

$$\frac{W(N,x)}{2^N} \cong \frac{1}{2^N}\frac{N!}{(N/2)!(N/2)!}\exp\left(-\frac{x^2}{2N}\right). \tag{2.74}$$

Using Stirling's approximation of $N!$ for large $N$

$$N! \cong \sqrt{2\pi N}\left(\frac{N}{\mathrm{e}}\right)^N, \tag{2.75}$$

the coefficient in front of the exponential can be rewritten:

$$\frac{1}{2^N}\frac{N!}{(N/2)!(N/2)!} \cong \frac{1}{2^N}\frac{\sqrt{2\pi N}N^N\exp(-N)}{\left(\sqrt{\pi N}(N/2)^{N/2}\exp(-N/2)\right)^2} = \sqrt{\frac{2}{\pi N}} \tag{2.76}$$

The final expression for the Gaussian approximation of the probability distribution is quite simple:

$$\frac{W(N,x)}{2^N} \cong \sqrt{\frac{2}{\pi N}}\exp\left(-\frac{x^2}{2N}\right). \tag{2.77}$$

Recall from Table 2.5 that $W(N,x)$ is non-zero only either for even or odd $x$ (depending on whether $N$ is even or odd). Therefore, the spacing between non-zero values of $W(N,x)$ is equal to 2 along the $x$ axis. The probability

distribution function $P_{1d}(N,x)$ is defined as the probability $P(N,x)\,dx$ that the drunk will be found in the interval $dx$ along the $x$ axis. Thus, the probability distribution function differs from Eq. (2.77) by a factor of 2:

$$P_{1d}(N,x) = \frac{1}{\sqrt{2\pi N}}\exp\left(-\frac{x^2}{2N}\right). \tag{2.78}$$

The square of the typical distance of the drunk from the pub after $N$ steps is determined from the mean-square displacement averaged over all the walks the drunk makes day after day:

$$\langle x^2\rangle = \int_{-\infty}^{\infty} x^2 P_{1d}(N,x)\,dx = \frac{1}{\sqrt{2\pi N}}\int_{-\infty}^{\infty} x^2 \exp\left(-\frac{x^2}{2N}\right)dx = N. \tag{2.79}$$

Therefore, the probability distribution function can be rewritten in terms of this mean-square displacement:

$$P_{1d}(N,x) = \frac{1}{\sqrt{2\pi\langle x^2\rangle}}\exp\left(-\frac{x^2}{2\langle x^2\rangle}\right). \tag{2.80}$$

This function has a maximum at $x=0$ and decays fast for distances larger than the root-mean-square displacement $x > \sqrt{\langle x^2\rangle}$ as can be seen from Fig. 2.10.

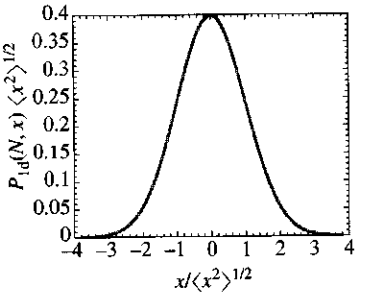


**Fig. 2.10**
Normalized one-dimensional Gaussian probability distribution function for occupying position $x$ after random $N$ steps from the origin ($x=0$).

This probability distribution function for the displacement of a one-dimensional random walk can be easily generalized to three-dimensional random walks. The probability of a walk, starting at the origin of the coordinate system, to end after $N$ steps, each of size $b$, within a volume $dR_x\,dR_y\,dR_z$ of the point with displacement vector $\vec{R}$ is $P_{3d}(N,\vec{R})\,dR_x\,dR_y\,dR_z$ (see Fig. 2.11). Since the three components of a three-dimensional random walk along the three Cartesian coordinates are independent of each other, the three-dimensional probability distribution function is a product of the three one-dimensional distribution functions:

$$P_{3d}(N,\vec{R})\,dR_x\,dR_y\,dR_z = P_{1d}(N,R_x)\,dR_x P_{1d}(N,R_y)\,dR_y P_{1d}(N,R_z)\,dR_z. \tag{2.81}$$

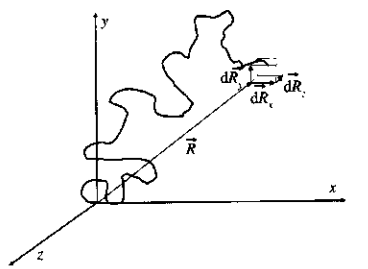


**Fig. 2.11**
One conformation of an ideal chain with one end at the origin and the other end within volume $dR_x\,dR_y\,dR_z$ of position $\vec{R}$.

The mean-square displacement of a random walk from the origin is equal to the mean-square end-to-end vector of a freely jointed chain with the number of monomers $N$ equal to the number of steps of the walk and the monomer length $b$ equal to the step size $\langle\vec{R}^2\rangle = Nb^2$. This mean-square displacement is composed of three mean-square displacements of the three independent one-dimensional walks:

$$\langle\vec{R}^2\rangle = \langle R_x^2\rangle + \langle R_y^2\rangle + \langle R_z^2\rangle = Nb^2. \tag{2.82}$$

Since each of the three Cartesian axes are equivalent, the mean-square displacement along each of them must be one-third of the total:

$$\langle R_x^2\rangle = \langle R_y^2\rangle = \langle R_z^2\rangle = \frac{Nb^2}{3}. \tag{2.83}$$

The one-dimensional probability distribution function for the components of a random walk along each of these three axes can be obtained by substituting these mean-square displacements into Eq. (2.80)

$$P_{1d}(N, R_x) = \frac{1}{\sqrt{2\pi\langle R_x^2\rangle}} \exp\left(-\frac{R_x^2}{2\langle R_x^2\rangle}\right) = \sqrt{\frac{3}{2\pi Nb^2}} \exp\left(-\frac{3R_x^2}{2Nb^2}\right). \tag{2.84}$$

The probability distribution function for the end-to-end vector $\vec{R}$ of an ideal linear chain of $N$ monomers is the product of the three independent distribution functions [Eq. (2.81)]:

$$P_{3d}(N, \vec{R}) = \left(\frac{3}{2\pi Nb^2}\right)^{3/2} \exp\left(-\frac{3(R_x^2 + R_y^2 + R_z^2)}{2Nb^2}\right) = \left(\frac{3}{2\pi Nb^2}\right)^{3/2} \exp\left(-\frac{3\vec{R}^2}{2Nb^2}\right). \tag{2.85}$$

As a function of each Cartesian component $R_i$ of the end-to-end vector $\vec{R}$, this probability distribution function looks the same as sketched in Fig. 2.10. The average of each component is $\langle R_i\rangle = 0$. As a function of the end-to-end distance $R = |\vec{R}|$ this probability distribution can be rewritten in the spherical coordinate system:

$$P_{3d}(N, R)4\pi R^2\,dR = 4\pi\left(\frac{3}{2\pi Nb^2}\right)^{3/2} \exp\left(-\frac{3R^2}{2Nb^2}\right) R^2\,dR. \tag{2.86}$$

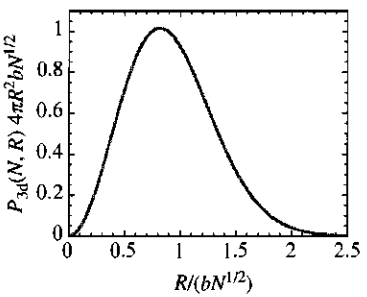


**Fig. 2.12**
Normalized distribution function of end-to-end distances for an ideal linear chain.

The probability distribution for the end-to-end distance $R$ is the probability for the end-to-end vector $\vec{R}$ to be in the spherical shell with radius between $R$ and $R + dR$. This probability of the end-to-end distance [Eq. (2.86)] is shown in Fig. 2.12. The Gaussian approximation is valid only for end-to-end vectors much shorter than the maximum extension of the chain (for $|\vec{R}| \ll R_{max} = Nb$). For $|\vec{R}| > Nb$, Eq. (2.85) predicts finite (though exponentially small) probability, which is physically unreasonable. For real chains $P_{3d}(N, R) \equiv 0$ for $R > Nb$ and this strong stretching is treated properly in Section 2.6.2.

## 2.6 Free energy of an ideal chain

The **entropy** $S$ is the product of the Boltzmann constant $k$ and the logarithm of the number of states $\Omega$:

$$S = k \ln \Omega. \tag{2.87}$$

Denote $\Omega(N, \vec{R})$ as the number of conformations of a freely jointed chain of $N$ monomers with end-to-end vector $\vec{R}$. The entropy is then a function

of $N$ and $\vec{R}$:

$$S\left(N,\vec{R}\right) = k\ln\Omega\left(N,\vec{R}\right). \tag{2.88}$$

The probability distribution function is the fraction of all conformations that actually have an end-to-end vector $\vec{R}$ between $\vec{R}$ and $\vec{R}+\mathrm{d}\vec{R}$:

$$P_{3d}\left(N,\vec{R}\right) = \frac{\Omega\left(N,\vec{R}\right)}{\int\Omega\left(N,\vec{R}\right)\mathrm{d}\vec{R}}. \tag{2.89}$$

The entropy of an ideal chain with $N$ monomers and end-to-end vector $\vec{R}$ is thus related to the probability distribution function:

$$S\left(N,\vec{R}\right) = k\ln P_{3d}\left(N,\vec{R}\right) + k\ln\left[\int\Omega\left(N,\vec{R}\right)\mathrm{d}\vec{R}\right]. \tag{2.90}$$

Equation (2.85) for the probability distribution function determines the entropy:

$$S\left(N,\vec{R}\right) = -\frac{3}{2}k\frac{\vec{R}^2}{Nb^2} + \frac{3}{2}k\ln\left(\frac{3}{2\pi Nb^2}\right) + k\ln\left[\int\Omega\left(N,\vec{R}\right)\mathrm{d}\vec{R}\right]. \tag{2.91}$$

The last two terms of Eq. (2.91) depend only on the number of monomers $N$, but not on the end-to-end vector $\vec{R}$ and can be denoted by $S(N,0)$:

$$S\left(N,\vec{R}\right) = -\frac{3}{2}k\frac{\vec{R}^2}{Nb^2} + S(N,0). \tag{2.92}$$

The **Helmholtz free energy** of the chain $F$ is the energy $U$ minus the product of absolute temperature $T$ and entropy $S$:

$$F\left(N,\vec{R}\right) = U\left(N,\vec{R}\right) - TS\left(N,\vec{R}\right). \tag{2.93}$$

The energy of an ideal chain $U(N,\vec{R})$ is independent of the end-to-end vector $\vec{R}$, since the monomers of the ideal chain have no interaction energy.[3] The free energy can be written as

$$F\left(N,\vec{R}\right) = \frac{3}{2}kT\frac{\vec{R}^2}{Nb^2} + F(N,0), \tag{2.94}$$

where $F(N,0) = U(N,0) - TS(N,0)$ is the free energy of the chain with both ends at the same point. As was demonstrated above, the largest number of chain conformations correspond to zero end-to-end vector. The number of conformations decreases with increasing end-to-end vector, leading to the decrease of polymer entropy and increase of its free energy. The free energy of an ideal chain $F(N,\vec{R})$ increases quadratically with the magnitude of the end-to-end vector $\vec{R}$. This implies that the entropic elasticity of an ideal

[3] The ideal chain never has long-range interactions, but short-range interactions are possible, and their consequences are discussed in problem 7.19.

chain satisfies Hooke's law. To hold the chain at a fixed end-to-end vector $\vec{R}$, would require equal and opposite forces acting on the chain ends that are proportional to $\vec{R}$. For example, to separate the chain ends by distance $R_x$ in $x$ direction, requires force $f_x$:

$$f_x = \frac{\partial F\left(N, \vec{R}\right)}{\partial R_x} = \frac{3kT}{Nb^2} R_x. \tag{2.95}$$

The force to hold chain ends separated by a general vector $\vec{R}$ is linear in $\vec{R}$, like a simple elastic spring:

$$\vec{f} = \frac{3kT}{Nb^2} \vec{R}. \tag{2.96}$$

The coefficient of proportionality $3kT/(Nb^2)$ is the **entropic spring constant** of an ideal chain. It is easier to stretch polymers with larger numbers of monomers $N$, larger monomer size $b$, and at *lower* temperature $T$. The fact that the spring constant is proportional to temperature is a signature of entropic elasticity. The entropic nature of elasticity in polymers distinguishes them from other materials. Metals and ceramics become softer as temperature is raised because their deformation requires displacing atoms from their preferred positions (energetic instead of entropic elasticity).

The force increases as the chain is stretched because there are fewer possible conformations for larger end-to-end distances. The linear entropic spring result for the stretching of an ideal chain [Eq. (2.96)] is extremely important for our subsequent discussions of rubber elasticity and polymer dynamics. This linear dependence [Hooke's law for an ideal chain, Eq. (2.96)] is due to the Gaussian approximation, valid only for $|\vec{R}| \ll R_{\max} = Nb$. If the chain is stretched to the point where its end-to-end vector approaches the maximum chain extension $|\vec{R}| \leq R_{\max}$, the dependence becomes strongly non-linear, with the force diverging at $|\vec{R}| = R_{\max}$, as will be discussed in Section 2.6.2.

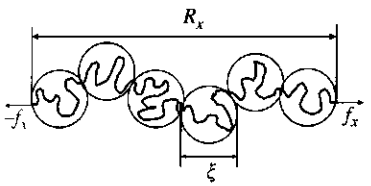


**Fig. 2.13**
An elongated chain is only stretched on its largest length scales. Inside the tension blob, the conformation of the chain is essentially unperturbed by the stretch.

### 2.6.1 Scaling argument for chain stretching

The linear relation between force and end-to-end distance can also be obtained by a very simple scaling argument. The key to understanding the scaling description is to recognize that most of the conformational entropy of the chain arises from local conformational freedom on the smallest length scales. For this reason, the random walks that happen to have end-to-end distance $R > bN^{1/2}$ can be visualized as a sequential array of smaller sections of size $\xi$ that are essentially unperturbed by the stretch, as shown in Fig. 2.13.

The stretched polymer is subdivided into sections of $g$ monomers each. We assume that these sections are almost undeformed so that the mean-square projection of the end-to-end vector of these sections of $g$ monomers onto any of the coordinate axes obeys ideal chain statistics [Eq. (2.83)]:

$$\xi^2 \approx b^2 g. \tag{2.97}$$

There are $N/g$ such sections and in the direction of elongation they are assumed to be arranged sequentially:

$$R_x \approx \xi \frac{N}{g} \approx \frac{Nb^2}{\xi}. \tag{2.98}$$

This can be solved for the size $\xi$ of the unperturbed sections and the number of monomers $g$ in each section:

$$\xi \approx \frac{Nb^2}{R_x}, \tag{2.99}$$

$$g \approx \frac{N^2 b^2}{R_x^2}. \tag{2.100}$$

The number of monomers $g$ and the size $\xi$ of these sections were specially chosen so that the polymer conformation changes from that of a random walk on smaller size scales to that of an elongated chain on larger length scales. Such sections of stretched polymers are called **tension blobs**. Being extended on only its largest length scales allows the chain to maximize its conformational entropy.

The physical meaning of a tension blob is the length scale $\xi$ at which external tension changes the chain conformation from almost undeformed on length scales smaller than $\xi$ to extended on length scales larger than $\xi$. The trajectory of the stretched chain (Fig. 2.13) shows that each tension blob is forced to go in a particular direction along the $x$ axis (rather than in a random direction as in an unperturbed chain). Therefore one degree of freedom is restricted per tension blob and the free energy of the chain increases by $kT$ per blob:[4]

$$F \approx kT \frac{N}{g} \approx kT \frac{R_x^2}{Nb^2}. \tag{2.101}$$

In comparing Eqs (2.94) and (2.101), we see that the scaling method gets the correct result within a prefactor of order unity. This is the character of all scaling calculations: they provide a simple means to extract the essential physics but do not properly determine numerical coefficients.

Equation (2.101) is the first of many instances where the free energy stored in the chain is of the order of $kT$ per blob, because the blobs generally describe a length scale at which the conformation of the chain changes and is the elementary unit of deformation. In the case of stretching, the free energy is $F/N$ per monomer. On length scales smaller than the tension blob, the thermal energy $kT$ that randomizes the conformation is larger than the cumulative stretching energy, and the conformation is essentially unperturbed. On length scales larger than the tension blob, the cumulative stretching energy is larger than $kT$, and the ideal chain gets strongly stretched (see Fig. 2.13). Similar arguments apply to other problems involving conformational changes beyond a particular length scale, making the free energy of order $kT$ per blob quite general.

[4] This is the consequence of the equipartition theorem.

The force needed to stretch the chain is given by the derivative of the free energy:

$$f_x = \frac{\partial F}{\partial R_x} \approx kT \frac{R_x}{Nb^2} \approx \frac{kT}{\xi}. \tag{2.102}$$

The tension blobs provide a simple framework for visualizing the chain stretching (Fig. 2.13) and provide simple relations for calculating the stretching force and free energy. They define the length scale at which elastic energy is of order $kT$. Since the force has dimensions of energy divided by length, Eq. (2.102) immediately follows from a dimensional analysis with length scale of tension blob $\xi$ corresponding to $kT$ of stored elastic energy.

The stretching along the $x$ axis, shown in Fig. 2.13, makes the stretched conformation of an ideal chain a **directed random walk** of tension blobs. This conformation is sequential in the $x$ direction, but the $y$ and $z$ directions have the usual random walk statistics that are unaffected by the stretching. The mean-square components of the end-to-end vector orthogonal to the stretching direction are obtained from one-dimensional random walks of $N/g$ sections of step length $\xi$:

$$\langle R_y^2 \rangle = \langle R_z^2 \rangle \approx \xi^2 \frac{N}{g} \approx Nb^2. \tag{2.103}$$

The linear relation between force $f_x$ and end-to-end distance $R_x$ (Hooke's law) is valid as long as there are many Kuhn monomers in each tension blob. As the end-to-end distance $R_x$ approaches a significant fraction of its maximal value $R_{\max}$, a deviation from Hooke's law is expected. Note that the Gaussian approximation assumes $R_x \ll R_{\max}$ and always leads to Hooke's Law. Below we derive the non-linear relation between force and elongation for strongly stretched chains. The limit of the linear regime corresponds to a force of the order of

$$\frac{kT}{b} \cong \frac{1.38 \times 10^{-23}\,\mathrm{J\,K^{-1}} \times 295\,\mathrm{K}}{1 \times 10^{-9}\,\mathrm{m}} \cong 4 \times 10^{-12}\,\mathrm{N} \tag{2.104}$$

for a chain with Kuhn length $b = 1$ nm at room temperature. Stiffer chains with larger Kuhn length get nearly fully stretched at weaker extension forces. For double-helical DNA with Kuhn length $b \cong 100$ nm (persistence length $l_p \cong 50$ nm) the force corresponding to the linear response limit is 100 times smaller ($4 \times 10^{-14}$ N).

### 2.6.2 Langevin dependence of elongation on force

Consider a freely jointed chain of $N$ bonds subject to a constant elongational force $f$ applied to its ends along the $z$ axis. An example could be a chain with two opposite charges $+q$ and $-q$ at its ends in a constant electric field $\vec{E}$ applied along the $z$ axis as sketched in Fig. 2.14. If the direct

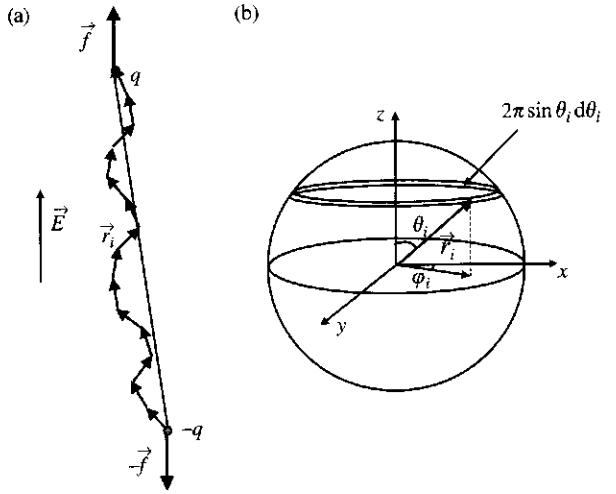


**Fig. 2.14**
(a) Freely jointed chain elongated by a pair of forces applied to its ends. (b) Spherical coordinate system for orientation of a bond.

Coulomb interaction between the charges is ignored, there is a constant force $\vec{f} = q\vec{E}$ acting along the $z$ axis on the positive charge and an opposite force $-\vec{f}$ acting on the negative charge. Different chain conformations are no longer equally likely, because they correspond to different energy of the chain in the external electric field. The energy of the chain is proportional to the projection of the end-to-end vector on the direction of the field:

$$U = -q\vec{E} \cdot \vec{R} = -\vec{f} \cdot \vec{R} = -fR_z. \tag{2.105}$$

This energy is equal to the work done by the chain upon separation of the charges by vector $\vec{R}$ in an external electric field $\vec{E}$. The direction of the end-to-end vector $\vec{R}$ of the chain is chosen from the negative to the positive charge at its ends. Displacement of the positive charge down the field with respect to the negative charge, lowers the electrostatic energy of the chain and corresponds to a more favorable conformation. Thus, different chain conformations have different statistical Boltzmann factors $\exp(-U/kT)$ that depend on their corresponding energy $U$ [Eq. (2.105)].

The sum of the Boltzmann factors over all possible conformations of the chain is called the **partition function**:

$$Z = \sum_{\text{states}} \exp\left(-\frac{U}{kT}\right) = \sum_{\text{states}} \exp\left(\frac{fR_z}{kT}\right). \tag{2.106}$$

The partition function is useful because we will calculate the free energy from it in Eq. (2.111). States with higher energy make a smaller contribution to the partition function because their Boltzmann factor determines that those states are less likely.

Different conformations in the freely jointed chain model correspond to different sets of orientations of bond vectors $\vec{r}_i$ in space [see Fig. 2.14(a)]. The orientation of each bond vector $\vec{r}_i$ can be defined by the two angles of the spherical coordinate system $\theta_i$ and $\varphi_i$ [Fig. 2.14(b)]. Therefore, the sum

over all possible conformations of a freely jointed chain corresponds to the integral over all possible orientations of all bond vectors of the chain:

$$Z = \sum_{\text{states}} \exp\left(\frac{fR_z}{kT}\right) = \int \exp\left(\frac{fR_z}{kT}\right) \prod_{i=1}^{N} \sin\theta_i \, \mathrm{d}\theta_i \, \mathrm{d}\varphi_i. \tag{2.107}$$

The notation $\prod_{i=1}^{N}$ denotes the product of $N$ terms. The $z$ component of the end-to-end vector can be represented as the sum of the projections of all bond vectors onto the $z$ axis:

$$R_z = \sum_{i=1}^{N} b \cos\theta_i. \tag{2.108}$$

Therefore, the partition function [Eq. (2.107)] becomes a product of $N$ identical integrals:

$$\begin{aligned} Z(T,f,N) &= \int \exp\left(\frac{fb}{kT}\sum_{i=1}^{N}\cos\theta_i\right) \prod_{i=1}^{N} \sin\theta_i \, \mathrm{d}\theta_i \, \mathrm{d}\varphi_i \\ &= \left[\int_0^{\pi} 2\pi \sin\theta_i \exp\left(\frac{fb}{kT}\cos\theta_i\right) \mathrm{d}\theta_i\right]^N \\ &= \left[\frac{2\pi}{fb/(kT)}\left[\exp\left(\frac{fb}{kT}\right) - \exp\left(-\frac{fb}{kT}\right)\right]\right]^N \qquad (2.109) \\ &= \left[\frac{4\pi \sinh(fb/(kT))}{fb/(kT)}\right]^N. \qquad (2.110) \end{aligned}$$

The Gibbs free energy $G$ can be directly calculated from the partition function:[5]

$$\begin{aligned} G(T,f,N) &= -kT \ln Z(T,f,N) \\ &= -kTN\left[\ln\left(4\pi \sinh\left(\frac{fb}{kT}\right)\right) - \ln\left(\frac{fb}{kT}\right)\right]. \end{aligned} \tag{2.111}$$

The average end-to-end distance corresponding to a given force can be obtained as the derivative of the free energy:

$$\langle R\rangle = -\frac{\partial G}{\partial f} = bN\left[\coth\left(\frac{fb}{kT}\right) - \frac{1}{fb/(kT)}\right]. \tag{2.112}$$

The expression in the square brackets of Eq. (2.112) is called the **Langevin function**:

$$\mathcal{L}(\beta) = \coth(\beta) - \frac{1}{\beta}. \tag{2.113}$$

The Langevin function relates average chain elongation $\langle R\rangle/R_{\max}$ and normalized extensional force $\beta = fb/(kT)$ for a freely jointed chain, as sketched in Fig. 2.15.

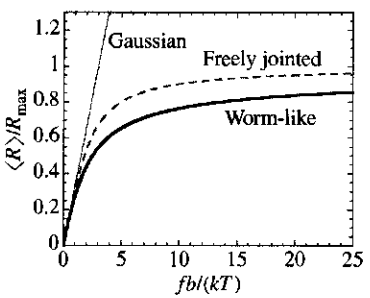


**Fig. 2.15**
Average end-to-end distance as a function of stretching force for a Gaussian chain [Eq. (2.95), thin line], a freely jointed chain [Langevin function, Eq. (2.112), dashed line], and a worm-like chain [Eq. (2.119), thick line].

[5] The Gibbs free energy is used here because the ensemble of chains corresponds to constant force $f$, not constant end-to-end distance $R$ (analogous to the isothermal–isobaric ensemble, which has constant pressure instead of constant volume).

For small relative elongations ($\langle R\rangle \ll R_{\max} = bN$) the dependence is approximately linear,

$$\mathcal{L}(\beta) \cong \frac{\beta}{3} \quad \text{for } \beta \ll 1, \tag{2.114}$$

and follows Hooke's law derived above [Eq. (2.96)] $\langle R\rangle/(bN) = fb/(3kT)$. For larger relative elongations, the Langevin function significantly deviates from linear dependence and saturates at unity (see Fig. 2.15). For large extensional force $f \gg kT/b$, the Langevin function has another simple limit:

$$\mathcal{L}(\beta) \cong 1 - \frac{1}{\beta} \quad \text{for } \beta \gg 1. \tag{2.115}$$

This means that the extension for strong stretching has a simple form

$$\frac{\langle R\rangle}{R_{\max}} \cong 1 - \frac{kT}{fb},$$

where $R_{\max} = Nb$. The extensional force of the equivalent freely jointed chain diverges reciprocally proportional to $R_{\max} - \langle R\rangle$:

$$\frac{fb}{kT} \cong \frac{R_{\max}}{R_{\max} - \langle R\rangle} \quad \text{for } 1 - \frac{\langle R\rangle}{R_{\max}} \ll 1. \tag{2.116}$$

In the case of the worm-like chain model (Section 2.3.2), the extensional force diverges reciprocally proportional to the square of $R_{\max} - \langle R\rangle$:

$$\frac{fb}{kT} \cong \frac{1}{2}\left(\frac{R_{\max}}{R_{\max} - \langle R\rangle}\right)^2 \quad \text{for } 1 - \frac{\langle R\rangle}{R_{\max}} \ll 1. \tag{2.117}$$

The differences between divergences of force near maximum extension [Eqs (2.116) and (2.117)] are due to bending modes on length scales shorter than Kuhn length $b$. These modes do not exist in freely jointed chains because sections of length $b$ are assumed to be absolutely rigid. In the worm-like chain model these bending modes with wavelength $\xi \ll b$ lead to much stronger divergence of the force [Eq. (2.117)].

At small relative extensions ($\langle R\rangle \ll R_{\max}$) worm-like chains behave as Hookean springs:

$$\frac{fb}{kT} \cong \frac{3\langle R\rangle}{R_{\max}} \quad \text{for } \langle R\rangle \ll R_{\max}. \tag{2.118}$$

There is no simple analytical solution for the worm-like chain model at all extensions, but there is an approximate expression valid both for small and for large relative extensions:[6]

$$\frac{fb}{kT} \cong \frac{2\langle R\rangle}{R_{\max}} + \frac{1}{2}\left(\frac{R_{\max}}{R_{\max} - \langle R\rangle}\right)^2 - \frac{1}{2}. \tag{2.119}$$

[6] J. F. Marko and E. D. Siggia, *Macromolecules* **28**, 8759 (1995).

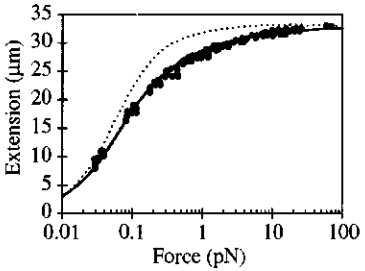


**Fig. 2.16**
Comparison of experimental force for 97 kilobase λ-DNA dimers with the worm-like chain model [solid curve is Eq. (2.119) with $R_{max} = 33\,\mu m$ and $b = 100\,nm$]. The dotted curve corresponds to the Langevin function of the freely jointed chain model [Eq. (2.112)]. Data are from R. H. Austin *et al.*, *Phys. Today*, Feb. 1997, p. 32.

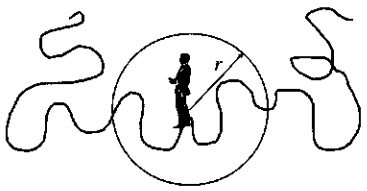


**Fig. 2.17**
A monomer can only reach other monomers with its CB radio if they are within the range of the radio.

Strong deviations from linear elasticity have been measured in polymer networks at large elongation (see Chapter 7). Optical tweezers and atomic force microscopy have been used to measure the dependence of the force applied to the ends of isolated chains on their elongation. In the optical tweezer experiments, beads were attached to the ends of long DNA segments. DNA is a biopolymer that exists as a double-stranded helix. Such stiff chains are best described by the worm-like chain model. The chain length of DNA is typically described in terms of the number of base pairs along the helix. The positions of the beads at the ends of DNA chains were manipulated by a focused laser beam (hence the name 'optical tweezers'). The force exerted on the chain ends was measured by the calibrated relative displacement of the beads with respect to the optical traps. In another type of nano-manipulation experiment a 97 kilobase λ-DNA dimer was chemically attached by one of its ends to a glass slide and by the other end to a small (3 μm) magnetic bead. The DNA was stretched by applying a known magnetic and hydrodynamic force to the bead. The stretching was measured by observing the position of the bead in an optical microscope. The extension of DNA as a function of applied force is compared with predictions of freely jointed and worm-like chain models in Fig. 2.16. The worm-like chain model is in excellent agreement with the experimental data.

## 2.7 Pair correlations of an ideal chain

Consider a monomer of an ideal polymer trying to reach fellow monomers of the same chain via a CB radio (see Fig. 2.17). The number of monomers it can call depends on the range $r$ of its transmitter. It can contact any monomer within the sphere of radius $r$ of itself. The number of monomers $m$ that can be reached via a CB radio with range $r$ is given by random walk statistics:

$$m \approx \left(\frac{r}{b}\right)^2. \tag{2.120}$$

The number density of these monomers within the volume $r^3$ is $m/r^3$. The probability of finding a monomer in a unit volume at a distance $r$ from a given monomer is called the **pair correlation function** $g(r)$. It can be approximated by the average number density within the volume $r^3$:

$$g(r) \approx \frac{m}{r^3} \approx \frac{1}{rb^2}. \tag{2.121}$$

The exact calculation of the pair correlation function of an ideal chain leads to an additional factor $3/\pi$:

$$g(r) = \frac{3}{\pi r b^2}. \tag{2.122}$$

Note that the pair correlation function decreases with increasing distance $r$. It is less likely to find a monomer belonging to the chain further away from

a given monomer because the average number density of monomers within the sphere of radius $r$ decreases. Large polymer coils are almost empty.

To illustrate this concept, divide the cube of size $R$, containing an ideal polymer with $N$ monomers of size $b$ and end-to-end distance $R = bN^{1/2}$, into smaller cubes of size $r$ (Fig. 2.18). There will be $(R/r)^3$ such smaller cubes. But only $(R/r)^2$ of these smaller cubes contain monomers of the chain. The average number of monomers in each of these occupied smaller cubes is $m \approx (r/b)^2$. The remaining $(R/r)^3 - (R/r)^2$ smaller cubes are empty. The local density of monomers strongly fluctuates from cell to cell. There are holes of all sizes inside a polymer chain.

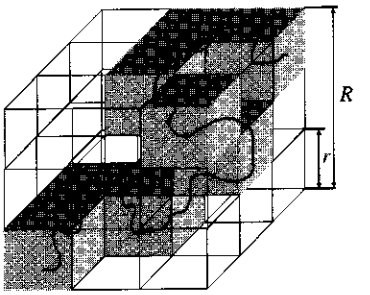


**Fig. 2.18**
Fractal nature of an ideal chain.

This description is a manifestation of the self-similarity (fractal nature) of polymers, discussed in Section 1.4. The fractal nature of ideal chains leads to the power law dependence of the pair correlation function $g(r)$ on distance $r$. This treatment for the ideal chain can be easily generalized to a linear chain with any fractal dimension $\mathcal{D}$. The number of monomers within range $r$ is $m \sim r^{\mathcal{D}}$. We use the proportionality sign '$\sim$' if the dimensional coefficient (in the particular case above $\approx 1/b^{\mathcal{D}}$) is dropped from the relation. The pair correlation function is still proportional to the ratio of $m$ and $r^3$:

$$g(r) \approx \frac{m}{r^3} \sim r^{\mathcal{D}-3}. \tag{2.123}$$

Hence, Eq. (2.121) is a special case of this result, with $\mathcal{D} = 2$ for an ideal chain. The fractal dimension of a rod polymer is $\mathcal{D} = 1$ and the pair correlation function is $g(r) \sim r^{-2}$.

## 2.8 Measurement of size by scattering

Polymer conformations are studied by various scattering experiments (light, small-angle X-ray and neutron scattering). These techniques are based on the contrast between the polymer and the surrounding media (solvent in the case of polymer solutions and other polymers in the case of polymer melts or blends). The contrast in light scattering arises from differences in refractive index between polymer and solvent, and the scattered intensity is proportional to the square of the refractive index increment $dn/dc$ [see Eq. (1.86)].

While neutron sources are not available in most laboratories, small-angle neutron scattering (SANS) has become a routine characterization method for polymer research using large-scale national and multinational facilities. To obtain the contrast needed for neutron scattering, some of the chains in a polymer melt have their hydrogen atoms replaced by deuterium. In a polymer solution, the solvent is often deuterated. This deuterium labelling appears to not alter the conformations of polymers.

### 2.8.1 Scattering wavevector

Consider an incident laser beam with wavelength $\lambda$ illuminating a polymer sample, represented by the large circle in Fig. 2.19, along the direction with

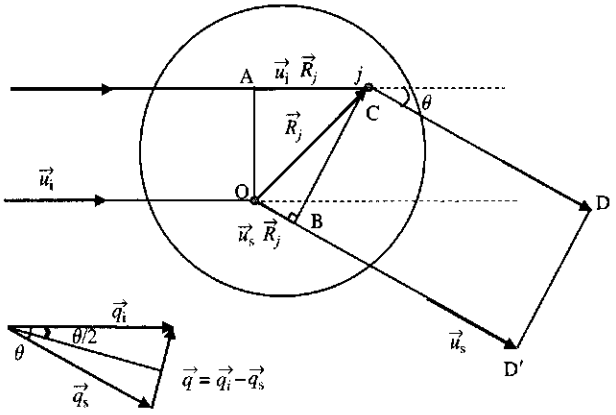


**Fig. 2.19**
Radiation scattered through angle $\theta$ from two distinct parts of the sample.

unit vector $\vec{u}_i$. This incident beam can be characterized by the **incident wavevector:**

$$\vec{q}_i \equiv \frac{2\pi n}{\lambda}\vec{u}_i, \tag{2.124}$$

where $n$ is the refractive index of the solution. The incident light is scattered through angle $\theta$ and leaves the sample along the direction with unit vector $\vec{u}_s$. The scattered beam is characterized by the **scattered wavevector:**

$$\vec{q}_s \equiv \frac{2\pi n}{\lambda}\vec{u}_s. \tag{2.125}$$

The incident beam is coherent, meaning that all photons are in-phase. When the incident beam enters the sample, monomers absorb the radiation and re-emit it in all directions. The difference in optical paths between the light scattered by different monomers makes the scattered beam incoherent, meaning that the scattered photons are no longer in-phase.[7] In the example sketched in Fig. 2.19, the difference in optical paths of the radiation scattered by the monomer $j$ at position $\vec{R}_j$ (at point C) and by the monomer at the origin O is easily calculated:

$$\mathrm{AC} + \mathrm{CD} - \mathrm{OD}' = \mathrm{AC} - \mathrm{OB}. \tag{2.126}$$

The section AC is the projection of the vector $\vec{R}_j$ onto the incident direction and has length $\vec{u}_i \cdot \vec{R}_j$. The section OB is the projection of the vector $\vec{R}_j$ onto the scattered direction and has length $\vec{u}_s \cdot \vec{R}_j$. Thus, the difference in the optical paths can be written in terms of these vectors:

$$\mathrm{AC} - \mathrm{OB} = \vec{u}_i \cdot \vec{R}_j - \vec{u}_s \cdot \vec{R}_j = (\vec{u}_i - \vec{u}_s) \cdot \vec{R}_j. \tag{2.127}$$

This difference in optical paths results in the phase difference $\varphi_j$, which is $2\pi n/\lambda$ times the optical path difference [see Eq. (1.77) with $\lambda$ replaced by the wavelength in the dielectric medium $\lambda/n$].

$$\varphi_j = \frac{2\pi n}{\lambda}(\vec{u}_i - \vec{u}_s) \cdot \vec{R}_j = (\vec{q}_i - \vec{q}_s) \cdot \vec{R}_j = \vec{q} \cdot \vec{R}_j. \tag{2.128}$$

[7] It is assumed that there is no multiple scattering, although this is not always a valid assumption.

The **scattering wavevector** $\vec{q}$ is defined as the difference of the incident and scattered wavevectors:

$$\vec{q} \equiv \vec{q}_i - \vec{q}_s. \tag{2.129}$$

From their definitions in Eqs (2.124) and (2.125), the magnitudes of the incident and scattered wavevectors are the same:

$$|\vec{q}_i| = |\vec{q}_s| = \frac{2\pi n}{\lambda}. \tag{2.130}$$

The isosceles triangle of wavevectors in Fig. 2.19 shows that half of the magnitude of the scattering wavevector is equal to the magnitude of wavevectors $\vec{q}_i$ or $\vec{q}_s$ times the sine of half the angle $\theta$ between them:

$$q \equiv |\vec{q}| = 2|\vec{q}_i| \sin\left(\frac{\theta}{2}\right) = \frac{4\pi n}{\lambda} \sin\left(\frac{\theta}{2}\right). \tag{2.131}$$

### 2.8.2 Form factor

We concentrate here on light scattering, but similar results are valid for small-angle X-ray and neutron scattering. We describe scattering from a single molecule, assuming that the solution is dilute, which is the relevant regime for determining the size and shape of individual coils.

The electric field of light scattered by the $j$th segment is

$$E_j = E_i A \cos(2\pi\nu t - \varphi_j), \tag{2.132}$$

where $\varphi_j$ is the phase difference [(Eq. (2.128)], $\nu$ is the frequency, $E_i$ is the amplitude of the incident electric field [Eq. (1.77)] and the coefficient $A$ contains the factors such as polarizability $\alpha$, the distance $r$ to the detector, the wavelength of light $\lambda$, etc. [see Eq. (1.81)]. Summing over the $N$ monomers gives the electric field scattered by an isolated polymer coil:

$$E_s = E_i \sum_{j=1}^{N} A \cos(2\pi\nu t - \varphi_j). \tag{2.133}$$

The intensity of scattered light is the energy of radiation that falls onto a unit area per unit time. It is proportional to the square of the electric field averaged over one oscillation period $1/\nu$:

$$\begin{aligned} I_s &= 2I_i A^2 \nu \int_0^{1/\nu} \left[\sum_{j=1}^{N} \cos(2\pi\nu t - \varphi_j)\right]^2 \mathrm{d}t \\ &= 2I_i A^2 \nu \int_0^{1/\nu} \left[\sum_{j=1}^{N}\sum_{k=1}^{N} \cos(2\pi\nu t - \varphi_j)\cos(2\pi\nu t - \varphi_k)\right] \mathrm{d}t \\ &= I_i A^2 \nu \int_0^{1/\nu} \left[\sum_{j=1}^{N}\sum_{k=1}^{N} (\cos(4\pi\nu t - \varphi_j - \varphi_k) + \cos(\varphi_k - \varphi_j))\right] \mathrm{d}t. \end{aligned} \tag{2.134}$$

The final result used the equation for the product of cosines:

$$\cos\alpha\cos\beta = \frac{\cos(\alpha+\beta)+\cos(\alpha-\beta)}{2}. \tag{2.135}$$

The first term in Eq. (2.134) oscillates exactly two full periods ($4\pi$) and its integral over the time interval $0 \le t \le 1/\nu$ is thus equal to zero. The second term (cosine of the phase difference) is time independent and determines the intensity of light scattered by the molecule

$$I_s = I_i A^2 \sum_{k=1}^{N}\sum_{j=1}^{N} \cos(\varphi_k - \varphi_j), \tag{2.136}$$

where the phases $\varphi_j$ are determined by the positions $\vec{R}_j$ of the corresponding monomers and the scattering wavevector $\vec{q}$ [Eq. (2.128)].

The dependence of the scattered intensity on the size and the shape of the polymer is usually described by the **form factor** defined as the ratio of intensity scattered at angle $\theta$ (scattering wavevector $\vec{q}$) to that extrapolated to zero angle ($\theta \to 0$) and therefore, zero scattering wavevector ($|\vec{q}| \to 0$):

$$P(\vec{q}) \equiv \frac{I_s(\vec{q})}{I_s(0)}. \tag{2.137}$$

All optical paths are the same at zero scattering angle ($q = 0$) and there is no phase shift ($\varphi_j = 0$ for all $j$) because the scattering wavevector $q = 0$ [Eq. (2.131)]. The intensity of light scattered by the molecule at zero angle,

$$I_s(0) = I_i A^2 \sum_{k=1}^{N}\sum_{j=1}^{N} 1 = I_i A^2 N^2, \tag{2.138}$$

leads directly to the form factor, defined by Eq. (2.137):

$$\begin{aligned} P(\vec{q}) &= \frac{1}{N^2}\sum_{i=1}^{N}\sum_{j=1}^{N}\cos(\varphi_i - \varphi_j) \\ &= \frac{1}{N^2}\sum_{i=1}^{N}\sum_{j=1}^{N}\cos[\vec{q}\cdot(\vec{R}_i - \vec{R}_j)]. \end{aligned} \tag{2.139}$$

It is important to stress that only the relative position of monomers

$$\vec{R}_{ij} \equiv \vec{R}_i - \vec{R}_j \tag{2.140}$$

enters into the form factor.

The form factor in Eq. (2.139) is defined for a specific orientation of the molecule with respect to the scattering wavevector $\vec{q}$. Often (but not always!), the system is isotropic with equal probabilities of all molecular

orientations in space. In this case, Eq. (2.139) can be averaged over all these orientations. This averaging can be carried out in the spherical coordinate system with the $z$ axis along the scattering wavevector $\vec{q}$ and the angle between $\vec{q}$ and $\vec{R}_{ij}$ denoted by $\alpha$. The polar angle in this spherical coordinate system is denoted by $\beta$. The scalar product of wavevector $\vec{q}$ and the relative vector between monomers $i$ and $j$ is

$$\vec{q} \cdot \left(\vec{R}_i - \vec{R}_j\right) = qR_{ij}\cos\alpha, \tag{2.141}$$

where $R_{ij}$ is the distance between monomers $i$ and $j$. Averaging the cosine of this scalar product over all orientations of the molecule leads to

$$\begin{aligned}\langle\cos[\vec{q}\cdot(\vec{R}_i - \vec{R}_j)]\rangle &= \frac{1}{4\pi}\int_0^{2\pi}\left[\int_0^{\pi}\cos(qR_{ij}\cos\alpha)\sin\alpha\,\mathrm{d}\alpha\right]\mathrm{d}\beta \\ &= \frac{1}{2}\int_{-1}^{1}\cos(qR_{ij}x)\,\mathrm{d}x = \frac{\sin(qR_{ij})}{qR_{ij}},\end{aligned} \tag{2.142}$$

where the integral was taken by the change of variables $x = \cos\alpha$. Thus, the form factor for any isotropic system is quite simple:

$$P(q) = \frac{1}{N^2}\sum_{i=1}^{N}\sum_{j=1}^{N}\frac{\sin(qR_{ij})}{qR_{ij}}. \tag{2.143}$$

### 2.8.3 Measuring $R_g^2$ by scattering at small angles

One important property of the form factor in dilute solutions is that at low scattering angle ($qR_g < 1$) it becomes independent of any assumption about the shape of the molecule. Using the Taylor series expansion,

$$\frac{\sin x}{x} = 1 - \frac{x^2}{3!} + \frac{x^4}{5!} - \cdots \tag{2.144}$$

the form factor at low angles can be rewritten, as

$$\begin{aligned}P(q) &= \frac{1}{N^2}\sum_{i=1}^{N}\sum_{j=1}^{N}\left[1 - \frac{(qR_{ij})^2}{3!} + \cdots\right] \\ &= 1 - \frac{q^2}{6N^2}\sum_{i=1}^{N}\sum_{j=1}^{N}R_{ij}^2 + \cdots \quad \text{for } qR_g < 1,\end{aligned} \tag{2.145}$$

$$P(q) = 1 - \frac{1}{3}q^2\langle R_g^2\rangle + \cdots \quad \text{for } qR_g < 1. \tag{2.146}$$

In the final relation, Eq. (2.47) was used for $R_g^2$ and the average $\langle\cdots\rangle$ is over different polymer conformations contributing to scattering.

Substituting the relation (2.131) between scattering wavevector $q$ and scattering angle $\theta$ provides the low-angle expression of the form factor in light scattering:

$$P(q) = 1 - \frac{16\pi^2 n^2}{3\lambda^2}\langle R_g^2\rangle\sin^2\left(\frac{\theta}{2}\right) + \cdots \tag{2.147}$$

Recall from Chapter 1 that it is convenient to plot the reciprocal Rayleigh ratio times concentration and optical constant $K$ [Eq. (1.96)] to determine the weight-average molar mass from the zero concentration limit. In Chapter 1, we considered the Rayleigh ratio in the zero wavevector limit, and since the Rayleigh ratio is a normalized intensity [Eq. (1.87)] it has the same $q$ dependence as the form factor [see Eq. (2.137)].

$$\left(\frac{Kc}{R_\theta}\right)_{c\to 0} = \frac{1}{M_w P(q)} = \frac{1}{M_w}\left[1 + \frac{16\pi^2 n^2}{3\lambda^2}\left\langle R_g^2\right\rangle \sin^2\left(\frac{\theta}{2}\right) + \cdots\right]. \quad (2.148)$$

Note that the plus sign in front of the $\langle R_g^2\rangle$ term arises because $(1-x)^{-1} \cong 1 + x$ for small values of $x$. Thus, extrapolation of the ratio $Kc/R_\theta$ to zero concentration plotted as a function of $\sin^2(\theta/2)$ allows determination of the radius of gyration of the polymer (or any other scattering object) from the slope for low scattering angles ($qR_g < 1$) and the mass of the object from the $y$-intercept. For polydisperse samples, this method leads to the weight-average molar mass $M_w$ and the $z$-average square radius of gyration $\langle R_g^2\rangle_z$. In order to understand this, we write the Rayleigh ratio for a mixture of different species with molar mass $M_N$, mean-square radius of gyration $\langle R_N^2\rangle$, and concentration $c_N$:

$$\begin{aligned} R_\theta &= K\left[\sum_N c_N M_N - \frac{q^2}{3}\sum_N c_N M_N \langle R_N^2\rangle + \cdots\right] \\ &= K\sum_N c_N \frac{\sum_N c_N M_N}{\sum_N c_N}\left[1 - \frac{q^2}{3}\frac{\sum_N c_N M_N \langle R_N^2\rangle}{\sum_N c_N M_N} + \cdots\right] \\ &= KcM_w\left[1 - \frac{q^2}{3}\langle R_g^2\rangle_z + \cdots\right]. \end{aligned} \quad (2.149)$$

The $z$-average mean-square radius of gyration is defined as

$$\langle R_g^2\rangle_z \equiv \frac{\sum_N c_N M_N \langle R_N^2\rangle}{\sum_N c_N M_N}, \quad (2.150)$$

and the low-concentration limit of the scattering expansion for a polydisperse solution takes a form similar to Eq. (2.148):

$$\left(\frac{Kc}{R_\theta}\right)_{c\to 0} = \frac{1}{M_w}\left[1 + \frac{16\pi^2 n^2}{3\lambda^2}\langle R_g^2\rangle_z \sin^2\left(\frac{\theta}{2}\right) + \cdots\right]. \quad (2.151)$$

An expansion similar to Eq. (2.151) for non-zero concentrations is the basis for the Zimm plot (see Problem 2.47).

The coil size of chains in dilute solution is typically measured by light scattering, using a laser. Visible light has a wavelength of order $\lambda \approx 500$ nm, which is much longer than the wavelength of neutrons ($\lambda \approx 0.3$ nm). This means that much smaller scattering wavevectors $q$ are realized in light scattering than in neutron scattering. The limit $qR_g < 1$, required for the expansion of the form factor in Eq. (2.146), is satisfied for all but the

highest molar mass chains in small-angle light scattering. At low scattering angles (for $qR_g < 1$), the form factor can also be approximated by an exponential:

$$P(q) \cong \exp\left(-\frac{q^2 R_g^2}{3}\right) \quad \text{for } qR_g < 1. \tag{2.152}$$

This last result is known as the **Guinier function** and is the basis for determining the radius of gyration from small-angle scattering experiments for objects with unknown form factor.

### 2.8.4 Debye function

Debye first calculated the form factor for scattering from an ideal chain in 1947. This form factor will be useful in interpretation of a wide variety of scattering experiments on polymers. The form factor for an ideal linear chain is obtained by averaging the form factor of isotropic scatterers [Eq. (2.143)] over the probability distribution for distances $R_{ij}$ between monomers $i$ and $j$ on the ideal chain:

$$P(q) = \frac{1}{N^2}\sum_{i=1}^{N}\sum_{j=1}^{N}\int_0^\infty \frac{\sin(qR_{ij})}{qR_{ij}} P_{3d}(|i-j|, R_{ij})\, 4\pi R_{ij}^2\, \mathrm{d}R_{ij}. \tag{2.153}$$

The probability distribution function $P_{3d}(|i-j|, R_{ij})$ is given by Eq. (2.86):

$$P_{3d}(|i-j|, R_{ij})4\pi R_{ij}^2\, \mathrm{d}R_{ij} = 4\pi\left(\frac{3}{2\pi|i-j|b^2}\right)^{3/2} \exp\left(-\frac{3R_{ij}^2}{2|i-j|b^2}\right) R_{ij}^2\, \mathrm{d}R_{ij}. \tag{2.154}$$

The integral over $R_{ij}$ can be evaluated by converting it into a Gaussian integral (by writing the complex representation of sine and completing the square in the exponent):

$$\int_0^\infty R_{ij} \sin(qR_{ij}) \exp\left(-\frac{R_{ij}^2}{x}\right) \mathrm{d}R_{ij} = \frac{\pi^{1/2} q x^{3/2}}{4} \exp\left(-\frac{q^2 x}{4}\right). \tag{2.155}$$

The variable

$$x = \frac{2|i-j|b^2}{3} \tag{2.156}$$

was defined for convenience and the form factor for an ideal linear chain becomes a double sum of exponentials:

$$P(q) = \frac{1}{N^2}\sum_{i=1}^{N}\sum_{j=1}^{N} \exp\left(-\frac{q^2 b^2 |i-j|}{6}\right). \tag{2.157}$$

Replacing the summations over monomer indices by integrations provides the integral form of the form factor of an ideal chain:

$$P(q) = \frac{1}{N^2}\int_0^N \left[\int_0^N \exp\left(-\frac{q^2b^2}{6}|u-\mathrm{v}|\right)\mathrm{d}u\right]\mathrm{dv}. \tag{2.158}$$

Next, we change the variables of integration $s \equiv u/N$ and $t \equiv \mathrm{v}/N$ and denote the coefficient in the exponent by $Q \equiv q^2b^2N/6 = q^2\langle R_g^2\rangle$ [we have used Eq. (2.54) for the radius of gyration of an ideal linear chain].

$$\begin{aligned}
P(q) &= \int_0^1 \left[\int_0^1 \exp(-Q|s-t|)\,\mathrm{d}s\right]\mathrm{d}t \\
&= \int_0^1 \left[\int_0^t \exp[-Q(t-s)]\,\mathrm{d}s + \int_t^1 \exp[-Q(s-t)]\,\mathrm{d}s\right]\mathrm{d}t \\
&= \int_0^1 \left[\exp(-Qt)\int_0^t \exp(Qs)\,\mathrm{d}s + \exp(Qt)\int_t^1 \exp(-Qs)\,\mathrm{d}s\right]\mathrm{d}t \\
&= \frac{1}{Q}\int_0^1 [\exp(-Qt)(\exp(Qt)-1) - \exp(Qt)(\exp(-Q)-\exp(-Qt))]\,\mathrm{d}t \\
&= \frac{1}{Q}\int_0^1 [2-\exp(-Qt)-\exp(-Q)\exp(Qt)]\,\mathrm{d}t \\
&= \frac{1}{Q}\left[2+\frac{\exp(-Q)-1}{Q} - \exp(-Q)\frac{\exp(Q)-1}{Q}\right] \\
&= \frac{2}{Q^2}[\exp(-Q)-1+Q].
\end{aligned} \tag{2.159}$$

This form factor of an ideal linear polymer is called the **Debye function** and can be rewritten in terms of the product of the square of scattering wavevector $q^2$ and the mean-square radius of gyration of the chain $\langle R_g^2\rangle$:

$$P(q) = \frac{2}{(q^2\langle R_g^2\rangle)^2}\,[\exp(-q^2\langle R_g^2\rangle) - 1 + q^2\langle R_g^2\rangle]. \tag{2.160}$$

The Debye function is plotted in Fig. 2.20.

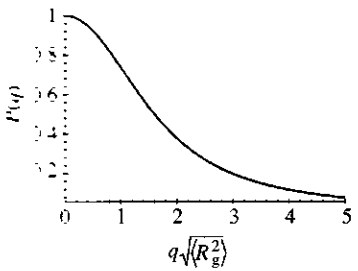


**Fig. 2.20**
The Debye function is the form factor of an ideal linear chain.

In the limit of small scattering angles, where $qR_g < 1$, the exponential can be expanded to simplify the Debye function:

$$\begin{aligned}
P(q) &\cong \frac{2}{(q^2\langle R_g^2\rangle)^2} \\
&\quad\times\left[1 - q^2\langle R_g^2\rangle + \frac{(q^2\langle R_g^2\rangle)^2}{2} - \frac{(q^2\langle R_g^2\rangle)^3}{6} + \cdots - 1 + q^2\langle R_g^2\rangle\right] \\
&\cong \left(1 - \frac{q^2\langle R_g^2\rangle}{3} + \cdots\right) \quad \text{for } q\sqrt{\langle R_g^2\rangle} < 1.
\end{aligned} \tag{2.161}$$

Note that we recover Eq. (2.146) for a general form factor for small values of $q\sqrt{\langle R_g^2\rangle}$.

At large scattering angles, the form factor describes the conformations of smaller sections of the chain on length scales $1/q < \sqrt{\langle R_g^2\rangle}$:

$$P(q) = \frac{2}{\left(q^2\langle R_g^2\rangle\right)^2}\left[\exp\left(-q^2\langle R_g^2\rangle\right) - 1 + q^2\langle R_g^2\rangle\right]$$
$$\cong \frac{2}{q^2\langle R_g^2\rangle} \quad \text{for } q\sqrt{\langle R_g^2\rangle} > 1. \tag{2.162}$$

This power law character of the form factor is related to the power law decay of the pair correlation function of an ideal chain [Eq. (2.121)]. Quite generally, the form factor is related to the Fourier transform of the intramolecular pair correlation function $g(r)$:

$$P(\vec{q}) = \frac{1}{N}\left[1 + \int g(\vec{r})\exp(i\vec{q}\cdot\vec{r})\,d^3r\right] \tag{2.163}$$

Equation (2.162) is a special case for a form factor of a fractal (with fractal dimension $\mathcal{D} = 2$). For any fractal, the wavevector dependence of the form factor gives a direct measure of the fractal dimension $\mathcal{D}$:

$$P(q) \sim \left(q\sqrt{\langle R_g^2\rangle}\right)^{-\mathcal{D}} \quad \text{for } q\sqrt{\langle R_g^2\rangle} > 1. \tag{2.164}$$

The reciprocal form factor $1/P(q)$ for a ideal linear chain [Eq. (2.160)] is shown in Fig. 2.21 as a function of $q^2\langle R_g^2\rangle$ (medium line) and is compared with the reciprocal form factors for a rigid rod (thin line) and for a solid sphere (thick line). The form factors of a rod,

$$P(q) = \frac{1}{\sqrt{3}qR_g}\int_0^{\sqrt{12}qR_g}\frac{\sin t}{t}\,dt - \left(\frac{\sin(\sqrt{3}qR_g)}{\sqrt{3}qR_g}\right)^2, \tag{2.165}$$

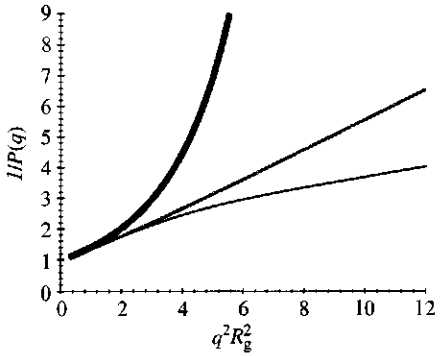


**Fig. 2.21**
Reciprocal form factors for simple objects: a solid sphere [Eq. (2.166), thick curve], an ideal linear chain [reciprocal Debye function, Eq. (2.160), medium line], and a rigid rod [Eq. (2.165), thin curve].

and a sphere,

$$P(q)=\left(\frac{3}{(\sqrt{5/3}qR_g)^3}[\sin(\sqrt{5/3}qR_g)-(\sqrt{5/3}qR_g)\cos(\sqrt{5/3}qR_g)]\right)^2, \tag{2.166}$$

are derived in Problems 2.44 and 2.45. Since all curves are plotted in Fig. 2.21 as functions of $q^2\langle R_g^2\rangle$, the initial slope of all of them is the same and is equal to 1/3 [see Eq. (2.146)].

The Debye function describes the $q$ dependence of scattering data from dilute solutions of ideal chains. Such dilute solutions can either be obtained in a $\theta$-solvent or by having a dilute solution of ordinary chains in a melt of perdeuterated chains. Small-angle neutron scattering data for four dilute concentrations of poly(methyl methacrylate) (PMMA with $M_w$= 250 000 g/mol$^{-1}$) in perdeuterated PMMA are shown to be fit by the Debye function in Fig. 2.22. Two parameters are used in the fits, $R_g = 13.3$ nm and a multiplicative intensity scale factor.

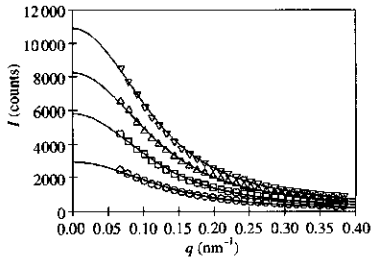


**Fig. 2.22**
Small-angle neutron scattering data fit to the Debye function multiplied by a zero wavevector scattering. Data are for 0.31% (circles), 0.63% (squares), 0.93% (triangles), and 1.19% (upside down triangles) PMMA with $M_w = 250\,000$ g mol$^{-1}$ in a melt of perdeuterated PMMA, from R. Kirste *et al.*, *Polymer* **16**, 120 (1975).

## 2.9 Summary of ideal chains

Polymers with no interactions between monomers separated by many bonds along the chain are called ideal chains. Chains are nearly ideal in polymer solutions at a special compensation temperature (the θ-temperature) as well as in polymer melts.

The mean-square end-to-end distance for an ideal chain with $n$ main-chain bonds of length $l$ is $\langle R^2\rangle = C_n n l^2$, where $C_n$ is called Flory's characteristic ratio. For long chains, this characteristic ratio converges to $C_\infty$, leading to a simple expression for the mean-square end-to-end distance of any long ideal linear chain:

$$\langle R^2\rangle \cong C_\infty n l^2. \tag{2.167}$$

It is convenient to define the Kuhn monomer of length $b$ and the number of Kuhn monomers $N$ such that the mean-square end-to-end distance of an ideal linear chain is a freely jointed chain of Kuhn monomers:

$$\langle R^2\rangle = Nb^2. \tag{2.168}$$

The mean-square radius of gyration is defined as the averaged square distance from all monomers to the center of mass of the polymer [Eq. (2.44)] and is related to the averaged square distance between all pairs of monomers [Eq. (2.48)]. The mean-square radius of gyration of an ideal linear polymer is one-sixth of its mean-square end-to-end distance:

$$\langle R_g^2\rangle = Nb^2/6. \tag{2.169}$$

The radius of gyration of ideal branched polymers can be calculated using the Kramers theorem [Eq. (2.65)].

The probability distribution of the end-to-end vector of an ideal chain is well described by the Gaussian function:

$$P_{3d}(N,\vec{R}) = \left(\frac{3}{2\pi Nb^2}\right)^{3/2} \exp\left(-\frac{3\vec{R}^2}{2Nb^2}\right) \quad \text{for } |\vec{R}| \ll R_{max} = Nb. \tag{2.170}$$

The free energy of an ideal chain is purely entropic and changes quadratically with the end-to-end vector:

$$F = \frac{3}{2}kT\frac{\vec{R}^2}{Nb^2} \quad \text{for } |\vec{R}| \ll Nb. \tag{2.171}$$

The quadratic form of the free energy implies a linear relationship between force and the end-to-end vector, that is valid for small extensions:

$$\vec{f} = \frac{3kT}{Nb^2}\vec{R} \quad \text{for } |\vec{R}| \ll Nb. \tag{2.172}$$

Thus, the ideal chain can be thought of as an entropic spring and obeys Hooke's law for elongations much smaller than the maximum elongation ($|\vec{R}| \ll R_{max} = bN$). For stronger deformations, the Langevin function [Eq. (2.112)] for freely jointed chains or Eq. (2.119) for worm-like chains can be used to describe the non-linear relation between force and elongation.

The probability to find a monomer within a distance $r$ of a given monomer is called the pair correlation function $g(r)$. For ideal linear chains, $g(r)$ is reciprocally proportional to the distance $r$:

$$g(r) = \frac{3}{\pi r b^2}. \tag{2.173}$$

The radius of gyration of any polymer can be determined from the wavevector $q$ dependence of the scattering intensity at low angles ($qR_g < 1$) in the limit of zero concentration:

$$P(q) = 1 - \frac{1}{3}q^2\langle R_g^2\rangle + \cdots \quad \text{for } q\sqrt{\langle R_g^2\rangle} < 1. \tag{2.174}$$

Distributions of monomers and correlations between them inside the chain can be determined from the angular dependence of scattering intensity in the range of higher wavevectors $q\sqrt{\langle R_g^2\rangle} > 1$:

$$P(q) \sim \left(q\sqrt{\langle R_g^2\rangle}\right)^{-\mathcal{D}} \quad \text{for } q\sqrt{\langle R_g^2\rangle} > 1, \tag{2.175}$$

where $\mathcal{D}$ is the fractal dimension of the polymer ($\mathcal{D} = 2$ for ideal chains). The Debye function is the form factor for scattering from an ideal linear chain:

$$P(q) = \frac{2}{(q^2\langle R_g^2\rangle)^2}\left[\exp(-q^2\langle R_g^2\rangle) - 1 + q^2\langle R_g^2\rangle\right]. \tag{2.176}$$

## Problems

### Section 2.2

**2.1** Prove that $\langle \cos\theta_{ij} \rangle = 0$ for the angle $\theta_{ij}$ between two bonds $i$ and $j$ if there are no correlations between bond vectors (see Fig. 2.3).

**2.2** Calculate the mean-square end-to-end distance of atactic polystyrene with degree of polymerization 100 assuming that it is an ideal chain with characteristic ratio $C_\infty = 9.5$. (Note that the characteristic ratio is defined in terms of the main-chain bonds of length $l = 1.54$ Å rather than monomers.)

**2.3** Calculate the root-mean-square end-to-end distance for polyethylene with $M = 10^7\,\mathrm{g\,mol^{-1}}$ in an ideal conformation with $C_\infty = 7.4$. Compare the end-to-end distance with the contour length of this polymer.

### Section 2.3

**2.4** Calculate Flory's characteristic ratio $C_n$ for a freely rotating chain consisting of $n$ bonds of length $l$ with bond angle $\theta$. Plot $C_n/C_\infty$ as a function of $n$ for bond angles $\theta = 68°$ and $10°$.

**2.5** Calculate the Kuhn monomer length $b$ and number of Kuhn monomers $N$ of a freely rotating chain consisting of $n$ bonds of length $l$ with angle $\theta$.

**2.6** Consider a restricted random walk on a square lattice. Let us assume that a walker is not allowed to step back (but can go forward, turn right, or turn left with equal probability). Calculate the mean-square end-to-end distance for such a restricted $n$-step random walk. What is the characteristic ratio $C_\infty$ for this walk? The lattice constant is equal to $l$.

**2.7** Consider a restricted random walk on a 3D cubic lattice. Let us assume that a walker is not allowed step back (but can go forward, turn up, down, right, or left with equal probability). The lattice constant is equal to $l$.

(i) Calculate the mean-square end-to-end distance for such a restricted $n$-step random walk.
(ii) What is the $C_\infty$ for this walk?

*Hint*: Recall for a freely rotating chain $C_\infty = (1 + \cos\theta)/(1 - \cos\theta)$.

**2.8*** Demonstrate that the mean-square end-to-end distance of a worm-like chain with contour length $R_{\max}$ and persistence length $l_p$ is

$$\langle R^2 \rangle = 2R_{\max}l_p - 2l_p^2\left(1 - \exp\left(-\frac{R_{\max}}{l_p}\right)\right), \tag{2.177}$$

and the mean-fourth end-to-end distance is

$$\begin{aligned}\langle R^4 \rangle = {} & \frac{20}{3}R_{\max}^2 l_p^2 - \frac{208}{9}R_{\max}l_p^3 - \frac{8}{27}l_p^4\left(1 - \exp\left(-\frac{3R_{\max}}{l_p}\right)\right) \\ & + 32l_p^4\left(1 - \exp\left(-\frac{R_{\max}}{l_p}\right)\right) - 8R_{\max}l_p^3\exp\left(-\frac{R_{\max}}{l_p}\right).\end{aligned} \tag{2.178}$$

**2.9*** Derive the characteristic ratio of the hindered rotation model [Eq. (2.40)].

**2.10** What are the common features of all models for ideal linear chains?

### Section 2.4

**2.11** The radius of gyration of a polystyrene molecule ($M_w = 3\times 10^7\,\mathrm{g\,mol^{-1}}$) was found to be $R_g = 1010$ Å. Estimate the overlap concentration $c^*$ in $\mathrm{g\,cm^{-3}}$, assuming that the pervaded volume of the chain is a sphere of radius $R_g$.

**2.12** Consider a polymer containing $N$ Kuhn monomers (of length $b$) in a dilute solution at the $\theta$-temperature, where ideal chain statistics apply.

Answer questions (i)–(vi) symbolically before substituting numerical values.

(i) What is the mean-square end-to-end distance $R_0^2$ of the polymer?
(ii) What is its fully extended length $R_{max}$?
(iii) What is the mean-square radius of gyration $R_g^2$ of this polymer?

The molar mass of the polymer is $M$

(iv) Estimate the overlap concentration $c^*$ for this polymer, assuming that the pervaded volume of the chain is a sphere of radius $R_g$. (*Hint*: It is of the order of the concentration inside the coil.)
(v) How does this overlap concentration depend on the degree of polymerization?
(vi) What is the ratio of its fully extended length to the average (root-mean-square) end-to-end distance $R_{max}/R_0$?
(vii) Consider an example of a polymer with molar mass $M = 10^4\,\mathrm{g\,mol^{-1}}$ consisting of $N = 100$ Kuhn monomers (of length $b = 10\,\text{Å}$) and determine $R_0$, $R_g$, $R_{max}$, $c^*$ and $R_{max}/R_0$.

**2.13** One property of an ideal chain is that its subsections are also ideal. Derive the general relation between the end-to-end distance of the chain $R$, the end-to-end distance of the section $\xi$, the number of monomers in the chain $N$ and the number of monomers in the section $g$.

**2.14** The previous problem showed that the equivalent freely jointed chain follows random walk statistics even if the effective monomer is renormalized to be larger than $b$. What is the smallest effective monomer size for which this renormalization works?

**2.15** Calculate the radius of gyration of a rod polymer with $N$ monomers of length $b$ using Eq. (2.51).

**2.16** Calculate the radius of gyration of a uniform disc of radius $R$ and negligible thickness.

**2.17** Calculate the radius of gyration of a uniform sphere of radius $R$.

**2.18** Calculate the radius of gyration of a uniform right cylinder of radius $R$ and length $L$.

**2.19** Consider a fractal line with fractal dimension $\mathcal{D}$. The mean-square distance between monomers $u$ and v along this line is

$$\langle(\vec{R}(u) - \vec{R}(\mathrm{v}))^2\rangle = b^2(\mathrm{v} - u)^{2/\mathcal{D}}. \tag{2.179}$$

Calculate the mean-square end-to-end distance $R^2$ and radius of gyration $R_g^2$ for this fractal line. Determine the ratio $R^2/R_g^2$ symbolically and then calculate this ratio for fractal dimensions $\mathcal{D} = 1$, 1.7 and 2.

**2.20** Show that the mean-square radius of gyration of a worm-like chain is

$$\langle R_g^2\rangle = \frac{1}{3}R_{max}l_p - l_p^2 + \frac{2l_p^3}{R_{max}} - \frac{2l_p^4}{R_{max}^2}\left(1 - \exp\left(-\frac{R_{max}}{l_p}\right)\right). \tag{2.180}$$

Verify that in the two simple limits (ideal chains $R_{max} \gg l_p$ and rigid rods $R_{max} \ll l_p$) the correct limiting expressions for the radius of gyration are recovered.

**2.21** Calculate the radius of gyration of an ideal symmetric $f$-arm star polymer with $N$ monomers of length $b$. *Hint*: Each arm of a symmetric star polymer can be treated as an ideal chain of $N/f$ monomers.

**2.22** Calculate the radius of gyration of an ideal H-polymer with all five sections containing equal number ($N/5$) of Kuhn monomers with length $b$.

**2.23**
(i) Calculate the radius of gyration of an asymmetric three arm star polymer with a short arm consisting of $n = N/4$ Kuhn monomers of length $b$ and two equal long arms containing $3N/8$ Kuhn monomers each.

(ii) Evaluate $R_g$ of this asymmetric star for $N = 1000$, $n = 250$, and $b = 3$ Å.
(iii) What length of the asymmetric arm $n$ corresponds to the largest and smallest radii of gyration of a star polymer for constant $N$ and $b$?

**2.24** Consider an ideal $f$-arm star with $n_j$ Kuhn monomers in the $j$th arm ($j = 1,2,\ldots,f$) and with Kuhn length $b$. The total number of Kuhn monomers in a molecule is $N = \sum_{j=1}^{f} n_j$. Show that the mean-square radius of gyration of this star is

$$\langle R_g^2 \rangle = Nb^2 \left( \frac{1}{2N^2} \sum_{j=1}^{f} n_j^2 - \frac{1}{3N^3} \sum_{j=1}^{f} n_j^3 \right). \tag{2.181}$$

**2.25*** Consider a tree polymer consisting of $f$ branches (but no loops). Each of these branches contains $N/f$ Kuhn monomers with Kuhn length $b$. Let $v_{ij}$ be the number of branches along the linear chain connecting branch $i$ and branch $j$. Demonstrate that the mean-square radius of gyration of this polymer is

$$\langle R_g^2 \rangle = Nb^2 \left( \frac{1}{2f} - \frac{1}{3f^2} + \frac{1}{f^3} \sum_{i=1}^{f} \sum_{j=i+1}^{f} v_{ij} \right). \tag{2.182}$$

**2.26*** Calculate the radius of gyration of an ideal ring polymer with $N$ Kuhn monomers of length $b$, and compare it to the radius of gyration of a linear chain with the same number of monomers.

**2.27** The radius of gyration of a spherical globule containing a single polymer and some solvent is 450 Å. Calculate the polymer density inside this globule if the molar mass of the polymer is $M = 2.6 \times 10^7\ \mathrm{g\,mol^{-1}}$.

## Section 2.5

**2.28** Derive Stirling's approximation for large $N$:

$$N! \cong \sqrt{2\pi N} N^N \exp(-N). \tag{2.183}$$

**2.29** Demonstrate that the Gaussian probability distribution function of a one-dimensional random walk is normalized to unity:

$$\int_{-\infty}^{\infty} P_{1d}(N,x)\,dx = \frac{1}{\sqrt{2\pi N}} \int_{-\infty}^{\infty} \exp\left(\frac{-x^2}{2N}\right) dx = 1. \tag{2.184}$$

**2.30** Show that the mean-square displacement of a one-dimensional random walker is

$$\int_{-\infty}^{\infty} x^2 P_{1d}(N,x)\,dx = \frac{1}{\sqrt{2\pi N}} \int_{-\infty}^{\infty} x^2 \exp\left(-\frac{x^2}{2N}\right) dx = N. \tag{2.185}$$

**2.31** Suppose a person walks from the origin in one dimension forward or backward. The probability for a step in each direction is 1/2. What is the probability of finding the person five steps ($x = 5$) forward from the origin after $N = 25$ steps.

**2.32** Calculate the location of the maximum of the distribution of end-to-end distances (Fig. 2.12) of an ideal chain with $N$ Kuhn monomers of length $b$.

**2.33** Calculate the average end-to-end distance of an ideal linear chain with $N$ Kuhn monomers of length $b$.

**2.34*** Demonstrate that the higher moments of the end-to-end vector of an ideal chain with $N$ Kuhn monomers of length $b$ is

$$\langle \vec{R}^{2p} \rangle = \frac{(2p+1)!}{6^p p!} (Nb^2)^p \tag{2.186}$$

within the Gaussian approximation [with probability distribution Eq. (2.85)].

**2.35*** Show that the mean-square distance of the $j$th monomer from the centre of mass of an ideal chain with $N$ Kuhn monomers of length $b$ is

$$\langle(\vec{R}_j - \vec{R}_{cm})^2\rangle = \frac{Nb^2}{3}\left[1 - \frac{3j(N-j)}{N^2}\right] \tag{2.187}$$

within the Gaussian approximation. What are the maximum and minimum values of this mean-square distance?

**2.36*** The mean-square radius of gyration is the second moment of the distribution of monomers around the centre of mass of the chain [Eq. (2.44)]. The mean-square radius of gyration of an ideal linear chain with $N$ Kuhn monomers of length $b$ is related to its mean-square end-to-end vector [Eq. (2.54)]:

$$\langle R_g^2\rangle = \frac{1}{N}\sum_{i=1}^{N}\langle(\vec{R}_i - \vec{R}_{cm})^2\rangle = \frac{1}{6}\langle\vec{R}^2\rangle. \tag{2.188}$$

(i) Show that higher moments of the distribution of monomers around the centre of mass are related to the corresponding higher moments of the end-to-end vector:

$$\frac{1}{N}\sum_{i=1}^{N}\langle(\vec{R}_i - \vec{R}_{cm})^4\rangle = \frac{1}{18}(Nb^2)^2 = \frac{1}{30}\langle\vec{R}^4\rangle, \tag{2.189}$$

$$\frac{1}{N}\sum_{i=1}^{N}\langle(\vec{R}_i - \vec{R}_{cm})^6\rangle = \frac{29}{972}(Nb^2)^3 = \frac{29}{3780}\langle\vec{R}^6\rangle. \tag{2.190}$$

(ii) Demonstrate that higher moments of the radius of gyration are

$$\left\langle\left[\frac{1}{N}\sum_{i=1}^{N}\left(\vec{R}_i - \vec{R}_{cm}\right)^2\right]^2\right\rangle = \frac{19}{540}(Nb^2)^2 = \frac{19}{15}\langle R_g^2\rangle^2, \tag{2.191}$$

$$\left\langle\left[\frac{1}{N}\sum_{i=1}^{N}\left(\vec{R}_i - \vec{R}_{cm}\right)^2\right]^3\right\rangle = \frac{631}{68040}(Nb^2)^3 = \frac{631}{315}\langle R_g^2\rangle^3. \tag{2.192}$$

**2.37*** Consider an ideal linear chain with $N$ Kuhn monomers of length $b$ and fixed end-to-end vector $\vec{R}$ directed along the $x$ axis. Demonstrate that the mean-square projection of the radius of gyration onto the direction of its end-to-end vector is

$$\frac{1}{N}\sum_{i=1}^{N}\langle(\vec{R}_i - \vec{R}_{cm})_x^2\rangle = \frac{1}{36}Nb^2\left(1 + \frac{3\vec{R}^2}{Nb^2}\right), \tag{2.193}$$

while the mean-square projection of the radius of gyration onto the perpendicular direction is independent of the magnitude of the end-to-end vector

$$\frac{1}{N}\sum_{i=1}^{N}\langle(\vec{R}_i - \vec{R}_{cm})_y^2\rangle = \frac{1}{N}\sum_{i=1}^{N}\langle(\vec{R}_i - \vec{R}_{cm})_z^2\rangle = \frac{1}{36}Nb^2. \tag{2.194}$$

Note that for $|\vec{R}| = 0$ the mean-square radius of gyration of a ring polymer $\langle R_g^2\rangle = Nb^2/12$ is recovered, for $|\vec{R}| = bN^{1/2}$ the mean-square

radius of gyration of an ideal linear chain $\langle R_g^2 \rangle = Nb^2/6$ is recovered, and for $|\vec{R}| = bN$ the mean-square radius of gyration of a rod $\langle R_g^2 \rangle \cong (Nb)^2/12$ is recovered. It is interesting to point out that the asymmetry of the ideal linear chain,

$$\left(1 + \frac{3\vec{R}^2}{Nb^2}\right),$$

is quite large and a typical shape is better represented by an elongated ellipsoid than by a sphere.

**2.38*** Show that the one-dimensional probability of finding a monomer of an ideal chain whose ends are fixed at positions $X_1$ and $X_2$ is the following Gaussian function.

$$P_{1d}(s, x) = \sqrt{\frac{3}{2\pi K_s b^2}} \exp\left(-\frac{3(x - x_s)^2}{2K_s b^2}\right). \tag{2.195}$$

Written in this way, the position of the monomer that is $s$ monomers from the end of the chain at $X_1$ is described as though that monomer was the end monomer of a single 'effective chain' of

$$K_s = \frac{1}{1/s + 1/(N - s)} = \frac{s(N - s)}{N} \tag{2.196}$$

monomers, whose other end is at position

$$x_s = X_1 \frac{N - s}{N} + X_2 \frac{s}{N}. \tag{2.197}$$

**2.39** Consider a linear chain consisting of $m + N$ monomers. The ends of this chain are fixed in space. The $x$ coordinates of the ends are $X_1'$ and $X_2'$, while the junction point fluctuates with $x$ coordinate $R'$. What is the mean-square $x$ coordinate of the end-to-end vector of the section containing $N$ monomers $\langle (R' - X_2')^2 \rangle$?

## Section 2.6

**2.40** Consider an ideal chain with $N$ Kuhn monomers of length $b$. The chain is carrying a positive charge $+e$ at one end and a negative charge $-e$ at the other end. What will be its average end-to-end distance $R_x$ in an electric field $E = 10^4$ V cm$^{-1}$ acting along the $x$ axis at room temperature, if $N = 10^4$ and $b = 6$ Å? What is the ratio of this average distance $R_x$ and root-mean-square projection $R_{x0}$ of the end-to-end vector along the $x$ axis in the absence of the field? Ignore the direct Coulomb interaction between the charges.

**2.41** Consider an ideal chain with $N$ Kuhn monomers of length $b$. The chain has two multivalent positive charges $+Ze$ at both of its ends (it is called a telechelic polymer). These two charges repel each other and stretch the polymer.

(i) What is the expression for the average distance $R$ between the chain ends in a polar solvent with dielectric constant $\epsilon$ at temperature $T$ (in terms of $Z$, $e$, $N$, $b$, $T$, $\epsilon$, etc.)?

(ii) What is the ratio of this average distance $R$ and the root-mean-square projection of the end-to-end vector along the $x$ axis $R_{x0}$ in the absence of Coulomb interaction for the chain with $N = 100$ Kuhn monomers

of length $b = 3$ Å in water (dielectric constant $\epsilon = 80$) at room temperature (20 °C) for charges of valency $Z = 10$?

*Hint*: The Coulomb force between two charges $+Ze$ separated by distance $R$ in a solution with dielectric constant $\epsilon$ is $(Ze)^2/(\epsilon R^2)$.

In order to avoid complicated conversions of units note that a combination of variables, called the Bjerrum length, is $l_B = e^2/(\epsilon kT) \cong 7$ Å in water at room temperature.

**2.42*** Demonstrate that the probability distribution function of the end-to-end distance $R$ of a freely jointed chain can be expressed in terms of the inverse Langevin function $\mathcal{L}^{-1}(x)$ of the ratio $x = R/R_{max}$ of the end-to-end distance $R$ to its maximum value $R_{max} = Nb$:

$$P(R) = \frac{[\mathcal{L}^{-1}(x)]^2}{(2\pi Nb^2)^{3/2} x\{1 - [\mathcal{L}^{-1}(x)\,\mathrm{csch}\,\mathcal{L}^{-1}(x)]^2\}^{1/2}} \times \left\{\frac{\sinh \mathcal{L}^{-1}(x)}{\mathcal{L}^{-1}(x)\exp[x\mathcal{L}^{-1}(x)]}\right\}^N. \tag{2.198}$$

Compare this distribution function with the Gaussian approximation [Eq. (2.85)].

**2.43** What is the difference between the probability distribution function and the pair correlation function?

## Section 2.8

**2.44** Calculate the form factor of a uniform sphere of radius $R$.

**2.45** Calculate the form factor of a long thin rod of length $L$.

**2.46** (i) Use the tabulated small-angle neutron scattering data[5] for a 1% solution of $M = 254\,000$ g mol$^{-1}$ deuterium-labelled polystyrene in $M = 110\,000$ g mol$^{-1}$ ordinary polystyrene to determine the radius of gyration by fitting the data to the Debye function [Eq. (2.160)].

(ii) Why is the Guinier limit [Eq. (2.146) or (2.152)] not useful for determining $R_g$ for these data?

(iii) If Eq. (2.146) were used to estimate $R_g$ from the five lowest $q$ data points, is $R_g$ overestimated or underestimated? Why?

| | | | | | | | |
|---|---|---|---|---|---|---|---|
| $q$ (1/Å) | 0.00980 | 0.0128 | 0.0158 | 0.0188 | 0.0218 | 0.0248 | 0.0278 |
| $I(q)$ | 4.43 | 3.37 | 2.55 | 2.05 | 1.58 | 1.23 | 0.966 |
| $q$ (1/Å) | 0.0308 | 0.0338 | 0.0368 | 0.0399 | 0.0429 | 0.0459 | 0.0504 |
| $I(q)$ | 0.804 | 0.758 | 0.592 | 0.509 | 0.445 | 0.370 | 0.275 |
| $q$ (1/Å) | 0.0564 | 0.0624 | 0.0684 | 0.0744 | 0.0804 | 0.0864 | 0.0940 |
| $I(q)$ | 0.246 | 0.197 | 0.175 | 0.139 | 0.128 | 0.107 | 0.081 |
| $q$ (1/Å) | 0.1060 | | | | | | |
| $I(q)$ | 0.077 | | | | | | |

[5] Data from M. R. Landry.

**2.47** In Chapter 1, we learned how to determine weight-average molar mass $M_w$ and second viral coefficient $A_2$ from the concentration dependence of light scattered at a very small angle from a polymer solution. In this chapter, we learned that the angular dependence of light scattering gives information about the radius of gyration $R_g$ of the polymer coil. In practice, these analyses are often combined to obtain $M_w$, $A_2$, and $R_g$ using a **Zimm plot.** The following equation is the basis of the Zimm plot and was obtained by combining the concentration expansion of Eq. (1.96) with the angular expansion of Eq. (2.147):

$$\frac{Kc}{R_\theta} = \left[\frac{1}{M_w} + 2A_2c + \cdots\right]\left[1 + \frac{16\pi^2 n^2}{3\lambda^2} R_g^2 \sin^2\left(\frac{\theta}{2}\right) + \cdots\right]. \tag{2.199}$$

Use the following table of data for $Kc/R_\theta$ of a polystyrene in benzene at four concentrations and five angles, to construct a Zimm plot by plotting $Kc/R_\theta$ against $100c + \sin^2(\theta/2)$ with $c$ in $\mathrm{g\,mL^{-1}}$ and extrapolating to $c \to 0$ and $\theta \to 0$ to determine $M_w$, $A_2$, and $R_g$.

Table of $10^6 Kc/R_\theta$ (in $\mathrm{mol\,g^{-1}}$) for a polystyrene in benzene:

| $c$ ($\mathrm{mg\,mL^{-1}}$) | $\theta = 30°$ | $\theta = 45°$ | $\theta = 60°$ | $\theta = 75°$ | $\theta = 90°$ |
|---|---|---|---|---|---|
| 0.5 | 1.92 | 1.98 | 2.16 | 2.33 | 2.51 |
| 1.0 | 2.29 | 2.37 | 2.53 | 2.66 | 2.85 |
| 1.5 | 2.73 | 2.81 | 2.94 | 3.08 | 3.27 |
| 2.0 | 3.18 | 3.25 | 3.45 | 3.56 | 3.72 |

For the laser used, $\lambda = 546\,\mathrm{nm}$ and the refractive index for light of this wavelength travelling though benzene is $n = 1.5014$. After plotting the 20 data points, the data at each angle must be extrapolated to zero concentration, making a $c = 0$ line of five points (corresponding to the five angles) whose slope determines $R_g$. The data at each concentration must be extrapolated to zero angle, making a $\theta = 0$ line of four points (corresponding to the four concentrations) whose slope determines $A_2$. Both the $c = 0$ line and the $\theta = 0$ line should have the same intercept, which is the weight-average molar mass $M_w$.

**2.48** Calculate the radius of gyration and the mean-square end-to-end distance of an ideal linear diblock copolymer consisting of $N_1$ Kuhn monomers of length $b_1$ connected at one end to $N_2$ Kuhn monomers of length $b_2$.

## Bibliography

Doi, M. *Introduction to Polymer Physics* (Clarendon Press, Oxford, 1996).

Flory, P. J. *Statistical Mechanics of Chain Molecules* (Wiley, New York, 1969).

Higgins, J. S. and Benoit, H. C. *Polymers and Neutron Scattering* (Clarendon Press, Oxford, 1994).

Yamakawa, H. *Modern Theory of Polymer Solutions* (Harper and Row, New York, 1971).

# Real chains

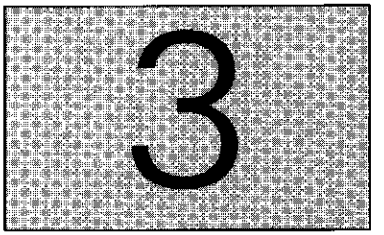


In Chapter 2, we studied the conformations of an ideal chain that ignore interactions between monomers separated by many bonds along the chain. In this chapter we study the effect of these interactions on polymer conformations. To understand why these interactions are often important, we need to estimate the number of monomer–monomer contacts within a single coil. This number depends on the probability for a given monomer to encounter any other monomer that is separated from it by many bonds along the polymer.

A mean-field estimate of this probability can be made for the general case of an ideal chain in $d$-dimensional space by replacing a chain with an ideal gas of $N$ monomers in the pervaded volume of a coil $\sim R^d$. The probability of a given monomer to contact any other monomer within this mean-field approximation is simply the overlap volume fraction $\phi^*$, of a chain inside its pervaded volume, determined as the product of the monomer 'volume' $b^d$ and the number density of monomers in the pervaded volume of the coil $N/R^d$:

$$\phi^* \approx b^d \frac{N}{R^d}. \tag{3.1}$$

Ideal chains obey Gaussian statistics in any dimension with $R = bN^{1/2}$, leading to the overlap volume fraction:

$$\phi^* \approx b^d \frac{N}{(bN^{1/2})^d} \approx N^{1-d/2}. \tag{3.2}$$

The overlap concentration of long ideal coils is very low in spaces with dimension $d$ greater than 2:

$$\phi^* \approx N^{1-d/2} \ll 1 \quad \text{for } d > 2 \text{ and } N \gg 1. \tag{3.3}$$

In particular, in three-dimensional space the probability of a given monomer contacting another monomer on the same chain is $\phi^* \approx N^{-1/2} \ll 1$.

The number of monomer–monomer contacts between pairs of monomers that are far away from each other along the chain, but get close

together in space, is the product of the number of monomers in the chain and the volume fraction of chains in the pervaded volume of the coil:

$$N\phi^* \approx N^{2-d/2}. \tag{3.4}$$

In spaces with dimension above 4, this number is small and monomer–monomer contacts are rare. Therefore, linear polymers are always ideal in spaces with dimension $d > 4$. In spaces with dimension less than 4 (in particular, in three-dimensional space relevant to most experiments), the number of monomer–monomer contacts for a long ideal chain is very large:

$$N\phi^* \approx N^{1/2} \gg 1 \quad \text{for } d = 3 \text{ and } N \gg 1. \tag{3.5}$$

It is important to understand how the energy arising from these numerous contacts affects the conformations of a real polymer chain. The effective interaction between a pair of monomers depends on the difference between a monomer's direct interaction with another monomer and with other surrounding molecules. An attractive effective interaction means that the direct monomer–monomer energy is lower and monomers would rather be near each other than in contact with surrounding molecules. In the opposite case of repulsive effective interactions, monomers 'do not like' to be near each other and prefer to be surrounded by other molecules. In the intermediate case, with zero net interaction, monomers 'do not care' whether they are in contact with other monomers or with surrounding molecules. In this case there is no energetic penalty for monomer–monomer contact and the chain conformation is nearly ideal. In the next section, this qualitative description of the monomer–monomer interaction is quantified.

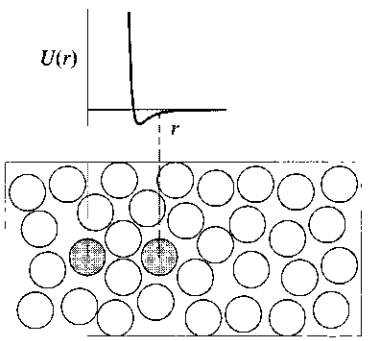


**Fig. 3.1**
Effective interaction potential between two monomers in a solution of other molecules.

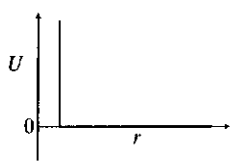


**Fig. 3.2**
The hard-core potential prevents monomers from overlapping.

## 3.1 Excluded volume and self-avoiding walks

### 3.1.1 Mayer $f$-function and excluded volume

Consider the energy cost $U(r)$ of bringing two monomers from $\infty$ to within distance $r$ of each other in a solvent. A typical profile of this function is sketched in Fig. 3.1. It contains a repulsive hard-core barrier that corresponds to the energy cost of steric repulsion of two overlapping monomers. Typical monomers 'like' each other more than they 'like' solvent and therefore there is usually an attractive well corresponding to this energy difference. On the other hand, if monomers are chemically identical to the solvent and there is no energy difference between their interactions, the energy $U(r)$ will contain only the hard-core repulsion (see Fig. 3.2). For reasons that become clear later, in this case the solvent is called **athermal**. On the other hand, if monomers 'like' each other less than surrounding solvent (for example, similarly charged monomers) there is no attractive well in $U(r)$ but instead, extra repulsion.

The probability of finding two monomers separated by a distance $r$ in a solvent at temperature $T$ is proportional to the Boltzmann factor

exp $[-U(r)/(kT)]$ which is plotted in Fig. 3.3 for the potential of Fig. 3.1. The relative probability is zero at short distances, corresponding to the **hard-core repulsion** (it is impossible to find two overlapping monomers). The probability is large in the attractive well (it is energetically more favourable and therefore more likely to find the two monomers at these distances). The Boltzmann factor is equal to one at large distances if there are no long-range interactions.

The **Mayer $f$-function** is defined as the difference between the Boltzmann factor for two monomers at distance $r$ and that for the case of no interaction (or at infinite distance):

$$f(r) = \exp\,[-U(r)/(kT)] - 1. \tag{3.6}$$

At short distances, the energy $U(r)$ is large because of the hard-core repulsion, making the Mayer $f$-function negative. The probability of finding monomers at these distances is significantly reduced relative to the non-interacting case (see Fig. 3.3). The Mayer $f$-function is positive in the attractive well and the probability of finding a second monomer there is enhanced compared to the non-interacting case.

The **excluded volume** v is defined as minus the integral of the Mayer $f$-function over the whole space:

$$\mathrm{v} = -\int f(r)\,\mathrm{d}^3r = \int (1 - \exp\,[-U(r)/(kT)])\,\mathrm{d}^3r. \tag{3.7}$$

This single parameter summarizes the *net* two-body interaction between monomers. As shown in Fig. 3.4, the hard-core repulsion ($r < 1$) makes a negative contribution to the integration of the Mayer $f$-function and a positive contribution to excluded volume. The example in Fig. 3.4 also has an effective attraction between monomers ($r > 1$) that makes a positive contribution to the integration of the Mayer $f$-function and a negative contribution to excluded volume. The attraction and repulsion largely offset each other for this example, making the net excluded volume quite small. A net attraction has a negative excluded volume $\mathrm{v} < 0$ and a net repulsion has $\mathrm{v} > 0$.

### 3.1.1.1 Non-spherical monomers

The simple calculation of excluded volume in Eq. (3.7) is only valid for spherical monomers. Particularly because of the 'monomer' being defined as a Kuhn monomer, the monomer is better described as a cylinder of length equal to the Kuhn length $b$, but smaller diameter $d$, as depicted in Fig. 3.5. Polymers without bulky side groups, such as polyethylene and poly(ethylene oxide), have effective diameter $d \cong 5$ Å. Polystyrene has $d \cong 8$ Å, and the diameter of the cylindrical Kuhn monomer steadily increases as side groups increase in size. Most flexible polymers have aspect ratio $b/d$ in the range 2–3, but this ratio is larger for stiffer polymers.

Excluded volume describes the two-body (pairwise) monomer–monomer interaction in solution. At low polymer concentrations, the interaction

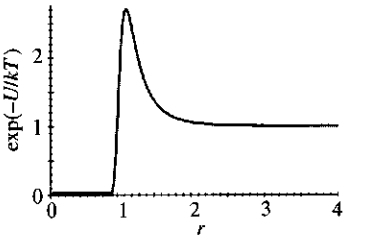


**Fig. 3.3**
The relative probability of finding a second monomer at distance $r$ from a given monomer is given by the Boltzmann factor.

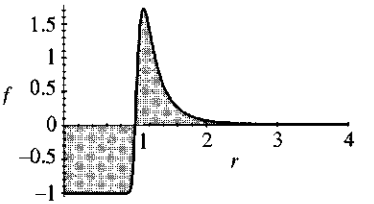


**Fig. 3.4**
The Mayer $f$-function and its integration (shaded regions) to determine excluded volume.

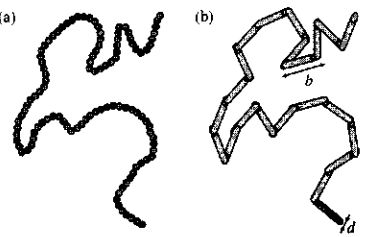


**Fig. 3.5**
(a) Chain with symmetric monomers. (b) Chain with strongly asymmetric cylindrical Kuhn segments of length $b$ and diameter $d$.

part of the free energy density $F_{\text{int}}/V$ can be written as a virial expansion in powers of the **monomer number density** $c_n$. The coefficient of the $c_n^2$ term is proportional to the excluded volume v and the coefficient of the $c_n^3$ term is related to the **three-body interaction coefficient** $w$:

$$\frac{F_{\text{int}}}{V} = \frac{kT}{2}(\mathrm{v}c_n^2 + wc_n^3 + \cdots) \approx kT\left(\mathrm{v}\frac{N^2}{R^6} + w\frac{N^3}{R^9} + \cdots\right). \tag{3.8}$$

This virial expansion is analogous to that used for the osmotic pressure in Chapter 1 [Eq. (1.74)] and we will see in Section 3.3.4, how the excluded volume is related to the second virial coefficient.

For athermal spherical monomers of diameter $d$, $\mathrm{v} \approx d^3$ and $w \approx d^6$. The interaction energy must not change if we redefine what is meant by a monomer. The chain in Fig. 3.5 can be thought of as a chain of $n$ spheres of diameter $d$ or a chain of $N = nd/b$ cylinders of length $b$ and diameter $d$. Each term in the virial expansion must be unchanged by these choices, which requires:

$$\mathrm{v}_s n^2 = \mathrm{v}_c N^2 \quad w_s n^3 = w_c N^3. \tag{3.9}$$

Using the renormalization of $N = nd/b$ and the spherical results $\mathrm{v}_s \approx d^3$ and $w_s \approx d^6$, the cylindrical Kuhn monomer has

$$\mathrm{v}_c \approx \mathrm{v}_s\left(\frac{n}{N}\right)^2 \approx \mathrm{v}_s\left(\frac{b}{d}\right)^2 \approx b^2 d, \tag{3.10}$$

$$w_c \approx w_s\left(\frac{n}{N}\right)^3 \approx w_s\left(\frac{b}{d}\right)^3 \approx b^3 d^3 \tag{3.11}$$

as coefficients in Eq. (3.8). The excluded volume of strongly asymmetric objects (long rods) $\mathrm{v}_c \approx b^2 d$ is much larger than their occupied volume $\mathrm{v}_0 \approx bd^2$, since $b \gg d$. The ratio of excluded volume and occupied volume is the aspect ratio $\mathrm{v}_c/\mathrm{v}_0 = b/d$. If the aspect ratio of the rod polymer is large enough, excluded volume creates nematic liquid crystalline ordering in solutions of rods, originally derived by Onsager. Once the excluded volumes of neighbouring rods overlap, these rods strongly interact and prefer to orient predominantly parallel to neighbouring rods. Similar nematic ordering is seen with polymers as well if the rigidity of the monomers is large enough (making the aspect ratio $b/d$ large). Further discussion of strongly asymmetric monomers is beyond the scope of this book. Here, we focus on flexible polymers, which typically have aspect ratios in the range 2–3. For this reason, we write results below in terms of cylindrical monomers, which reduce to the results for a spherical monomer when $b \approx d$. The spherical monomer results are often used in the rest of this book, owing to the simplicity of a single length scale to describe the monomer. The excluded volume discussed in this book always refers to the excluded volume of a Kuhn monomer. The transformation rules of

Eq. (3.9) can be used to recast the excluded volume in terms of any part of the chain, including the chemical monomer.

(A) *Athermal solvents.* In the high-temperature limit, the Mayer $f$-function has a contribution only from hard-core repulsion. The excluded volume becomes independent of temperature at high temperatures, making the solvent athermal. An example is polystyrene in ethyl benzene (essentially polystyrene's repeat unit). The excluded volume in athermal solvent was derived in Eq. (3.10):

$$\mathrm{v} \approx b^2 d. \tag{3.12}$$

(B) *Good solvents.* In the athermal limit, the monomer makes no energetic distinction between other monomers and solvent. In a typical solvent, the monomer–monomer attraction is slightly stronger than the monomer–solvent attraction because dispersion forces usually favor identical species. Benzene is an example of a good solvent for polystyrene. The net attraction creates a small attractive well $U(r) < 0$ that leads to a lower excluded volume than the athermal value:

$$0 < \mathrm{v} < b^2 d. \tag{3.13}$$

As temperature is lowered, the Mayer $f$-function increases in the region of the attractive well, reducing the excluded volume.

(C) *Theta solvents.* At some special temperature, called the **$\theta$-temperature**, the contribution to the excluded volume from the attractive well exactly cancels the contribution from the hard-core repulsion, resulting in a net zero excluded volume:

$$\mathrm{v} = 0. \tag{3.14}$$

The chains have nearly ideal conformations at the $\theta$-temperature[1] because there is no net penalty for monomer–monomer contact. Polystyrene in cyclohexane at $\theta \cong 34.5\,^{\circ}\mathrm{C}$ is an example of a polymer–solvent pair at the $\theta$-temperature.

(D) *Poor solvents.* At temperatures below $\theta$, the attractive well dominates the interactions and it is more likely to find monomers close together. In such poor solvents the excluded volume is negative signifying an effective attraction:

$$-b^2 d < \mathrm{v} < 0. \tag{3.15}$$

Ethanol is a poor solvent for polystyrene.

(E) *Non-solvents.* The limiting case of the poor solvent is called non-solvent:

$$\mathrm{v} \approx -b^2 d. \tag{3.16}$$

In this limit of strong attraction, the polymer's strong preference for its own monomers compared to solvent nearly excludes all solvent from being

[1] There are actually logarithmic corrections at the $\theta$-temperature that make the chain conformation not quite ideal.

within the coil. Water is a non-solvent for polystyrene, which is why styrofoam coffee cups are made from polystyrene.

In a typical case of the Mayer $f$-function with an attractive well, repulsion dominates at higher temperatures and attraction dominates at lower temperatures. In athermal solvents with no attractive well there is no temperature dependence of the excluded volume. It is possible to have monomer–solvent attraction stronger than the monomer–monomer attraction. In this case, there is a soft barrier in addition to the hard-core repulsion and the excluded volume $\mathrm{v} > b^2 d$ decreases to the athermal value $\mathrm{v} = b^2 d$ at high temperatures.

### 3.1.2 Flory theory of a polymer in a good solvent

The conformations of a real chain in an athermal or good solvent are determined by the balance of the effective repulsion energy between monomers that tends to swell the chain and the entropy loss due to such deformation. One of the most successful simple models that captures the essence of this balance is the **Flory theory**, which makes rough estimates of both the energetic and the entropic contributions to the free energy.

Consider a polymer with $N$ monomers, swollen to size $R > R_0 = bN^{1/2}$. Flory theory assumes that monomers are uniformly distributed within the volume $R^3$ with no correlations between them. The probability of a second monomer being within the excluded volume v of a given monomer is the product of excluded volume v and the number density of monomers in the pervaded volume of the chain $N/R^3$. The energetic cost of being excluded from this volume (the energy of excluded volume interaction) is $kT$ per exclusion or $kT\mathrm{v}N/R^3$ per monomer. For all $N$ monomers in the chain, this energy is $N$ times larger [see the first term of Eq. (3.8) with $V \approx R^3$]:

$$F_{\mathrm{int}} \approx kT\mathrm{v}\frac{N^2}{R^3}. \tag{3.17}$$

The Flory estimate of the entropic contribution to the free energy of a real chain is the energy required to stretch an ideal chain to end-to-end distance $R$ [Eq. (2.101)]:

$$F_{\mathrm{ent}} \approx kT\frac{R^2}{Nb^2}. \tag{3.18}$$

The total free energy of a real chain in the Flory approximation is the sum of the energetic interaction and the entropic contributions:

$$F = F_{\mathrm{int}} + F_{\mathrm{ent}} \approx kT\left(\mathrm{v}\frac{N^2}{R^3} + \frac{R^2}{Nb^2}\right). \tag{3.19}$$

The minimum free energy of the chain (obtained by setting $\partial F/\partial R = 0$) gives the optimum size of the real chain in the Flory

theory, $R = R_F$:

$$\frac{\partial F}{\partial R} = 0 = kT\left(-3v\frac{N^2}{R_F^4} + 2\frac{R_F}{Nb^2}\right),$$
$$R_F^5 \approx vb^2N^3,$$
$$R_F \approx v^{1/5}b^{2/5}N^{3/5}. \tag{3.20}$$

The size of long real chains is much larger than that of ideal chains with the same number of monomers, as reflected in the swelling ratio:

$$\frac{R_F}{bN^{1/2}} \approx \left(\frac{v}{b^3}N^{1/2}\right)^{1/5} \quad \text{for } \frac{v}{b^3}N^{1/2} > 1. \tag{3.21}$$

If the total interaction energy of a chain in its ideal conformation $F_{int}(R_0)$ [Eq. (3.17) for $R = R_0 = bN^{1/2}$] is less than $kT$, the chain will not swell. In this case, $N^{1/2}v/b^3 < 1$ and the chain's conformation remains nearly ideal. Excluded volume interactions only swell the chain when the **chain interaction parameter**,

$$z \equiv \left(\frac{3}{2\pi}\right)^{3/2}\frac{v}{b^3}N^{1/2} \approx \frac{F_{int}(R_0)}{kT} \approx v\frac{N^2}{R_0^3} \approx \frac{v}{b^3}N^{1/2}, \tag{3.22}$$

becomes sufficiently large. Equation (3.20) is therefore only valid for chain interaction parameters that are larger than some number of order unity. The precise value of this number is discussed in Section 3.3.4.

The predictions of the Flory theory are in good agreement with both experiments and with more sophisticated theories (renormalization group theory, exact enumerations and computer simulations). However, the success of the Flory theory is due to a fortuitous cancellation of errors. The repulsion energy is overestimated because the correlations between monomers along the chain are omitted. The number of contacts per chain is estimated to be $b^3N^2/R^3 \approx N^{1/5}$. Computer simulations of random walks with excluded volume show that the number of contacts between monomers that are far apart along the chain does not grow with $N$. Hence, Flory overestimated the interaction energy. The elastic energy is also overestimated in the Flory theory because the ideal chain conformational entropy is assumed. The conformations of real chains are qualitatively different from the ideal chains as will be demonstrated in the remainder of this chapter. Simple modifications of the Flory theory that take into account only some of these effects usually fail. However, Flory theory is useful because it is simple and provides a reasonable answer. We will make calculations in a similar spirit throughout this book. Mean-field estimates of the energetic part of the free energy, ignoring correlations between monomers, are used with entropy estimates based on ideal chain statistics. We will refer to such simple calculations as 'Flory theory' and will hope that the errors will cancel again.

It is important to realize that Flory theory leads to a universal power law dependence of polymer size $R$ on the number of monomers $N$:

$$R \sim N^{\nu} \tag{3.23}$$

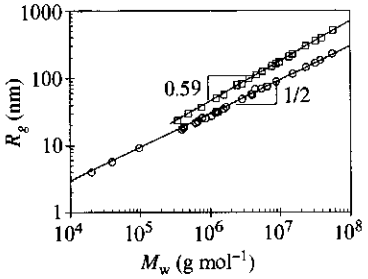


**Fig. 3.6**
Molar mass dependence of the radius of gyration from light scattering in dilute solutions for polystyrenes in a $\theta$-solvent (cyclohexane at $\theta = 34.5\,^{\circ}C$, circles) and in a good solvent (benzene at 25 °C, squares). Data are compiled in L. J. Fetters, *et al.*, *J. Phys. Chem. Ref. Data*, **23**, 619 (1994).

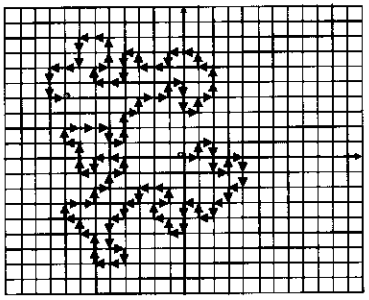

**Fig. 3.7**
A two-dimensional self-avoiding walk on a square lattice. The direction of each step is randomly chosen from four possible directions (up, down, right or left) with the requirement that previously visited sites cannot be visited again.

The quality of solvent, reflected in the excluded volume v, enters only in the prefactor, but does not change the value of the scaling exponent $\nu$ for any $v > 0$. The Flory approximation of the scaling exponent is $\nu = 3/5$ for a swollen linear polymer. For the ideal linear chain the exponent $\nu = 1/2$. In the language of fractal objects, the fractal dimension of an ideal polymer is $\mathcal{D} = 1/\nu = 2$, while for a swollen chain it is lower $\mathcal{D} = 1/\nu = 5/3$. More sophisticated theories lead to a more accurate estimate of the scaling exponent of the swollen linear chain in three dimensions:

$$\nu \cong 0.588. \tag{3.24}$$

Comparison of Eq. (3.23) with experimental data for polystyrenes in cyclohexane at the $\theta$-temperature (a $\theta$-solvent) and in toluene (a good solvent) is shown in Fig. 3.6. Both data sets obey Eq. (3.23), with $\nu = 1/2$ in $\theta$-solvent and $\nu \cong 0.59$ in good solvent.

While the ideal chain discussed in Chapter 2 has a random walk conformation, the real chain has additional correlations because two monomers cannot occupy the same position in space. The real chain's conformation is similar to that of a **self-avoiding walk**, which is a random walk on a lattice that never visits the same site more than once. An example of a self-avoiding walk is shown in Fig. 3.7, on a two-dimensional square lattice.

## 3.2 Deforming real and ideal chains

### 3.2.1 Polymer under tension

In order to emphasize the difference between ideal and real chains, we compare their behaviour under tension. Consider a polymer containing $N$ monomers of size $b$, under tension in two different solvents: a $\theta$-solvent with nearly ideal chain statistics and an athermal solvent with excluded volume $v \approx b^3$. An ideal chain under tension was already discussed in Section 2.6.1 and is repeated for comparison with that of a swollen chain. The major difference between ideal and real chains is that in the latter there are excluded volume interactions between monomers that are far apart along the chain when they approach each other in space.

The end-to-end distances of the chains in the unperturbed state (with no applied external force) are given by Eqs (2.18) and (3.20) with $v \approx b^3$:

$$R_0 \approx bN^{1/2} \quad \text{ideal}, \tag{3.25}$$

$$R_F \approx bN^{3/5} \quad \text{real}. \tag{3.26}$$

Since both ideal and real chains are self-similar fractals, the same scaling applies to subsections of the chains of size $r$ containing $n$ monomers:

$$r \approx bn^{1/2} \quad \text{ideal}, \tag{3.27}$$

$$r \approx bn^{3/5} \quad \text{real}. \tag{3.28}$$

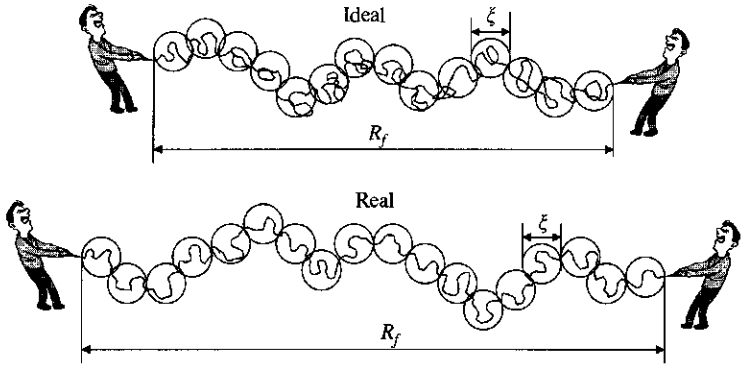


**Fig. 3.8**
Maxwell demons stretching ideal and real chains of the same contour length with the same force $f$.

Note that there are fewer monomers within the same distance $r$ in the real chain case compared with the ideal chain because the real chain is swollen.

Let us now employ Maxwell demons to put both chains under tension with force of magnitude $f$ applied at both ends of each chain, stretching them out as sketched in Fig. 3.8. As in Section 2.6.1, we subdivide each chain into tension blobs of size $\xi$ containing $g$ monomers each, such that on length scales smaller than these tension blobs the chain statistics are unperturbed,

$$\xi \approx bg^{1/2} \quad \text{ideal,} \tag{3.29}$$

$$\xi \approx bg^{3/5} \quad \text{real,} \tag{3.30}$$

while on larger length scales both chains are fully extended arrays of tension blobs.

Since each chain is a stretched array of tension blobs, their end-to-end distance $R_f$ in an extended state is the product of the tension blob size $\xi$ and the number of these blobs $N/g$ per chain:

$$R_f \approx \xi \frac{N}{g} \approx \frac{Nb^2}{\xi} \approx \frac{R_0^2}{\xi} \quad \text{ideal,} \tag{3.31}$$

$$R_f \approx \xi \frac{N}{g} \approx \frac{Nb^{5/3}}{\xi^{2/3}} \approx \frac{R_F^{5/3}}{\xi^{2/3}} \quad \text{real.} \tag{3.32}$$

These equations can be solved for the size of the tension blobs in terms of the normal size ($R_0$ or $R_F$) and stretched size ($R_f$) of the chains:

$$\xi \approx \frac{R_0^2}{R_f} \quad \text{ideal,} \tag{3.33}$$

$$\xi \approx \frac{R_F^{5/2}}{R_f^{3/2}} \quad \text{real.} \tag{3.34}$$

As discussed in Section 2.6.1, the free energy cost for stretching the chains is of the order $kT$ per tension blob (we are neglecting coefficients of order unity):

$$F(N, R_f) \approx kT\frac{N}{g} \approx kT\frac{R_f}{\xi} \approx kT\left(\frac{R_f}{R_0}\right)^2 \quad \text{ideal,} \tag{3.35}$$

$$F(N, R_f) \approx kT\frac{N}{g} \approx kT\frac{R_f}{\xi} \approx kT\left(\frac{R_f}{R_F}\right)^{5/2} \quad \text{real.} \tag{3.36}$$

The force necessary to stretch the chain to end-to-end distance $R_f$ is of the order of the thermal energy $kT$ per tension blob of size $\xi$:

$$f \approx \frac{kT}{\xi} \approx \frac{kT}{R_0^2}R_f \approx \frac{kT}{R_0}\frac{R_f}{R_0} \quad \text{ideal,} \tag{3.37}$$

$$f \approx \frac{kT}{\xi} \approx \frac{kT}{R_F^{5/2}}R_f^{3/2} \approx \frac{kT}{R_F}\left(\frac{R_f}{R_F}\right)^{3/2} \quad \text{real.} \tag{3.38}$$

The same result (up to numerical prefactors of order unity) can be obtained by differentiation of the free energy with respect to end-to-end distance:

$$f = \frac{\partial F(N, R_f)}{\partial R_f}. \tag{3.39}$$

It is very important to notice the difference between the results for ideal and real chains under tension. Ideal chains satisfy Hooke's law with force $f$ linearly proportional to elongation $R_f$. For real chains the dependence of force $f$ on chain elongation $R_f$ is non-linear with the exponent equal to 3/2 for the Flory value of $\nu = 3/5$. This non-linear dependence of force on elongation for real chains was first derived by Pincus and tension blobs are often called **Pincus blobs**. The differences between real and ideal chains can be clearly seen when we consider the dimensionless stretching force:

$$\frac{fb}{kT} \approx \frac{R_f}{Nb} \quad \text{ideal} \quad \text{for } R_f < Nb, \tag{3.40}$$

$$\frac{fb}{kT} \approx \left(\frac{R_f}{Nb}\right)^{3/2} \quad \text{real} \quad \text{for } R_f < Nb. \tag{3.41}$$

The stretching energy is of order $kT$ per monomer when either chain is nearly fully stretched ($R_f \approx Nb$) resulting in $f \approx kT/b$. The force required to stretch the real chain increases more rapidly with $R_f$, but is always *smaller* than the force required to stretch the ideal chain to the same end-to-end distance $R_f$, as shown in Fig. 3.9. Both chains have fewer possible conformations when they are stretched, but the real chain has fewer possible conformations to lose, resulting in a smaller stretching force.

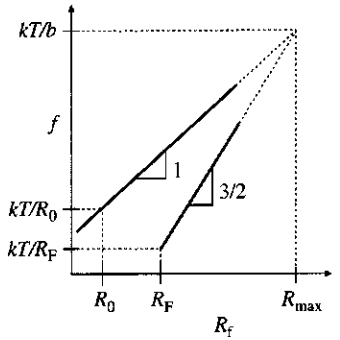


**Fig. 3.9**
Extensional force $f$ as a function of end-to-end distance $R_f$ on logarithmic scales. Comparison between ideal chains (upper line) and real chains (lower line).

A similar scaling calculation can be carried out for stretching a linear chain with fractal dimension $1/\nu$. The free energy cost of stretching a chain from its original size $bN^{\nu}$ to end-to-end distance $R$ is (derived in Problem 3.15)

$$F \approx kT\left(\frac{R}{bN^{\nu}}\right)^{1/(1-\nu)}. \tag{3.42}$$

The fractal dimension of an ideal chain is $1/\nu = 2$ and Eq. (3.42) reduces to free energy of stretching an ideal chain [Eq. (3.35)]. The Flory estimate of the fractal dimension of a real chain is $1/\nu = 5/3$ and Eq. (3.42) reduces to Eq. (3.36). A more accurate estimate of the fractal dimension of a real chain is $1/\nu \cong 1/0.588 \cong 1.7$ with corresponding free energy of stretching [Eq. (3.42)] $F \approx kT\,(R/R_F)^{2.4}$.

The divergence of the force near maximal extension ($f \to \infty$ as $R_f \to R_{max}$) is not described by this scaling approach and is not shown in Fig. 3.9. This divergence is discussed in Section 2.6.2 for freely jointed and worm-like chain models.

### 3.2.2 Polymer under compression

Two simple examples comparing the properties of ideal and real chains are discussed in this section: uniaxial and biaxial compression. A related example of triaxial confinement shall be discussed in Section 3.3.2 for the case where polymers collapse into globules due to attraction between monomers.

#### 3.2.2.1 Biaxial compression

We consider first biaxial compression corresponding to squeezing of a chain into a cylindrical pore of diameter $D$. The diameter of the pore defines a natural **compression blob** size. On length scales smaller than $D$, sections of the chain do not 'know' that it is compressed and their statistics are still the same as the statistics of an undeformed chain:

$$D \approx bg^{1/2} \quad \text{ideal}, \tag{3.43}$$

$$D \approx bg^{3/5} \quad \text{real}. \tag{3.44}$$

These equations can be solved for the number of monomers $g$ in a compression blob of size $D$:

$$g \approx \left(\frac{D}{b}\right)^{2} \quad \text{ideal}, \tag{3.45}$$

$$g \approx \left(\frac{D}{b}\right)^{5/3} \quad \text{real}. \tag{3.46}$$

The above relations are identical to the corresponding equations for tension blobs (Section 3.2.1) because in both examples the conformational statistics are unperturbed on the shortest scales.

The length of a tube $R_{\|}$ occupied by an ideal chain can be estimated as a random walk of $N/g$ compression blobs along the contour of the tube:

$$R_{\|} \approx D\left(\frac{N}{g}\right)^{1/2} \approx bN^{1/2} \quad \text{ideal.} \tag{3.47}$$

As expected, the size of the ideal chain along the contour of the tube is not affected by the confinement. This is an important property of an ideal chain. Deformation of the ideal chain in one direction does not affect its properties in the other directions because each coordinate's random walk is *independent*.

In the case of confinement of a real chain, the compression blobs repel each other and fill the pore in a sequential array. Therefore, the length of the tube $R_{\|}$ occupied by a real chain is the size of one compression blob $D$ times the number $N/g$ of these blobs:

$$R_{\|} \approx D\left(\frac{N}{g}\right) \approx \left(\frac{b}{D}\right)^{2/3} Nb \quad \text{real in a cylinder.} \tag{3.48}$$

Note that in the case of a real chain confined to a tube, the occupied length of the tube $R_{\|}$ is linearly proportional to the number of monomers $N$ in the chain. The occupied length increases as the tube diameter $D$ decreases. Ideal and real chains of the same length, confined in a cylinder of diameter $D$, are shown schematically in Fig. 3.10. There is no penalty to overlap the compression blobs of an ideal chain, whereas the compression blobs of the real chain have strong excluded volume interactions that prevent overlap.

The free energy of confinement is of the order of $kT$ per compression blob for either chain:

$$F_{\text{conf}} \approx kT\frac{N}{g} \approx kTN\left(\frac{b}{D}\right)^{2} \approx kT\left(\frac{R_0}{D}\right)^{2} \quad \text{ideal,} \tag{3.49}$$

$$F_{\text{conf}} \approx kT\frac{N}{g} \approx kTN\left(\frac{b}{D}\right)^{5/3} \approx kT\left(\frac{R_{\text{F}}}{D}\right)^{5/3} \quad \text{real.} \tag{3.50}$$

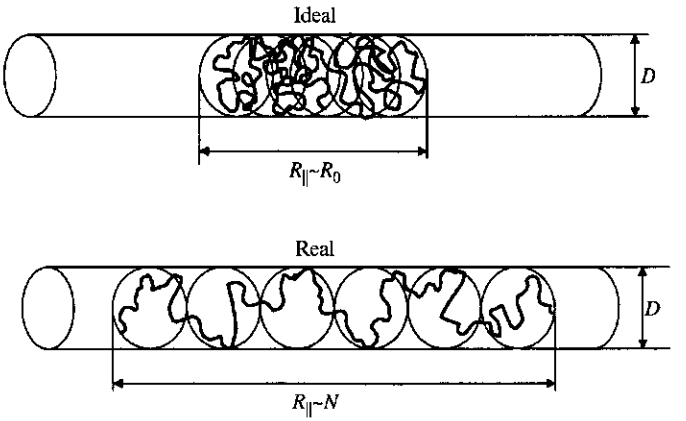


**Fig. 3.10**
Ideal and real chains of the same length, confined in a cylinder of diameter $D$.

$R_0$ and $R_F$ are the end-to-end distances of unconfined ideal and real chains, respectively. These calculations can be generalized to confinement a polymer with fractal dimension $1/\nu$ from its original size $bN^{\nu}$ to a cylinder with diameter $D$. The confinement free energy in this case is (derived in Problem 3.16)

$$F_{\text{conf}} \approx kT\left(\frac{bN^{\nu}}{D}\right)^{1/\nu}, \tag{3.51}$$

with Eq. (3.49) corresponding to an ideal chain with $1/\nu = 2$ and Eq. (3.50) being the result for a real chain with the Flory estimate of fractal dimension $1\ \nu = 5/3$. For a more accurate estimate of the fractal dimension of real chains $1/\nu = 1.70$ the confinement free energy is $F_{\text{conf}} \approx kT\,(R_F/D)^{1.70}$.

### 3.2.2.2 Uniaxial compression

The free energy of confinement of a chain between parallel plates in a slit of spacing $D$ is the same as in the cylindrical pore (up to numerical prefactors of order unity [Eqs (3.49) and (3.50)]. The longitudinal size $R_{\|}$ of an ideal chain confined between parallel plates is still the same as for an unperturbed ideal chain [Eq. (3.47)] because the different $x$, $y$, $z$ components of an ideal chain's random walk are not coupled. In the case of a real chain confined between parallel plates, the compression blobs repel each other, leading to a two-dimensional swollen conformation (see Fig. 3.11). The size of a two-dimensional swollen chain of compression blobs can be estimated from the Flory theory (Section 3.1.2). The 'excluded area' of each compression blob is $\approx D^2$, making the two-dimensional analogue of Eq. (3.17) for the repulsive interaction energy of the chain of $N/g$ compression blobs $kTD^2(N/g)^2/R_{\|}^2$, where $R_{\|}^2$ is the area of the chain. The entropic part of the free energy that resists increasing the area of the chain of $N/g$ compression blobs of size $D$ is $kTR_{\|}^2/\left[(N/g)D^2\right]$ for a real chain confined between two parallel plates:

$$F \approx kT\left(D^2\frac{(N/g)^2}{R_{\|}^2} + \frac{R_{\|}^2}{(N/g)D^2}\right). \tag{3.52}$$

Minimizing this free energy with respect to $R_{\|}$ gives the size of a real chain between plates of spacing $D$:

$$R_{\|} \approx D\left(\frac{N}{g}\right)^{3/4} \approx N^{3/4}b\left(\frac{b}{D}\right)^{1/4} \quad \text{real between plates} \tag{3.53}$$

The size of the real chain confined between plates is again much larger than that of an ideal chain (where $R_{\|} \approx bN^{1/2}$) because the compression blobs of the real chain repel each other. The maximum confinement corresponds to thickness $D$ of the order of the Kuhn monomer size $b$. In this case the chain becomes effectively two-dimensional with size

$$R_{\|} \approx N^{3/4}b \quad \text{real two-dimensional.} \tag{3.54}$$

The exponent $\nu = 3/4$ is universal for two-dimensional linear chains with excluded volume repulsion.

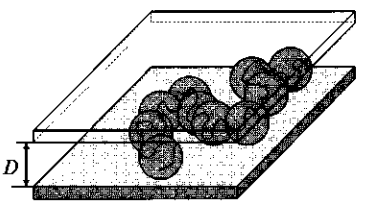


**Fig. 3.11**
Uniaxial compression—a real chain in a slit of spacing $D$ between two parallel plates.

### 3.2.3 Adsorption of a single chain

For the final example comparing the properties of ideal and real chains, consider a polymer in dilute solution near a weakly adsorbing surface. Let the energy gain for a monomer in contact with the surface be $-\delta kT$, where we assume that $0 < \delta < 1$ (weak adsorption). The chain would like to increase the number of monomers in contact with the surface in order to gain adsorption energy. In order to do that, however, it would have to confine itself to a layer of thickness smaller than its unperturbed polymer size ($\xi_{ads} < R$), thereby losing conformational entropy.

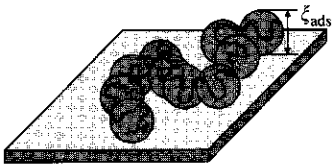


**Fig. 3.12**
A chain adsorbed to a weakly attractive surface.

#### 3.2.3.1 Scaling calculation

The thickness $\xi_{ads}$ of the adsorbed layer defines the **adsorption blob** size (see Fig. 3.12). This adsorption blob size is the length scale on which the cumulative interaction energy of a small section of the chain with the surface is of the order of the thermal energy $kT$. On smaller length scales, the interaction energy is weaker than the thermal energy and the chain remains in an unperturbed conformation, which is Gaussian for ideal chains [Eq. (3.45)] and swollen for real chains [Eq. (3.46)]. On scales larger than the adsorption blob, the interaction energy of the chain with the surface is larger than $kT$ and the consecutive adsorption blobs are forced to be in contact with the surface. Therefore, the conformation of an adsorbed chain is a two-dimensional array of adsorption blobs and is similar to that for a chain confined between two parallel plates, discussed in the previous section.

In order to calculate the size of the adsorption blob $\xi_{ads}$, we need to calculate the number of monomers in contact with the surface for a chain section of size $\xi_{ads}$. The average volume fraction in a chain section of size $\xi_{ads}$ containing $g_{ads}$ monomers is $\phi$:

$$\phi \approx \frac{b^3 g_{ads}}{\xi_{ads}^3} \approx \frac{b}{\xi_{ads}} \quad \text{ideal,} \tag{3.55}$$

$$\phi \approx \frac{b^3 g_{ads}}{\xi_{ads}^3} \approx \left(\frac{b}{\xi_{ads}}\right)^{4/3} \quad \text{real.} \tag{3.56}$$

The number of monomers in each adsorption blob that are in direct contact with the surface (within a layer of thickness $b$ from it) is estimated as the product of the mean-field number density of monomers in the blob $\phi/b^3$ and the volume of this layer within distance $b$ of the surface, $\xi_{ads}^2 b$:

$$\frac{\phi}{b^3}\xi_{ads}^2 b \approx \frac{\xi_{ads}}{b} \quad \text{ideal,} \tag{3.57}$$

$$\frac{\phi}{b^3}\xi_{ads}^2 b \approx \left(\frac{\xi_{ads}}{b}\right)^{2/3} \quad \text{real.} \tag{3.58}$$

The energy gain per monomer in contact with the surface is $\delta kT$. Therefore, the energy gain per adsorption blob is

$$\delta kT \frac{\xi_{ads}}{b} \approx kT \quad \text{ideal,} \tag{3.59}$$

$$\delta kT \left(\frac{\xi_{ads}}{b}\right)^{2/3} \approx kT \quad \text{real,} \tag{3.60}$$

leading to the adsorption blob size:

$$\xi_{ads} \approx \frac{b}{\delta} \quad \text{ideal,} \tag{3.61}$$

$$\xi_{ads} \approx \frac{b}{\delta^{3/2}} \quad \text{real.} \tag{3.62}$$

The free energy of an adsorbed chain can be estimated as the thermal energy $kT$ per adsorption blob:

$$F_{ads} \approx -kT \frac{N}{g_{ads}} \approx -kTN\delta^2 \quad \text{ideal,} \tag{3.63}$$

$$F_{ads} \approx -kT \frac{N}{g_{ads}} \approx -kTN\delta^{5/2} \quad \text{real.} \tag{3.64}$$

The adsorbed layer is thicker and bound less strongly for the real chain (since for weak adsorption $0 < \delta < 1$) because it pays a higher confinement penalty than the ideal chain. The excluded volume interaction of real chains make them more difficult to compress or adsorb than ideal chains. These scaling calculations can be generalized to adsorption of a polymer with general fractal dimension $1/\nu$:

$$F_{ads} \approx kTN\delta^{1/(1-\nu)}. \tag{3.65}$$

The same result can be obtained using the Flory theory, as demonstrated below.

### 3.2.3.2 Flory theory of an adsorbed chain

A mean-field estimate of the free energy of adsorption and the thickness of the adsorbed chain can be made by assuming the monomers are uniformly distributed at different distances from the surface up to thickness $\xi_{ads}$. Then the fraction of monomers in direct contact with the surface (within distance $b$ from the surface) is $b/\xi_{ads}$. The number of adsorbed monomers $Nb/\xi_{ads}$ is multiplied by the adsorption energy per monomer–surface contact ($-\delta kT$) to calculate the energetic gain from the surface interaction:

$$F_{int} \approx -\delta kTN \frac{b}{\xi_{ads}}. \tag{3.66}$$

In order to gain this energy, the chain must pay the entropic confinement free energy $F_{\text{conf}}$, derived in the example above [Eqs (3.49) and (3.50)]. Therefore, the total free energy of a weakly adsorbing chain is

$$F = F_{\text{conf}} + F_{\text{int}} \approx kTN\left(\frac{b}{\xi_{\text{ads}}}\right)^2 - kTN\delta\frac{b}{\xi_{\text{ads}}} \quad \text{ideal,} \tag{3.67}$$

$$F = F_{\text{conf}} + F_{\text{int}} \approx kTN\left(\frac{b}{\xi_{\text{ads}}}\right)^{5/3} - kTN\delta\frac{b}{\xi_{\text{ads}}} \quad \text{real.} \tag{3.68}$$

The minimum of the free energy corresponds to the optimal thickness of the adsorbed layer, determined from $\partial F/\partial\xi_{\text{ads}} = 0$:

$$\xi_{\text{ads}} \approx \frac{b}{\delta} \quad \text{ideal,} \tag{3.69}$$

$$\xi_{\text{ads}} \approx \frac{b}{\delta^{3/2}} \quad \text{real.} \tag{3.70}$$

These estimates are identical to the scaling results [Eqs (3.61) and (3.62)]. Substituting Eqs (3.69) and (3.70) into each individual term[2] in Eqs (3.67) and (3.68) shows that each term is actually of order the free energy of adsorption [Eqs (3.63) and (3.64)].

The adsorbed layer thickness for a polymer with general fractal dimension $1/\nu$ is derived in Problem 3.18:

$$\xi_{\text{ads}} \approx b\delta^{-\nu/(1-\nu)}. \tag{3.71}$$

Substituting this adsorbed layer thickness into the confinement free energy [Eq. (3.51)] or into the interaction free energy [Eq. (3.66)] gives the expected result for the free energy of adsorption [Eq. (3.65)].

### 3.2.3.3 Proximity effects

Both theories of single-chain adsorption, described above, ignore a very important effect—the loss of conformational entropy of a strand due to its proximity to the impenetrable surface. Each adsorption blob has $1/\delta$ contacts with the surface and each strand of the chain near these contacts loses conformational entropy due to the proximity effect. In order to overcome this entropic penalty, the chain must gain finite energy $E_{\text{cr}}$ per contact between a monomer and the surface. This critical energy $E_{\text{cr}}$ corresponds to the adsorption transition. For ideal chains $E_{\text{cr}} \approx kT$. The small additional free energy gain per contact $kT\delta$ should be considered in excess of the critical value $E_{\text{cr}}$,

$$E = E_{\text{cr}} + \delta kT. \tag{3.72}$$

Polymer adsorption is, therefore, a sharp transition with chain thickness changing rapidly in the small interval $\delta kT$ of monomer–surface interaction energy $E$ above $E_{\text{cr}}$ (Fig. 3.13). Strictly speaking, this correction [Eq. (3.72)]

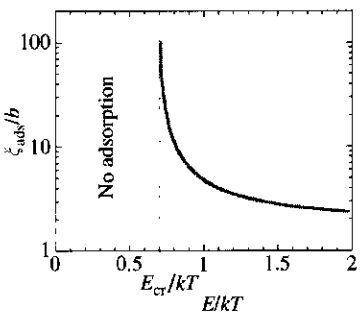


**Fig. 3.13**
The thickness $\xi_{\text{ads}}$ of an adsorbed ideal chain decreases rapidly as the adsorption energy $E$ is increased above the adsorption transition $E_{\text{cr}}$.

[2] Notice that if Eqs (3.69) and (3.70) are blindly substituted into Eqs (3.67) and (3.68), the conclusion would be that the adsorption free energy is zero for both ideal and real chains. This exemplifies the disadvantage of scaling calculations. There are unspecified prefactors of order unity in both terms of Eqs (3.67) and (3.68), which invalidates the blind substitution.

for the proximity effect is valid only for ideal chains. It is much harder to take into account the proximity effect for real chains due to strong correlation effects in these polymers. However, qualitatively there is still a threshold value of energy needed for the real chain to adsorb, as depicted in Fig. 3.13. For adsorption of real chains, the actual concentration inside each adsorption blob decays as a power law in distance from the surface. This power law decay modifies the exponent in Eqs (3.62) and (3.70) (see Problem 3.22).

## 3.3 Temperature effects on real chains

### 3.3.1 Scaling model of real chains

Several examples of scaling with different types of scaling blobs have already been introduced for tension, compression, and adsorption. The main idea in all scaling approaches is a separation of length scales. The blob in each case corresponds to the length scale at which the interaction energy is of the order of the thermal energy $kT$. On smaller scales the interaction is not important and smaller sections of the chain follow the unperturbed statistics (either ideal or swollen). On length scales larger than the blob size, the interaction energy is larger than $kT$ and polymer conformations are controlled by interactions.

In this section, we will consider the excluded volume interaction following a similar scaling approach. The main idea is that of a thermal length scale (the **thermal blob**). On length scales smaller than the thermal blob size $\xi_T$, the excluded volume interactions are weaker than the thermal energy $kT$ and the conformations of these small sections of the chain are nearly ideal. The thermal blob contains $g_T$ monomers in a random walk conformation:

$$\xi_T \approx b g_T^{1/2} \tag{3.73}$$

The thermal blob size can be estimated by equating the Flory excluded volume interaction energy [Eq. (3.17)] for a single thermal blob and the thermal energy $kT$.

$$kT|\mathrm{v}|\frac{g_T^2}{\xi_T^3} \approx kT. \tag{3.74}$$

In this section, we discuss both good ($\mathrm{v} > 0$) and poor ($\mathrm{v} < 0$) solvents and therefore, use $|\mathrm{v}|$ in the definition of the thermal blob. The above two equations are combined to estimate the number of monomers in a thermal blob

$$g_T \approx \frac{b^6}{\mathrm{v}^2}, \tag{3.75}$$

and the size of the thermal blob

$$\xi_T \approx \frac{b^4}{|\mathrm{v}|}, \tag{3.76}$$

in terms of the monomer size b and the excluded volume v.

The thermal blob size is the length scale at which excluded volume becomes important. For $v \approx b^3$, the thermal blob is the size of a monomer ($\xi_T \approx b$) and the chain is fully swollen in an athermal solvent [Eq. (3.12)]. For $v \approx -b^3$, the thermal blob is again the size of a monomer ($\xi_T \approx b$) and the chain is fully collapsed in a non-solvent [Eq. (3.16)]. For $|v| < b^3 N^{-1/2}$, the thermal blob is larger than the chain size ($\xi_T > R_0$) and the chain is nearly ideal. For $b^3 N^{-1/2} < |v| < b^3$ the thermal blob is between the monomer size and the chain size, with either intermediate swelling in a good solvent [$v > 0$, Eq. (3.13)] or intermediate collapse in a poor solvent [$v < 0$, Eq. (3.15)].

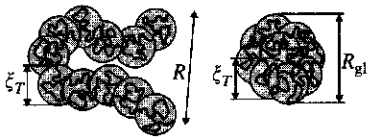


**Fig. 3.14**
The conformation of a single chain in a good solvent (left side) is a self-avoiding walk of thermal blobs while the conformation in a poor solvent (right side) is a collapsed globule of thermal blobs.

#### 3.3.1.1 Excluded volume repulsion ($v > 0$)

On length scales larger than the thermal blob size $\xi_T$, in athermal and good solvents, the excluded volume repulsion energy is larger than the thermal energy $kT$ and the polymer is a swollen chain of $N/g_T$ thermal blobs (Fig. 3.14). The end-to-end distance of this chain is determined as a self-avoiding walk of thermal blobs with fractal dimension $D = 1/\nu \cong 1.7$:

$$R \approx \xi_T \left(\frac{N}{g_T}\right)^{\nu} \approx b \left(\frac{v}{b^3}\right)^{2\nu-1} N^{\nu}. \tag{3.77}$$

For the swelling exponent $\nu \cong 0.588$ the expression for the chain size is $R \approx b\,(v/b^3)^{0.18} N^{0.588}$. Note that this scaling result reduces to the prediction of the Flory theory [Eq. (3.20)] for exponent $\nu = 3/5$.

#### 3.3.1.2 Excluded volume attraction ($v < 0$)

In poor solvents on length scales larger than the thermal blob size $\xi_T$, the excluded volume attraction energy is larger than the thermal energy $kT$. This causes the thermal blobs to adhere to each other, forming a dense globule (Fig. 3.14). The size of the globule is calculated by assuming a dense packing of thermal blobs:

$$R_{gl} \approx \xi_T \left(\frac{N}{g_T}\right)^{1/3} \approx \frac{b^2}{|v|^{1/3}} N^{1/3}. \tag{3.78}$$

Thermal blobs in a poor solvent attract each other like molecules in a liquid droplet. The shape of the globule is roughly spherical to reduce the area of the unfavourable interface between it and the pure solvent. The volume fraction inside the globule is independent of the number of monomers $N$ and is the same as inside a thermal blob:

$$\phi \approx \frac{Nb^3}{R_{gl}^3} \approx \frac{|v|}{b^3}. \tag{3.79}$$

The dependence of the size $R$ of the chain on the number of monomers $N$. for solvents of different quality, is sketched in Fig. 3.15. In athermal solvent ($v = b^3$), in $\theta$-solvent ($v = 0$) and in non-solvent ($v = -b^3$) the dependence of size $R$ on number of monomers $N$ is a single power law $R \approx bN^{\nu}$ for $N \gg 1$. The scaling exponent $\nu$ adopts three values: $\nu \cong 3/5$ in an athermal solvent, $\nu = 1/2$ in a $\theta$-solvent, and $\nu = 1/3$ in a non-solvent. In good and

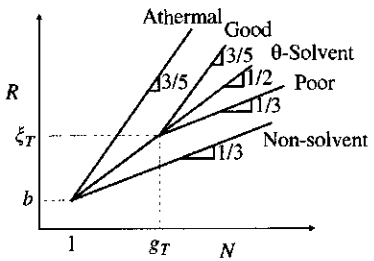


**Fig. 3.15**
End-to-end distance of dilute polymers in various types of solvents, sketched on logarithmic scales. In a $\theta$-solvent the thermal blob size is infinite. For athermal solvent and non-solvent the thermal blob is the size of a single monomer. Good and poor solvents have intermediate thermal blob size (shown here for the specific example of equivalent thermal blobs in good and poor solvent.

poor solvents the dependence follows the ideal chain scaling for polymers (or sections of polymers) smaller than the thermal blob $\xi_T$. On larger scales, the chain follows the corresponding limiting scaling, with good solvent exponent $\nu \cong 3/5$ for $v > 0$ and with collapsed globule exponent $\nu = 1/3$ for $v < 0$. Fig. 3.15 shows that finite length chains have essentially ideal conformations for small values of the excluded volume. Chains have approximately ideal conformations as long as $N < g_T \approx b^6/v^2$ because the net excluded volume interaction in the whole chain is still of smaller magnitude than the thermal energy. Note that Fig. 3.15 suggests the crossover at the thermal blob size is abrupt, while in reality the crossover will be smooth with intermediate effective slopes observed over limited ranges of data.

### 3.3.2 Flory theory of a polymer in a poor solvent

The scaling result for a polymer in a poor solvent can also be found using Flory theory. The Flory free energy for a polymer chain is given by Eq. 3.19:

$$F \approx kT\left(\frac{R^2}{Nb^2} + v\frac{N^2}{R^3}\right). \tag{3.80}$$

In poor solvent, the excluded volume is negative, indicating a net attraction and the minimum of the free energy of Eq. (3.80) corresponds to $R = 0$. Both entropic and energetic contributions decrease with decreasing $R$. Such strong collapse of a polymer into a point is unphysical and we need to add a stabilizing term to this free energy.

#### 3.3.2.1 Entropy of confinement

Earlier in this chapter, we have discussed the entropic cost due to confinement of an ideal chain into a cylindrical tube or in a slit between two parallel walls. A similar entropic penalty has to be paid if a chain is confined within a spherical cavity of size $R < bN^{1/2}$. Each compression blob corresponds to a random walk that fills the cavity. Thus, the number of monomers in each compression blob is determined by ideal chain statistics within the blob:

$$g \approx \left(\frac{R}{b}\right)^2. \tag{3.81}$$

The $N/g$ compression blobs of the ideal chain fully overlap for a chain confined in a spherical pore. The free energy cost of confinement within the spherical cavity is of the order of the thermal energy $kT$ per compression blob:

$$F_{\text{conf}} \approx kT\frac{N}{g} \approx kT\frac{Nb^2}{R^2}. \tag{3.82}$$

The entropic part of the free energy, that includes both the penalty for stretching and one for confinement, and is valid for both $R > bN^{1/2}$ and for

$R < bN^{1/2}$, is a simple sum of the stretching and confinement terms:

$$F_{\text{ent}} \approx kT\left(\frac{R^2}{Nb^2} + \frac{Nb^2}{R^2}\right). \tag{3.83}$$

Note that this entropic free energy alone has a minimum at $R = Nb^2$, which is the conformation of an ideal chain.

Adding the excluded volume interaction term, we obtain a total free energy of the chain with three terms:

$$F \approx kT\left(\frac{R^2}{Nb^2} + \frac{Nb^2}{R^2} + \mathrm{v}\frac{N^2}{R^3}\right). \tag{3.84}$$

This free energy still has a minimum at $R = 0$. The confinement entropy term is not strong enough to stabilize the collapse of the chain due to excluded volume attraction because $Nb^2/R^2 \ll |\mathrm{v}|N^2/R^3$ for $R \to 0$.

### 3.3.2.2 Three-body repulsion

The stabilization of the collapsing coil comes from other terms of the interaction part of the free energy. The interaction energy per unit volume is an intrinsic property of any mixture, that is often expressed as a virial expansion in powers of the number density of monomers $c_n$ [Eq. (3.8)]. The relevant volume of interest here is the pervaded coil volume $R^3$. The excluded volume term is the first term in the virial series and counts two-body interactions as $\mathrm{v}c_n^2$. The next term in the expansion counts three-body interactions as $wc_n^3$, where $w$ is the three-body interaction coefficient:

$$\frac{F_{\text{int}}}{R^3} \approx kT(\mathrm{v}c_n^2 + wc_n^3 + \cdots). \tag{3.85}$$

At low concentration, the two-body term dominates the interaction. The three-body term becomes important at higher concentrations and can stabilize the collapse of the globule (since $w > 0$). The interaction free energy within the coil is estimated using the monomer concentration inside the coil $c_n = N/R^3$:

$$F_{\text{int}} \approx kT\left(\mathrm{v}\frac{N^2}{R^3} + w\frac{N^3}{R^6}\right). \tag{3.86}$$

The total free energy of the chain is dominated by the interaction terms at higher densities (smaller chain sizes $R$):

$$\begin{aligned} F &\approx kT\left(\frac{R^2}{Nb^2} + \frac{Nb^2}{R^2} + \mathrm{v}\frac{N^2}{R^3} + w\frac{N^3}{R^6}\right) \\ &\approx kT\left(\mathrm{v}\frac{N^2}{R^3} + w\frac{N^3}{R^6}\right) \text{ for } R \ll R_0. \end{aligned} \tag{3.87}$$

The globule seeks to minimize this free energy, by balancing the two-body attraction ($\mathrm{v} < 0$) and three-body repulsion ($w > 0$) terms:

$$R_{\text{gl}} \approx \left(\frac{wN}{|\mathrm{v}|}\right)^{1/3}. \tag{3.88}$$

A typical value of the three-body interaction coefficient for almost symmetric monomers is $w \approx b^6$ leading to the prediction of the globule size identical to that of the scaling approach [Eq. (3.78)]. For the cylindrical Kuhn monomer of length $b$ and diameter $d$, Eq. (3.11) gives $w \approx (bd)^3$, making the globule size

$$R_{gl} \approx bd\left(\frac{N}{|v|}\right)^{1/3}, \tag{3.89}$$

and the volume fraction within this globule is proportional to the magnitude of the excluded volume:

$$\phi \approx \frac{Nbd^2}{R_{gl}^3} \approx \frac{|v|}{b^2 d}. \tag{3.90}$$

In a non-solvent, $v \approx -b^2 d$ [Eq. (3.16)] and the globule is fully collapsed with volume fraction $\phi \approx 1$ and size $R_{gl} \approx (bd^2 N)^{1/3}$. This state is the result of a dense packing of $N$ monomers, since the volume of the cylindrical Kuhn monomer is $bd^2$.

### 3.3.3 Temperature dependence of the chain size

All results for chain size are now written in terms of the excluded volume. To understand how the chain size changes with temperature, we simply need the temperature dependence of the excluded volume. There are two important parts of the Mayer $f$-function, from which the excluded volume is calculated [Eq. (3.7)]. The first part is the hard-core repulsion, encountered when two monomers try to overlap each other (monomer separation $r < b$). In the hard-core repulsion, the interaction energy is enormous compared to the thermal energy, so the Mayer $f$-function for $r < b$ is $-1$:

$$f(r) = \exp\left[-\frac{U(r)}{kT}\right] - 1 \cong -1 \quad \text{for } r < b, \text{ where } U(r) \gg kT. \tag{3.91}$$

The second part is for monomer separations larger than their size ($r > b$), where the magnitude of the interaction potential is small compared to the thermal energy. In this regime, the exponential can be expanded and the Mayer $f$-function is approximated by the ratio of the interaction energy and the thermal energy:

$$f(r) = \exp\left[-\frac{U(r)}{kT}\right] - 1 \cong -\frac{U(r)}{kT} \quad \text{for } r > b, \text{ where } |U(r)| < kT. \tag{3.92}$$

The excluded volume v can be estimated using Eq. (3.7) with these two parts of the Mayer $f$-function:

$$\begin{aligned} v &= -4\pi \int_0^\infty f(r) r^2 \, dr \approx 4\pi \int_0^b r^2 \, dr + \frac{4\pi}{kT} \int_b^\infty U(r) r^2 \, dr \\ &\approx \left(1 - \frac{\theta}{T}\right) b^3. \end{aligned} \tag{3.93}$$

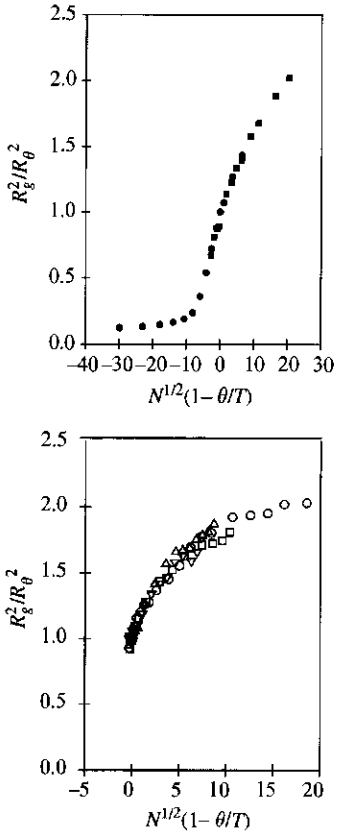


**Fig. 3.16**
Temperature dependence of radius of gyration in universal form. Upper plot shows Monte-Carlo simulation data on Lennard-Jones chains, with the filled squares from W. W. Graessley *et al.*, *Macromolecules* **32**, 3510 (1999) and the filled circles are courtesy of I. Withers. Lower plot shows experimental data on polystyrene in decalin: open circles have $M_w = 4\,400\,000$ g mol$^{-1}$, open squares have $M_w = 1\,560\,000$ g mol$^{-1}$, open triangles have $M_w = 1\,050\,000$ g mol$^{-1}$ and open upside-down triangles have $M_w = 622\,000$ g mol$^{-1}$, from G. C. Berry, *J. Chem. Phys.* **44**, 4550 (1966).

The first term is the contribution of the hard-core repulsion, and is of the order of the monomer volume $b^3$. The second term contains the temperature dependence, and the coefficient of $1/T$ defines an effective temperature called the $\theta$-temperature:

$$\theta \approx -\frac{1}{b^3 k}\int_b^\infty U(r) r^2 \, \mathrm{d}r. \tag{3.94}$$

Since $U(r) < 0$ in the attractive well, the $\theta$-temperature is positive. This results in a very simple approximate temperature dependence of the excluded volume [Eq. (3.93)]:

$$\mathrm{v} \approx \frac{T-\theta}{T} b^3. \tag{3.95}$$

For $T < \theta$ the excluded volume is negative, indicating a net attraction between monomers (poor solvent). For temperatures far below $\theta$, the chain collapses into a dry globule that excludes nearly all solvent (with $\mathrm{v} \approx -b^3$) at $\theta - T \approx T$ and Eq. (3.95) does not apply below this temperature. For $T = \theta$ the net excluded volume is zero and the chain adopts a nearly ideal conformation ($\theta$-solvent). $T > \theta$ has a positive excluded volume, resulting in swelling of the coil (good solvent). For $T \gg \theta$, excluded volume becomes independent of temperature ($\mathrm{v} \approx b^3$) and such solvents are termed athermal.

The temperature dependence of the radius of gyration, reduced by the radius of gyration at the $\theta$-temperature $R_\theta = bN^{1/2}$, is shown in Fig. 3.16 for both experimental data and Monte-Carlo simulations of chains made of $N$ freely jointed monomers interacting via a **Lennard-Jones potential**:

$$U(r) = 4\epsilon\left[\left(\frac{\sigma}{r}\right)^{12} - \left(\frac{\sigma}{r}\right)^{6}\right] \tag{3.96}$$

The abscissa of Fig. 3.16 is proportional to the chain interaction parameter [Eq. (3.22)]:

$$z \approx \frac{\mathrm{v}}{b^3} N^{1/2} \approx \frac{T-\theta}{T} N^{1/2}. \tag{3.97}$$

Note that the square of the chain interaction parameter $z$ is equal to the number of thermal blobs in a chain $z^2 \approx N/g_T$.

$$g_T \approx \frac{N}{z^2} \approx \left(\frac{T}{T-\theta}\right)^2. \tag{3.98}$$

The data reduction for $R_g/R_\theta$ as a function of chain interaction parameter $z$ in Fig. 3.16 is remarkable for both simulation and experiment. Notice in Fig. 3.16 that the $\theta$-temperature is a *compensation point* where the excluded volume happens to be zero. Below the $\theta$-temperature, the chains are collapsed in poor solvent ($\mathrm{v} < 0$), while above the $\theta$-temperature, the coils are swollen in good solvent ($\mathrm{v} > 0$).

The relative contraction of chains in poor solvents can be expressed in terms of the chain interaction parameter $z$ [Eqs. (3.78) and (3.97)]:

$$\frac{R}{bN^{1/2}} \approx \frac{b}{|\mathrm{v}|^{1/3} N^{1/6}} \approx |z|^{-1/3} \quad \text{for } T < \theta. \tag{3.99}$$

The relative swelling in good solvents can also be written as a function of the chain interaction parameter $z$ [Eq. (3.21)].

$$\frac{R}{bN^{1/2}} \approx z^{2\nu-1} \quad \text{for } T > \theta. \tag{3.100}$$

The relative swelling is proportional to $z^{0.18}$ for $\nu \cong 0.588$.

### 3.3.4 Second virial coefficient

The second virial coefficient $A_2$ is determined from the concentration dependence of osmotic pressure [Eq. (1.76)] or scattered light intensity [Eq. (1.91)] from dilute polymer solutions. $A_2$ is a direct measure of excluded volume interactions between pairs of chains.

In solvents near the $\theta$-temperature, the thermal blob is larger than the chain ($g_T > N$ meaning $|z| < 1$ or $|T-\theta|/T < N^{-1/2}$) and the excluded volume interactions are weak. The interaction energy of two overlapping chains is less than the thermal energy $kT$, so chains can easily interpenetrate each other. In this limit, monomers interact directly and $A_2$ *is proportional to the excluded volume* v of a Kuhn monomer. The second virial coefficient of Eqs (1.76) and (1.91) has units of $\mathrm{m^3\,mol\,kg^{-2}}$, making the relation

$$\mathrm{v} = \frac{2M_0^2}{\mathcal{N}_{\mathrm{Av}}} A_2 \quad \text{for } \left|\frac{T-\theta}{T}\right| < N^{-1/2}, \tag{3.101}$$

as will be derived in Chapter 4 [see Eq. (4.72)]. Using Eq. (3.97), $A_2$ can be written in terms of the chain interaction parameter $z$:

$$A_2 \approx \frac{\mathcal{N}_{\mathrm{Av}}\mathrm{v}}{M_0^2} \approx \frac{\mathcal{N}_{\mathrm{Av}} b^3}{M_0^{3/2}} \frac{z}{M^{1/2}} \quad \text{for } |z| < 1. \tag{3.102}$$

For good solvents ($z > 1$), chains repel each other strongly and do not interpenetrate. The volume excluded by a chain is of the order of its pervaded volume $R^3$ and the molar mass of the chain is $M$:

$$\frac{A_2 M^2}{\mathcal{N}_{\mathrm{Av}}} \approx R^3 \quad \text{for } \frac{T-\theta}{T} > N^{-1/2}. \tag{3.103}$$

Using Eq. (3.100) for the chain size $R$ allows the second virial coefficient in good solvent to be determined:

$$A_2 \approx \frac{\mathcal{N}_{\mathrm{Av}}}{M^2} R^3 \approx \frac{\mathcal{N}_{\mathrm{Av}} b^3}{M_0^{3/2}} \frac{z^{6\nu-3}}{M^{1/2}} \quad \text{for } z > 1. \tag{3.104}$$

The second virial coefficient is proportional to $z^{0.53}$ for exponent $\nu \cong 0.588$. Combining Eqs (3.102) and (3.104), we see that both $\theta$-solvent and good solvent should have $A_2 M^{1/2}$ a function of chain interaction parameter $z$ alone:

$$\frac{A_2 M^{1/2} M_0^{3/2}}{\mathcal{N}_{\mathrm{Av}} b^3} = f(z) \approx \left\{ \begin{array}{cc} z & |z| < 1 \\ z^{6\nu-3} & z > 1 \end{array} \right\}. \tag{3.105}$$

The success of this functional form is demonstrated in Fig. 3.17 for polystyrene of various molar masses in decalin from slightly below $\theta$ to

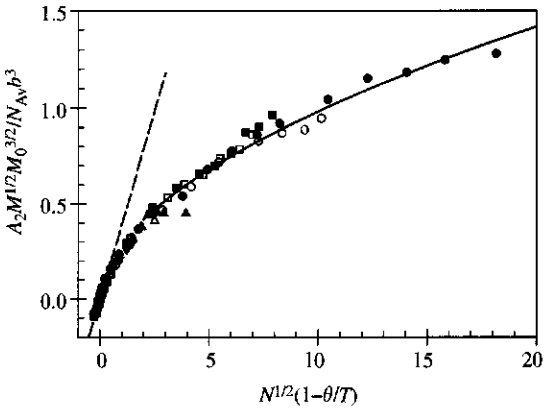


**Fig. 3.17**
Universal plot of second virial coefficient for linear polystyrenes in decalin (filled circles have $M_w = 4\,400\,000$ g mol$^{-1}$, open circles have $M_w = 1\,560\,000$ g mol$^{-1}$, filled squares have $M_w = 1\,050\,000$ g mol$^{-1}$, open squares have $M_w = 622\,000$ g mol$^{-1}$, filled triangles have $M_w = 186\,000$ g mol$^{-1}$, open triangles have $M_w = 125\,000$ g mol$^{-1}$ and filled inverted triangles have $M_w = 48\,200$ g mol$^{-1}$. Data from G. C. Berry, *J. Chem. Phys.* **44**, 4550 (1966).

$\theta + 100\,K$. The collapse of the data is superb. The solid curve is the large $z$ branch of Eq. (3.105), $0.29\,[N^{1/2}(1-\theta/T)]^{6\nu-3}$. The slope of the dashed line drawn in Fig. 3.17 is 0.39. The crossover between these two branches occurs when there is a single thermal blob per chain ($N = g_T$). Using Eq. (3.98) allows the second virial coefficient to be written in terms of the number of thermal blobs per chain $N/g_T$.

$$\frac{A_2 M^{1/2} M_0^{3/2}}{\mathcal{N}_{Av} b^3} \cong 0.20 \left\{ \begin{array}{ll} (N/g_T)^{1/2} & N < g_T \\ (N/g_T)^{0.264} & N > g_T \end{array} \right\}. \tag{3.106}$$

This identifies the prefactors in Eq. (3.98)

$$g_T \cong 0.25 \left( \frac{T}{T-\theta} \right)^2, \tag{3.107}$$

and in Eq. (3.95)

$$\frac{v}{b^3} \cong 0.78 \frac{T-\theta}{T} \cong \frac{0.39}{\sqrt{g_T}}. \tag{3.108}$$

Examples of excluded volume and numbers of Kuhn monomers per thermal blob are given in Table 3.1.

Indeed, data on the temperature dependence of second virial coefficient for a variety of polymer–solvent combinations and from computer simulation show that Eq. (3.106) can be written as a simple crossover function:

$$\frac{A_2 M^{1/2} M_0^{3/2}}{\mathcal{N}_{Av} b^3} = 0.20 \left[ \left( \frac{g_T}{N} \right)^{1.32} + \left( \frac{g_T}{N} \right)^{0.70} \right]^{-0.38}. \tag{3.109}$$

**Table 3.1** Number of Kuhn monomers per thermal blob and excluded volume of a Kuhn monomer for polystyrene in various solvents

| Polymer/solvent | $T$ (°C) | $T-\theta$ (K) | $g_T$ | $v/b^3$ | v (Å$^3$) |
|---|---|---|---|---|---|
| Polystyrene/cyclohexane | 50 | 15 | 120 | 0.036 | 210 |
| Polystyrene/cyclohexane | 70 | 35 | 24 | 0.079 | 460 |
| Polystyrene/decalin | 115 | 100 | 4 | 0.21 | 1200 |
| Polystyrene/benzene | 25 | $\sim 200^a$ | 0.6 | 0.5 | 3000 |

[a] For benzene (and most other good solvents) the $\theta$-temperature is far below all measurement temperatures and use of Eq. (3.107) to extrapolate to the $\theta$-temperature has considerable error.

Measurement of the temperature dependence of second virial coefficient $A_2$ for polymers with known molar mass $M$ and Kuhn length $b$ allows estimation of the number of thermal blobs per chain $N/g_T$ using Eq. (3.109).

## 3.4 Distribution of end-to-end distances

We have seen numerous examples of the qualitative difference in properties between ideal and real chains with excluded volume interactions. It is therefore not surprising that the distribution of end-to-end vectors of real chains is significantly different from the Gaussian distribution function of ideal chains [Eq. (2.86)].

Relative probabilities to find chain ends at distances much larger than the average end-to-end distance are related to the free energy penalty due to chain elongation [see Problem 3.15 and Eq. (3.42):

$$F \approx kT\left(\frac{R}{\sqrt{\langle R^2\rangle}}\right)^{\delta}, \tag{3.110}$$

where the exponent $\delta = 1/(1-\nu)$ is related to the exponent $\nu$ of the root-mean-square end-to-end distance of the chain:

$$\sqrt{\langle R^2\rangle} \approx bN^{\nu}. \tag{3.111}$$

For ideal chains, $\nu = 1/2$ and $\delta = 2$ [see Eq. (3.35)], while for real chains in a good solvent $\nu \cong 0.588$ and $\delta \cong 2.43$ [see Eq. (3.36)]. The tail of the probability distribution function for end-to-end distances is determined by the Boltzmann factor arising from this free energy penalty [Eq. (3.110)]

$$P(N,R) \sim \exp\left(-\frac{F}{kT}\right) \sim \exp\left[-\alpha\left(\frac{R}{\sqrt{\langle R^2\rangle}}\right)^{\delta}\right] \quad \text{for } R > \sqrt{\langle R^2\rangle}, \tag{3.112}$$

where $\alpha$ is a numerical coefficient of order unity. For ideal chains ($\delta = 2$) this leads to the Gaussian distribution function [Eq. (2.86)]. For real chains, a faster decay of the distribution function is expected due to the higher power $\delta \cong 2.43$ in the exponential:

$$P(N,R) \sim \exp\left[-\alpha\left(\frac{R}{\sqrt{\langle R^2\rangle}}\right)^{2.43}\right] \quad \text{for } R > \sqrt{\langle R^2\rangle}. \tag{3.113}$$

Another major difference between ideal and real chains is the reduced probability of two ends of a real chain to be near each other due to excluded volume repulsion of these and neighboring monomers. Recall from Section 2.5 that the probability of finding one end of an ideal chain within a small spherical shell of volume $4\pi R^2\,dR$ around the other end is proportional to the volume of this shell [see Eq. (2.86) for $R \ll bN^{1/2}$]. This probability is significantly reduced for real chains by an additional factor

$$P(N,R) \sim \left(\frac{R}{\sqrt{\langle R^2\rangle}}\right)^g \quad \text{for } R \ll \sqrt{\langle R^2\rangle}, \tag{3.114}$$

due to excluded volume repulsion between sections of the polymer, as they approach each other. The exponent $g = 0$ for ideal chains because there is no reduction of probabilities for small end-to-end distances. For real chains, the exponent $g \cong 0.28$ in three dimensions and $g = 11/24$ in two dimensions.

By combining the two limits [Eqs. (3.113) and (3.114)], the distribution function of normalized end-to-end distances can be constructed:

$$P(x) \sim x^g \exp(-\alpha x^\delta), \tag{3.115}$$

where

$$x = \frac{R}{\sqrt{\langle R^2\rangle}}. \tag{3.116}$$

An approximate expression for the three-dimensional distribution function for real chains results:

$$P(x) \cong 0.278x^{0.28} \exp(-1.206x^{2.43}) \quad \text{real.} \tag{3.117}$$

For ideal chains, the corresponding function is Gaussian:

$$P(x) = \left(\frac{3}{2\pi}\right)^{3/2} \exp(-1.5x^2) \quad \text{ideal.} \tag{3.118}$$

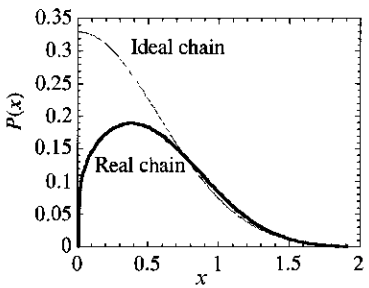


**Fig. 3.18**
Distribution function $P(x)$ of normalized end-to-end distances $x = R/\sqrt{\langle R^2\rangle}$. Thin curve, ideal chain; thick curve, real chain.

The two functions are compared in Fig. 3.18. Note the dramatic difference between them. Real chains in an athermal solvent rarely have ends in close proximity. The probability to find chain ends within relative distance $dx$ of $x$ is $4\pi x^2 P(x)\,dx$. The coefficients of the distributions of end-to-end distances are chosen so that they are normalized:

$$\int P(x)\,d^3x = \int_0^\infty P(x)4\pi x^2\,dx = 1. \tag{3.119}$$

Their second moment is also equal to unity

$$\int x^2 P(x)\,d^3x = \int_0^\infty x^2 P(x)4\pi x^2\,dx = 1, \tag{3.120}$$

due to the definition of the relative distance $x$ [Eq. (3.116)].

## 3.5 Scattering from dilute solutions

The size and shape of a polymer chain in dilute solution is best studied using scattering methods. Each monomer absorbs the incident radiation

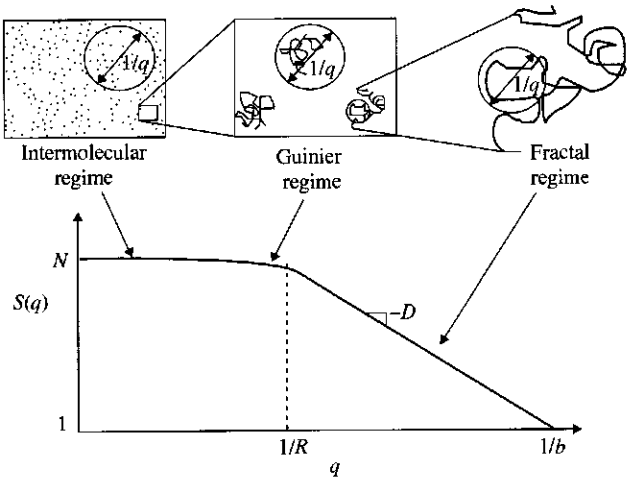


**Fig. 3.19**
Scattering function for a dilute solution on logarithmic scales.

and re-emits it in all directions. If there is contrast between monomers and solvent they can be distinguished. The scattered intensity at a given scattering wavevector is determined by this contrast and by the coherence of the re-emitted radiation from pairs of monomers. The **scattering function** $S(\vec{q})$ is defined as a sum over all pairs of $n$ monomers in the scattering volume,

$$S(\vec{q}) = \frac{1}{n}\sum_{j=1}^{n}\sum_{k=1}^{n}\langle \exp[-i\vec{q}\cdot(\vec{r}_j - \vec{r}_k)]\rangle, \tag{3.121}$$

where $\vec{q}$ is the scattering wavevector [Eq. (2.131)] and $\vec{r}_j$ is the position vector of $j$th monomer. This scattering function is simply a dimensionless version of the ratio of scattering intensity at wavevector $\vec{q}$ and concentration. The isotropic scattering function from dilute solution is sketched in Fig. 3.19. At large wavevectors $q \gg 1/R$ for each monomer $j$ the sum over $k$ has contribution of order unity from each of the $n_q$ monomers within distance $1/q$ from monomer $j$ since for $\vec{q}\cdot(\vec{r}_j - \vec{r}_k) < 1$ the exponential is close to one. On the other hand, the contribution from monomers further away from monomer $j$ averages to zero. The scattering function at large wavevectors is

$$S(q) \approx \frac{1}{n}\sum_{j=1}^{n} n_q = n_q \quad \text{for } q \gg 1/R \tag{3.122}$$

where $n_q$ is the number of monomers in the volume $1/q^3$. The number of monomers $n_q$ is related to the size of the chain segment $1/q$ through the fractal dimension of the chain $\mathcal{D}$:

$$S(q) \approx n_q \approx (qb)^{-\mathcal{D}} \quad \text{for } 1/R < q < 1/b. \tag{3.123}$$

This power law extends from the monomer size $b$ to the size of the chain $R$, provided that the entire chain has the same fractal dimension $\mathcal{D}$. Scattering on such small scales is dominated by **intra-molecular scattering** from

monomers inside individual coils and is related to the pair correlation function within the coil [Eq. (2.123)]:

$$g(r) \approx \frac{m}{r^3} \sim r^{\mathcal{D}-3}. \tag{3.124}$$

For real chains in an athermal solvent, $\mathcal{D} = 1/\nu \cong 1.7$, so $S(q) \sim q^{-1.7}$ and $g(r) \sim r^{-1.3}$ within the coil.

For smaller wavevectors $q < 1/R$, the number of monomers $n_q$ within distance $1/q$ from monomer $j$ saturates at the number of monomers in the chain $N$. The exact form of the scattering function in this Guinier regime enables calculation of the radius of gyration $R_g$ [Eq. (2.152)]. In both the Guinier and fractal regimes, the scattering comes from pairs of monomers on the same chain and the scattering function is proportional to the form factor:

$$S(q) = NP(q) \quad \text{for } q > \left(\frac{c_n}{N}\right)^{1/3}. \tag{3.125}$$

The **inter-molecular scattering** dominates the scattering function at wavevectors $q$ smaller than the reciprocal distance between chains $(c_n/N)^{1/3}$, where $c_n$ is the number density of monomers in solution. The inter-molecular regime is controlled by concentration fluctuations arising from the difference in the number of chains in volumes $1/q^3$. Assuming there are no interactions between chains (strictly valid only in very dilute solutions), the mean-square fluctuation in the number of chains in the volume $1/q^3$ is of the order of the average number $n_q/N \approx c_n/(Nq^3)$. The fluctuation in the number of monomers in volumes of size $1/q^3$ is $\sqrt{\langle(\delta n_q)^2\rangle} = N\sqrt{c_n/(Nq^3)}$. The scattering function is the mean-square fluctuation in the number of monomers in the volume $1/q^3$ normalized by the number of monomers $n_q$ in this volume:

$$S(q) = \frac{\langle(\delta n_q)^2\rangle}{n_q} = \frac{N^2 c_n/(Nq^3)}{Nc_n/(Nq^3)} = N \quad \text{for } q \ll \left(\frac{c_n}{N}\right)^{1/3}. \tag{3.126}$$

Note that this value matches the low-$q$ end of the fractal regime. It is hardly surprising that the scattering function contains information about the chain length, since in Chapter 1 we demonstrated how light scattering can be used to determine molar mass from the low concentration limit of $R_\theta/(Kc)$, where $R_\theta$ is Rayleigh ratio [Eq. (1.87)], $K$ is the optical constant [Eq. (1.89)], and $c$ is mass concentration. The scattering function for light scattering is related to the Rayleigh ratio as

$$S(q) = \frac{R_\theta}{KcM_0}, \tag{3.127}$$

where $M_0$ is the molar mass of a monomer. We give this relation for light scattering for completeness, but scattering inside the polymer coils is usually measured using neutrons and X-rays, which extend the range of wavevectors to $1\ \text{nm}^{-1}$. The scattering function from all of these scattering experiments is the same, with the prefactor relating the scattering function to scattered intensity being specific to the type of radiation used.

## 3.6 Summary of real chains

Real chains have interactions between monomers. If the attraction between monomers just balances the effect of the hard core repulsion, the net excluded volume is zero ($v = 0$) and the chain will adopt a nearly ideal conformation (see Chapter 2):

$$R_0 = bN^{1/2} \quad \text{for } \theta\text{-solvent.} \tag{3.128}$$

Such a situation with zero net excluded volume is called the $\theta$-condition, corresponding to a particular $\theta$-temperature for a given solvent.

If the attraction between monomers is weaker than the hard-core repulsion, the excluded volume is positive and the chain swells. This corresponds to a good solvent at a temperature above the $\theta$-temperature, and the coil size is larger than the ideal size:

$$R_F \approx b\left(\frac{v}{b^3}\right)^{2\nu-1} N^{\nu} \approx b\left(\frac{v}{b^3}\right)^{0.18} N^{0.588} \quad \text{for good solvent.} \tag{3.129}$$

The chain conformation is a self-avoiding walk of thermal blobs, whose size decreases as temperature is raised.

In an athermal solvent, the monomer–solvent energetic interaction is identical to the monomer–monomer interaction. This makes the net interaction between monomers zero, leaving only the hard core repulsion between monomers. The excluded volume is independent of temperature ($v \approx b^3$), and the chain is a self-avoiding walk of monomers:

$$R \approx bN^{\nu} \approx bN^{0.588} \quad \text{for athermal solvent.} \tag{3.130}$$

If the attraction between monomers is stronger than the hard-core repulsion, the excluded volume is negative and the chain collapses. This occurs below the $\theta$-temperature, and corresponds to a poor solvent. In a poor solvent, the polymer is in a collapsed globular conformation corresponding to a dense packing of thermal blobs. The size of a globule is smaller than the ideal size:

$$R_{gl} \approx |v|^{-1/3} b^2 N^{1/3} \quad \text{for poor solvent.} \tag{3.131}$$

A chain in a poor solvent collapses into a globule with significant amounts of solvent inside. Most chains agglomerate with other chains and precipitate from solution. Only a very small number of polymers remain in the solvent-rich phase of a poor solvent in a globular conformation described by Eq. (3.131). Far below the $\theta$-temperature, the attraction dominates completely and the excluded volume $v \approx -b^3$. This limit is called a non-solvent, and an individual chain in that solvent would have a fully collapsed conformation:

$$R \approx bN^{1/3} \quad \text{for non-solvent.} \tag{3.132}$$

In this case, most chains precipitate from solution into a melt excluding nearly all solvent, and the chains then adopt ideal conformations to maximize their entropy.

The good solvent and poor solvent results only apply to chains that are sufficiently long. Short chains with degree of polymerization less than the number of monomers in a thermal blob remain ideal, as depicted in Fig. 3.15.

Several examples were given of scaling models that utilize blobs to separate regimes of chain conformation. The common idea in these scaling models is that, on the smallest length scales (inside the blobs), there is not enough cumulative interaction to alter the chain conformation. On length scales larger than the blob size, the cumulative interactions become larger than the thermal energy, and can then modify the conformation of the chain of blobs. Since the cumulative interaction energy of each blob is roughly the thermal energy $kT$, the total interaction energy can be conveniently estimated as $kT$ per blob.

The free energy of stretching a real linear chain in a good solvent has a stronger dependence on size $R$ than the quadratic dependence of the ideal chain:

$$F \approx kT\left(\frac{R}{R_F}\right)^{1/(1-\nu)} \approx kT\left(\frac{R}{R_F}\right)^{2.43}. \tag{3.133}$$

The stretching force for a real chain increases non-linearly with elongation:

$$\frac{fb}{kT} = \frac{b}{kT}\frac{\partial F}{\partial R} \approx \left(\frac{R}{Nb}\right)^{\nu/(1-\nu)} \approx \left(\frac{R}{Nb}\right)^{1.43}. \tag{3.134}$$

The free energy of confining a real linear chain in a good solvent either into a slit of spacing $D$ or to a cylindrical pore of diameter $D$ is larger than for an ideal chain because the real chain has repulsive interactions:

$$F \approx kT\left(\frac{R_F}{D}\right)^{1/\nu} \approx kT\left(\frac{R_F}{D}\right)^{1.7}. \tag{3.135}$$

Excluded volume changes with temperature in the vicinity of the $\theta$-temperature:

$$\mathrm{v} \approx b^3\left(\frac{T-\theta}{T}\right). \tag{3.136}$$

Good solvents typically have $T \gg \theta$, and their $\theta$-temperature is not accessible because the solvent crystallizes at much higher temperatures. Similarly, $\theta$-solvents cannot usually be heated far enough above the $\theta$-temperature to reach the athermal limit because the solvent will boil at a lower temperature.

# Problems

## Section 3.1

**3.1** (i) Taking the volume of a cylindrical Kuhn monomer to be $bd^2$, derive an expression for the cylindrical monomer diameter $d$ in terms of the characteristic ratio, molar mass per backbone bond, melt density, Kuhn length $b$ and bond angle $\theta$.

(ii) Using the melt density of polyethylene $\rho = 0.784\ \mathrm{g\,cm^{-3}}$ and the melt density of polystyrene $\rho = 0.784\ \mathrm{g\,cm^{-3}}$, along with the data of Table 2.1 for $C_\infty$ and $b$, calculate the diameter of the Kuhn cylindrical monomer for these two polymers.

**3.2** Consider the excluded volume interaction between hard spheres of radius $R$.

(i) What is the shortest possible distance between their centres?
(ii) What is the interaction potential between these spheres?
(iii) Demonstrate that the excluded volume of hard spheres is eight times larger than the volume $v_0$ a sphere:

$$v = \frac{32\pi}{3} R^3 = 8v_0.$$

**3.3** Consider the excluded volume interaction between spherical particles with effective pairwise interaction potential

$$U(r) = \left\{ \begin{array}{cc} \infty & \text{for } r \leq 2R \\ -kT_0(2 - r/(2R)) & \text{for } 2R \leq r \leq 4R \\ 0 & \text{for } r > 4R \end{array} \right\},$$

where $kT_0$ is the strength of the attractive potential with $T_0 = 100\,\mathrm{K}$.

(i) Calculate the excluded volume of these particles.
(ii) Plot the dimensionless excluded volume $v/R^3$ as a function of temperature and determine the $\theta$-temperature of these particles.

**3.4** Consider two cylindrical rods of length $b$ and diameter $d$ with $b \gg d$. Fix the centre of one of the rods at the origin of the coordinate system, pointing in the $x$ direction.

(i) Estimate the volume excluded for the second rod if it is fixed to always point in the $y$ direction (perpendicular rods).
(ii) Estimate the volume excluded for the second rod if it is fixed to always point in the $x$ direction (parallel rods).
(iii) How do you expect the excluded volume to change at different fixed angles between the two rods?

**3.5** Consider a linear polymer chain with $N$ monomers of length $b$, restricted to the air–water interface (two-dimensional conformations). Repeat the Flory theory calculation and demonstrate that the size $R$ of the chain as a function of the 'excluded area' $a$ per monomer (two-dimensional analogue of excluded volume v) is

$$R = a^{1/4} b^{1/2} N^{3/4}. \tag{3.137}$$

Compare the size of this chain at the interface to that in the bulk for parameters $N = 1000$, $b = 3\,\text{Å}$, $a = 7.2\,\text{Å}^2$, $v = 21.6\,\text{Å}^3$.

**3.6** Consider a randomly branched polymer in a dilute solution. Let us assume that the radius of gyration for this polymer in an ideal state (in the absence of

excluded volume interactions) is

$$R_0 = bN^{1/4},$$

where $b$ is the Kuhn monomer size and $N$ is the number of Kuhn monomers. Use a Flory theory to determine the size $R$ of this randomly branched polymer in a good solvent with excluded volume v. What is the size $R$ of a randomly branched polymer with $N = 1000$, $b = 3$ Å, $v = 21.6$ Å$^3$? Compare this size to the size of a linear chain with the same degree of polymerization in the same good solvent and in $\theta$-solvent.

**3.7** Using the results of Problem 3.6, calculate the overlap volume fraction for the three cases:

(i) randomly branched monodisperse polymer in good solvent.
(ii) linear chain in good solvent.
(iii) linear chain in $\theta$-solvent.

**3.8** Consider a randomly branched polymer with $N$ monomers of length $b$. The polymer is restricted to the air–water interface and thus assumes a two-dimensional conformation. The ideal size of this polymer $R_0$ in the absence of excluded volume interactions is

$$R_0 = bN^{1/4}.$$

(i) Repeat the Flory theory calculation to determine the size $R$ of the branched polymer at the interface as a function of the 'excluded area' $a$ per monomer (two-dimensional analogue of the excluded volume v). degree of polymerization $N$ and monomer length $b$.
(ii) Calculate the size of the branched polymer with $N = 1000$, $b = 3$ Å, $a = 7.2$ Å$^2$ at the air–water interface.
(iii) Calculate the surface coverage (number of monomers per square Angstrom) at overlap for this randomly branched polymer at the air–water interface in good solvent.
(iv) How much higher is the surface coverage at the overlap of randomly branched chains with $N = 100$, $b = 3$ Å, $a = 7.2$ Å$^2$ at the air–water interface, compared with $N = 1000$?

**3.9** Consider a linear polymer chain with $N = 400$ Kuhn monomers of Kuhn length $b = 4$ Å in a solvent with $\theta$-temperature of 27 °C. The mean-field approximation of the interaction part of the free energy for a chain of size $R$ is

$$F_{\text{int}} \approx kTR^3\left[v\left(\frac{N}{R^3}\right)^2 + w\left(\frac{N}{R^3}\right)^3 + \cdots\right],$$

where the excluded volume of a monomer is

$$v \approx \left(1 - \frac{\theta}{T}\right)b^3,$$

and $w \approx b^6$ is the three-body interaction coefficient.

(i) Use Flory theory to estimate the size of the chain swollen at the $\theta$-temperature due to three-body repulsion.
(ii) For what values of the excluded volume v does the two-body repulsion dominate over the three-body repulsion? Is the chain almost ideal or swollen if the two interactions are of the same order of magnitude?
(iii) For what values of temperature $T$ does the two-body repulsion dominate over the three-body repulsion?

(iv) Use Flory theory to estimate the size of the chain swollen at 60 °C due to excluded volume repulsion (ignore the three-body repulsion).
(v) Estimate the overlap volume fraction $\phi^*$ of the chain at 60 °C.
(vi) What is the number of Kuhn monomers in the largest chain that stays ideal at 60 °C?

**3.10** Consider an oligomer with $N = 3$ bonds occupying four lattice sites on a two-dimensional square lattice with lattice constant $b$. One end of the oligomer is fixed at the origin of the lattice.

(i) How many different conformations would such an oligomer have if it *can* occupy the same lattice site many times (simple random walk)?
(ii) How many different conformations would such an oligomer have if it *cannot* occupy the same lattice site (self-avoiding walk)?
(iii) Find the root-mean-square end-to-end distance of the oligomer for the first case.
(iv) Find the root-mean-square end-to-end distance of the oligomer for the second case.

**3.11** Why is there no temperature dependence of the excluded volume in an athermal solvent?

**3.12** If the monomer–solvent interaction potential is identical to the monomer–monomer interaction potential, the solvent is called:

(i) good,
(ii) $\theta$,
(iii) athermal.

Explain your answer.

**3.13** (i) Construct a Flory theory for the free energy of a polyelectrolyte chain consisting of $N$ monomers of length $b$ and net charge of the chain $Q = efN$, where $f$ is the fraction of Kuhn monomers bearing a charge.

*Hint*: The electrostatic energy of the chain is $Q^2/(\epsilon R)$, where $\epsilon$ is the dielectric constant of the solvent and $R$ is the size of the chain.

(ii) Show that the size of the chain at temperature $T$ is

$$R \approx Nbf^{2/3}\left(\frac{l_B}{b}\right)^{1/3},$$

where the Bjerrum length is defined as $l_B \equiv e^2/(\epsilon kT)$.

**3.14** (i) What is the relation of the fourth virial coefficients of spherical ($v_{4,s}$) and cylindrical ($v_{4,c}$) monomers if there are $b/d$ spheres per cylinder?
(ii) What is the relation of the $k$th virial coefficients of spherical ($v_{k,s}$) and cylindrical ($v_{k,c}$) monomers?

## Section 3.2

**3.15** Calculate the free energy $F(N, R_f)$ and the force $f$ for stretching a chain with an arbitrary scaling exponent $\nu$ in the dependence of the end-to-end distance on the number of monomers $R = bN^{\nu}$.

**3.16** Calculate the free energy for compressing a real chain into a cylindrical tube with diameter $D$. Assume an arbitrary scaling exponent $\nu$ in the dependence of end-to-end distance of the chain on the number of monomers $R = bN^{\nu}$.

**3.17** Calculate the free energy for squeezing a real chain between parallel plates into a slit of width $D$. Assume an arbitrary scaling exponent $\nu$ in the dependence of the end-to-end distance of the chain on the number of monomers $R = bN^{\nu}$.

**3.18** Calculate the thickness $\xi_{ads}$ of the adsorbed layer for a polymer with $N$ monomers of size $b$. The interaction energy of a monomer in contact with the (planar) surface is $-\delta KT$. Assume an arbitrary scaling exponent $\nu$ in the dependence of end-to-end distance of the chain on the number of monomers $R = bN^{\nu}$.

**3.19** Scaling theory of two-dimensional adsorption.
Consider a linear chain confined to an air–water interface. The attraction of each monomer at the contact line between the edge of the interface and the walls of the container is $-\delta kT$.

(i) Estimate the thickness and length of the ideal adsorbed chain of $N$ Kuhn monomers with Kuhn length $b$.
(ii) Calculate the energy of adsorption of the ideal polymer of part (i) to the contact line.
(iii) Estimate the thickness and length of the real adsorbed chain of $N$ Kuhn monomers with Kuhn length $b$. Recall that the unperturbed size of the real chain confined to the air–water interface in good solvent is $R \approx bN^{3/4}$ [Eq. (3.54)].
(iv) Calculate the energy of adsorption of the real polymer of part (iii) to the contact line.

**3.20** Flory theory of adsorption from a two-dimensional interface onto a one-dimensional line.
Consider a real linear chain confined to an air–water interface. The attraction of a monomer at the contact line between the edge of the interface and the walls of the container is $-\delta kT$.
Calculate the thickness $\xi_{ads}$ of the adsorbed real chain and the energy of adsorption using Flory theory. Recall that the unperturbed size of the real chain confined to the air–water interface in good solvent is given by Eq. (3.54).

**3.21** Consider a polymer chain consisting of $N$ Kuhn monomers of length $b$, adsorbed from a good solvent onto a solid substrate. A monomer in contact with the surface has interaction energy $-\delta kT$.

(i) What is the thickness $\xi_{ads}$ of the adsorbed chain?
(ii) What is the size of the adsorption blob if $N = 1000$, $b = 3$ Å, and $\delta = 0.4$?

Suppose that one of the ends of the adsorbed chain is attached to the tip of an atomic force microscope and is pulled away from the surface (still in a good solvent) with force $f$.

(iii) What is the minimal force $f$ required to pull the chain away from the surface at room temperature?
(iv) What would be the minimal force $f$ required to pull the chain away from the surface if the tip of the atomic force microscope were attached to a middle monomer rather than to the end monomer?
(v) Would the minimal force required to pull the chain away from the surface in a $\theta$-solvent be smaller or larger (as compared to a good solvent) for the same attractive energy $-\delta kT$? Explain your answer.

**3.22** Consider a real chain adsorbed at a surface with an excess free energy gain per monomer $\delta kT$. Assume that the monomer concentration decreases as a power law of the distance $z$ from the surface

$$c(z) = c(0)\left(\frac{b}{z}\right)^{a} \quad \text{for } 0 < z < \xi_{ads},$$

where exponent $0 < a < 1$ and $\xi_{ads}$ is the thickness of the adsorbed chain.

(i) Calculate the fraction of monomers within distance $b$ of the surface. These are the monomers that lower their energy by favourable contacts with the surface.

(ii) Construct a modified Flory theory for the adsorption of a real chain and estimate the thickness $\xi_{ads}$ of the adsorbed chain as a function of the excess free energy gain per monomer $\delta kT$. Ignore the effects of the density profile $c(z)$ on the confinement free energy penalty.

**3.23** The effective interaction between each monomer and an adsorbing surface is

$$W(z) = -kT\frac{b^3}{z^3}A,$$

where $A$ is the **Hamaker constant** of the polymer–surface interaction. Consider an ideal chain adsorbed at the surface. Find the relation between the free energy gain per contact $-\delta kT$ and the effective Hamaker constant $A$.

## Section 3.3

**3.24** Calculate the force needed to stretch a chain, of $N = 1000$ Kuhn monomers with Kuhn length $b = 5$ Å in a good solvent with excluded volume $v = 37.5$ Å$^3$, by a factor of 4 from its unperturbed root-mean-square end-to-end distance at room temperature.

**3.25** Consider a chain of $N$ Kuhn monomers with Kuhn length $b$ in a good solvent with excluded volume v confined between parallel plates in a slit of width $D$.

(i) What is the size of a thermal blob and the number of monomers in a thermal blob?

(ii) What is the size of a compression blob?

(iii) What is the number of monomers in a compression blob? Note: Be careful with respect to relative sizes of compression and thermal blobs.

(iv) What is the free energy of confinement of the chain in a slit?

(v) At what thickness of the slit $D$ does the free energy change form between real and ideal chain expressions?

(vi) Estimate the value of this crossover thickness $D$ for a chain with $N = 1000$ Kuhn monomers with Kuhn length $b = 5$ Å in a good solvent with excluded volume $v = 20$ Å$^3$.

**3.26** Consider a randomly branched polymer in a dilute solution. The ideal size of this polymer, $R_0$, in the absence of excluded volume interactions is

$$R_0 = bN^{1/4},$$

where $b$ is the monomer size and $N$ is the degree of polymerization.

(i) Use the scaling theory to determine the size $R$ of this randomly branched polymer in a good solvent with excluded volume v.

(ii) What is the number of monomers in a thermal blob for this randomly branched polymer as a function of excluded volume v and monomer size $b$. How does it compare to the similar expression for the number of monomers in a thermal blob in linear polymers?

(iii) What is the size, $\xi_T$, of a thermal blob for a randomly branched polymer? How does it compare to the similar expression for the size of the thermal blob in linear polymers.

*Hint*: Recall that the cumulative energy of all excluded volume interactions inside a thermal blob is equal to $kT$.

(iv) What is the size of a randomly branched polymer with $N = 1000$, $b = 3$ Å, in a good solvent with $v = 2.7$ Å$^3$?

(v) What is the size of a linear chain for the same set of parameters?

(vi) What are the size and the number of monomers in the largest randomly branched polymer that stays ideal for monomer length $b = 3$ Å, and excluded volume $v = 2.7$ Å$^3$? (*Hint*: Thermal blob.)

(vii) What are the size and the number of monomers in the largest linear polymer that stays ideal for monomer length $b = 3$ Å, and excluded volume $v = 2.7$ Å$^3$? (*Hint*: Thermal blob.)

**3.27** Assume the simple approximation for a temperature dependence of the excluded volume:

$$v = \left(1 - \frac{\theta}{T}\right) b^3.$$

Consider a chain with degree of polymerization $N = 1000$ and monomer size $b = 3$ Å in a solvent with $\theta$-temperature of 30 °C.

(i) What would be the chain size at temperatures: $T = 10$, 30, and 60 °C?

(ii) Sketch the temperature dependence of the size of this polymer.

(iii) What is the degree of polymerization of the largest chain that stays ideal at $T = 60$ °C (*Hint*: Thermal blob)?

(iv) Estimate the degree of polymerization of the largest chain that dissolves in the solvent at $T = 10$ °C (*Hint*: Thermal blob)?

**3.28** Use the following light scattering data for the temperature dependence of the second virial coefficient of a linear poly(methyl methacrylate) with $M_w = 2\,380\,000$ g mol$^{-1}$ in a water/*t*-butyl alcohol mixture to determine the temperature dependence of excluded volume, assuming the Kuhn length of PMMA is 17 Å:

| $T$ (°C) | 37.0 | 38.0 | 40.0 | 43.8 | 50.0 | 55.8 |
|---|---|---|---|---|---|---|
| $10^5 A_2$ (cm$^3$ mol g$^{-2}$) | −6.4 | −3.4 | −0.4 | 0.5 | 3.5 | 4.1 |

(i) Estimate the excluded volume at each of the six temperatures.

(ii) Estimate the $\theta$-temperature from these data.

(iii) To measure the excluded volume of this polymer/solvent system at lower temperature, should a higher or lower molar mass sample be studied?

Data from M. Nakata, *Phys. Rev. E* **51**, 5770 (1995).

**3.29** Derive an equation for the second virial coefficient in a solution of collapsed globules below their $\theta$-temperature, in terms of the number of Kuhn monomers per chain $N$, the Kuhn monomer size $b$ and the reduced temperature $(\theta - T)/T$. Can this second virial coefficient be related to the chain interaction parameter of Eq. (3.97)?

**3.30** Determine the relation between the chain interaction parameter $z$ [defined in Eq. (3.22)] and the number of thermal blobs per chain $N/g_T$.

## Section 3.4

**3.31** Polymerization of ring polymers.

Ring polymers are synthesized by linking two reactive ends of linear polymers in dilute solution. The cyclization probability can be defined as the

probability of two ends of a chain being found within monomeric distance $b$ of each other.

(i) What are the cyclization probabilities of $N$-mers in $\theta$-solvent and in good solvent? What is the ratio of these probabilities for $N = 100$?

(ii) Are the resulting ring polymers obtained by cyclization in $\theta$-solvent and good solvent statistically equivalent? In other words will these rings have the same size if they are placed in the same solvent? If they are different, which one is larger? Explain your answer.

### Section 3.5

**3.32** A pair correlation function $g(\vec{r})$ was defined in Section 2.7 as the probability of finding a monomer in a unit volume at distance $\vec{r}$ away from a given monomer (labeled by $j = 1$). Note that $j = 1$ is not necessarily the end monomer of any chain. The pair correlation function $g(\vec{r})$ can be written in terms of the delta function summed over all monomers except for the one at $\vec{r}_1$

$$g(\vec{r}) = \left\langle \sum_{j \neq 1} \delta(\vec{r} - (\vec{r}_j - \vec{r}_1)) \right\rangle \tag{3.138}$$

(i) Show that the Fourier transform of the pair correlation function is

$$g(\vec{q}) = \int g(\vec{r}) \exp(-i\vec{q} \bullet \vec{r}) \mathrm{d}^3 r = \sum_{j=1}^{n} \langle \exp[-i\vec{q} \bullet (\vec{r}_j - \vec{r}_1)] \rangle - 1 \tag{3.139}$$

(ii) Recognize that the choice of the $j = 1$ monomer was arbitrary and use the definition of the scattering function (Eq. 3.121) to show that

$$S(\vec{q}) = 1 + g(\vec{q}) = 1 + \int g(\vec{r}) \exp(-i\vec{q} \bullet \vec{r}) \mathrm{d}^3 r \tag{3.140}$$

## Bibliography


des Cloizeaux, J. and Jannink, G. *Polymers in Solution: Their Modelling and Structure* (Clarendon Press, Oxford, 1990).

Eisenriegler, E. *Polymers near Surfaces* (World Scientific, Singapore, 1993).

Flory, P. J. *Principles of Polymer Chemistry* (Cornell University Press, Ithaca, NY, 1953).

Freed, K. *Renormalization Group Theory of Macromolecules* (Wiley, New York, 1987).

de Gennes, P. G. *Scaling Concepts in Polymer Physics* (Cornell University Press, Ithaca, NY, 1979).

Grosberg, A. Yu. and Khokhlov, A. R. *Statistical Physics of Macro-molecules* (AIP Press, Woodbury, NY, 1994).

McQuarrie, D. A. *Statistical Mechanics* (University Science, 2000).

Yamakawa, H. *Modern Theory of Polymer Solutions* (Harper & Row, New York, 1971).

This page is intentionally left blank